Tetraether lipid Liposomes for the Preparation of Novel Liposomal Drug Carriers

Dissertation

zur Erlangung des Doktorgrades der Naturwissenschaften (Dr. rer. nat.)

dem

Fachbereich Pharmazie der Philipps-Universität Marburg

vorgelegt von

Aybike Özçetin

aus İzmit, Türkei

Marburg/Lahn 2011

Vom Fachbereich Pharmazie der Philipps-Universität Marburg als Dissertation am 19.04.2011 angenommen.

Erstgutachter: Prof. Dr. Udo Bakowsky
Zweitgutachter: Prof. Dr. Achim Aigner

Tag der mündlichen Prüfung: 20.04.2011

Die vorliegende Arbeit entstand auf Anregung und unter Leitung von

Herrn Prof. Dr. Udo Bakowsky

am Institut für Pharmazeutische Technologie und Biopharmazie
der Philipps-Universität Marburg.

„Ich hinterlasse keinen Vers, kein Dogma und keine unumstößlichen Gesetze. Mein geistiges Erbe sind Wissenschaft und Vernunft.“

“I give you no verse as my spiritual heritage; no dogma or irrevocable laws either. My spiritual inheritance is only science and reason.”

„Ben manevi miras olarak hiç bir ayet ve, hiç bir dogma, hiç bir donmuş ve kalıplaşmış kural bırakmıyorum. Benim manevi mirasım ilim ve akıldır.“

30.08.1925 Kastamonu

Mustafa Kemal Atatürk

TABLE OF CONTENTS

1 Introduction

1.1 Tetraether lipids

Archaea is the third domain of life; its members are distinguished from *Eukarya* and *Bacteria* by their unique structure and composition characteristics. (1). Therefore the members of Archaea survive in extreme habitats with acidic pH, high temperatures, low pressure or hypersaline conditions due to their physiological adaptations (2).

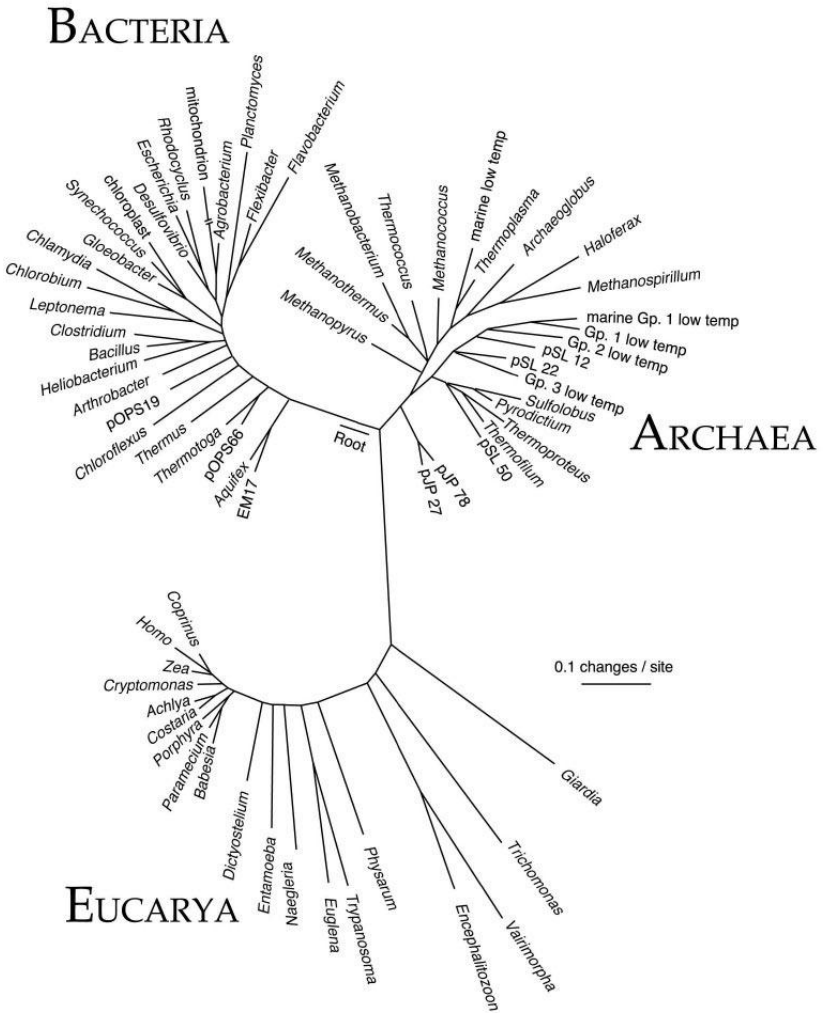

Figure 1. Three domains of life (Ref: http://epicofevolution.com/treeoflife.html)

This study focuses on two species of the Archea domain, namely *Sulfolobus acidocaldarius* and *Thermoplasma acidophilum*. The tetraether lipids used in this study were extracted form both of these species. *Sulfolobus acidocaldarius* is a hyper-thermophilic archaeon from the family Sulfolobaceae with optimum living conditions of about 80° C and pH 3 which makes them thermophiles and acidophiles respectively (2). *Thermoplasma acidophilum* is a thermoacidophilic archaebacterium which has optimal growth conditions at 59° C - 100° C and in acidic environments at pH 1-2. *Thermoplasma acidophilum* was isolated from a coal refuse pile by Darland *et al*. in 1970 (3).

The ability of these organisms to survive in extreme environments is based on their specific lipid structure, which is highly distinctive from bacterial lipids, e.g. (i) the hydrocarbon "tails" are linked to the glycerol backbone with an ether linkage instead of an ester linkage, (ii) these tails are attached to each other (iii) the carbon bonds are saturated with methyl groups (4) (Figure 2, 3). In the membrane of Archaea more than 15 different ether lipid structures are present (5). In this ether linkage, *sn*-2,3 configurations of the saturated phytanyl chains are attached to a glycerol backbone. This linkage is a *sn*-1,2 configuration in conventional ester lipids (1).

The core lipid consists of 5-carbon repeating units that are bound together to form saturated isporanoid chains. These units are attached via ether bonds in sn-2,3 carbon positions to the glycerol backbone (6). The archaeol (standard ether, 2,3-di-O-phytanyl-sn-glycerol) with $C_{20,20}$ is most common and dominant in Archaea and found in extreme halophiles (1). The tail to tail condensation of two archaeol moieties reveals caldarchaeols with $C_{40,40}$ (standard caldarchaeol or standard tetraether, 2,2',3,3'-tetra-O-dibiphytanyl-sn-diglycerol).

Caldarchaeol is not found in extreme halophiles, but 0 to 65 % of methanogens and up to 90 % of thermoacidophiles consist of Caldarchaeols (7).

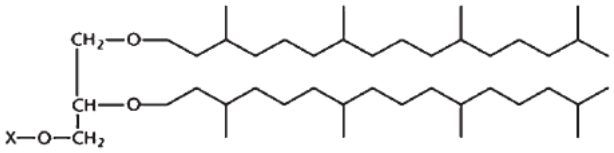

Figure 2. Chemical structure of Archaeol. (Ref: Patel, G.B. Sprott, G.D. (2006) Archaeal Membrane Lipids, Wiley, doi: 10.1038/npg.els.0004316)

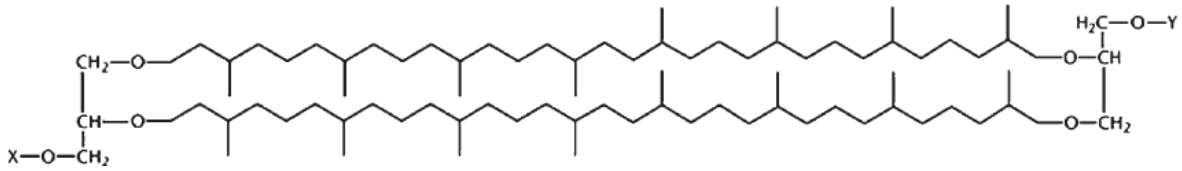

Figure 3. Chemical Structure of Cardarchaeol. (Ref: Patel, G.B. Sprott, G.D. (2006) Archaeal Membrane Lipids, Wiley, doi: 10.1038/npg.els.0004316)

In the selected Archaea, *Thermoplasma* and sulfur-dependent thermophiles consist of head groups bound to core lipids of most caldarchaeol. The core glycerolipids of *Sulfolobus sulfataricus* and *Thermoplasma acidophilum* consist of up to 95 % caldarchaeols. The increased amount of caldarchaeol stabilizes the membrane. Furthermore, the pentacyclic rings which can be found in *Sulfolobus acidocaldarius* and *Thermoplasma acidophilum* species have an crucial impact on stability against high temperatures. The core lipid of these species can contain up to 4 rings per alkyl chain (7).

As mentioned above, the high stability of the native archaebacterial membranes can be attributed to the unique chemical structures of one of the lipids purified; glycerol dialkyl

nonitol tetraether (GDNT) (8) (Figure 4a, 4b). For the successful extraction of glycerol dialkyl nonitol tetraether (GDNT) from *Sulfolobus acidocaldarious,* we applied the extraction method proposed by Bode *et al.* and described in Chapter 2. The freeze-dried material of *Sulfolobus acidocaldarious* extracted with $CHCl_3$:MeOH was then stirred with $CHCl_3$:MeOH:5 % trichloroacetic acid (TCA) mixture. The mixture was washed thoroughly with $CHCl_3$:MeOH:H_2O (9).

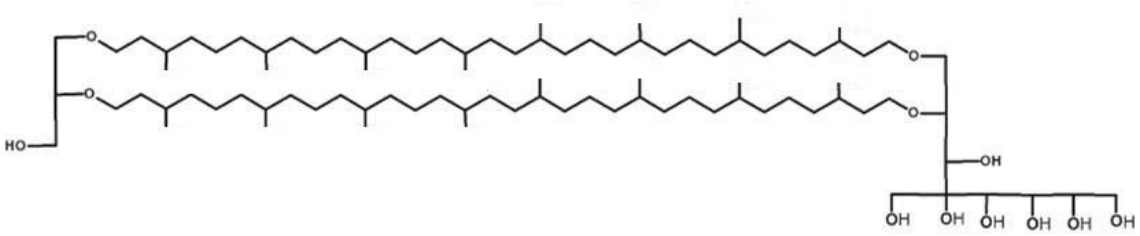

a

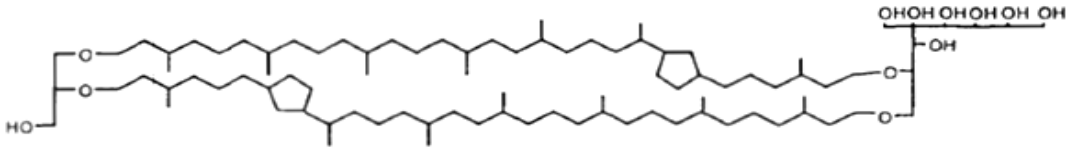

b

Figure 4. (a) Chemical structure of glycerol dialkyl nonitol tetraether (GDNT), (b) Chemical structure of GDNT with two cyclopentanes. (Ref: Shi-Lung, L, Charles E.M., Chang, E.L. (1989) Purfication of glycerol dialkyl nonitol tetraether from *Sulfolobus acidocaldarius*, , Vol:30 J Lip Res)

The major class of archaeal lipids is bipolar tetraether lipids. Considering the stability properties of these lipids, it was proposed to employ them for the liposome formation to provide more durability to membranes compared to conventional liposomes (4).

In 1959 E.G. Bligh and W.J. Dyer published a lipid extraction method (10). This Bligh-Dyer method applied with the use of a basic solvent system of chloroform/methanol provides an

effective extraction of the total lipid amount from biomass. This total lipid mixture consists of a large variety of lipids of different configuration and properties. The mix of these lipids provides comprehensive stability of the liposomes which shows the inessentiality of purification of individual lipid species and may provide a unique character in a wide range of applications (11).

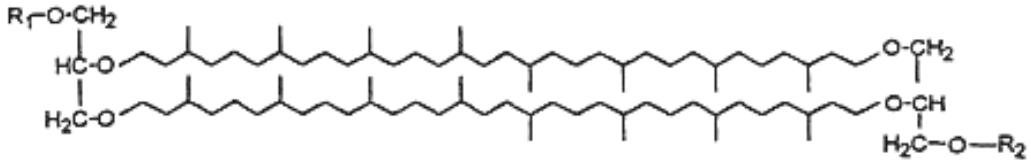

Figure 5. Tetraether lipids general structure. (Ref: Albers, S.-V., van de Vossenberg, J.L.C.M., Driessen, A. J.M. Konings,W.N. (2000) Adaptation of the archaeal cell membrane to heat stress, Vol. 5, pp. 796-803 Front Biosci)

1.2 Tetraether lipid liposomes

Tetraether lipid liposomes are spherical soft-matter particles constructed from tetraether lipids instead of ester lipids. These lipids are extracted from archaeal membranes (12). The method of lipid extraction is mentioned above. Lipids of tetraether lipid liposomes consist of fully saturated phytanyl chains with 20-40 carbons in length. They are attached to the glycerol backbone via ether bonds (1) (Figure 5). Fully saturated bonds are playing an important role in oxidation resistance, and methyl side groups provide fluidity to hydrocarbon chains (13).

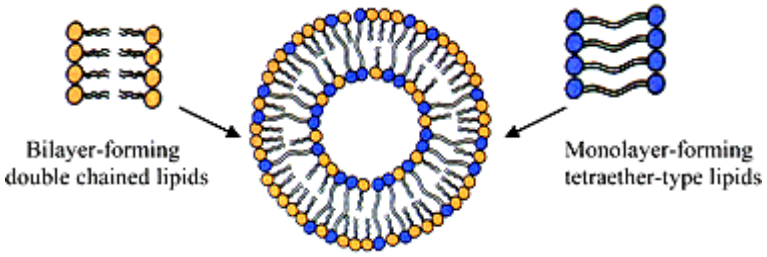

Figure 6. Monolayer-forming tetraether lipid and bilayer forming double chained lipid mixture in a liposome structure. (Ref: Réthoré, G., Montier, T. Gall T. Le, Delépine, P. Cammas-Marion, S. Lemiègre, L. Lehn, P. and Benvegnu, T. (2007) Archaeosomes based on synthetic tetraether-like lipids as novel versatile gene delivery systems, pp. 2054-2056 Chem Commun)

Liposomes have lately become a matter of particular interest as drug and gene carriers because of their biocompatibility and biodegradability properties. However, besides many advantages, one of the most important handicaps of liposomes concerns stability. So far, conventional lipids were incorporated with high amounts of cholesterol in their bilayers (14). Other methods include coating the lipids with polymers (15) or mixing with fluorinated phospholipids (16). With all these methods it was not possible to achieve sufficient stability. Tetraether lipids overcome this handicap due to their chemical properties, which do not exist in conventional lipids.

1.3 Stability properties of liposomes

High mechanical stability of tetraether lipids offers a wide range of potential usage in biotechnological applications, such as delivery systems. A significant stability is expected from gene or drug carriers, particularly if the environment of the destination has the potential to harm to the composition of the vesicle. For instance, a carrier for oral drug delivery in the gastrointestinal tract is expected to be stable at low pH and withstand protein degradation conditions (17).

The gastrointestinal tract contains pancreatic fluids with 1.5-16.0 U of phospholipase A_2 activity in each ml (18). A drug loaded conventional liposome will undergo burst release when the lipids are hydrolyzed. Similar to stability against bile salts, tetraether liposomes provide convincing results on stability against phospholipases (19). Besides that, several other stability studies with tetraether lipid liposomes were undertaken, among these, stability in alcohols, detergents, phenol, high salinity and combinations of those.

The lipid mixture consists of a large variety of lipids with different properties. The mix of these lipids provides comprehensive stability to the liposomes which makes it an inessentiality to purify individual lipid species (11).

Tetraether lipid liposomes are also convenient for storage; they do not fuse or aggregate at 4° C for more than four months. It is as well possible to store them at higher temperatures and at a wide pH range (20).

The extreme stability of liposomes is attributed to the chemical structures of membrane lipids of Archaea. A typical biological membrane consists of a monolayer or bilayer of lipid molecules. These lipids have one hydrophilic head group which is oriented towards the

aqueous medium surrounding the membrane. This hydrophilic head group is linked to the hydrophobic tails. These lipid molecules form a bilayer or monolayer membrane with van der Waals and Coulomb interactions. Non-covalent bonds in membranes provide higher impermeability to small ions (21). In consequence of this feature, high energy is required for transport of ions across the membrane. At higher temperatures the permeability will increase. It is expected that a conventional lipid membrane will be more permeable at higher temperatures. A tetraether lipid membrane provides an additional energy barrier to proton permeability. However, at a certain point of very high temperature, far upon the optimal growth temperature, the membrane will be unable to compensate the proton permeability. This proton permeability is strongly connected to the upper boundary of the growth temperature of the microorganism (22). On the other hand, sodium permeability is occurring via a solubility-diffusion mechanism (23). The bioenergetic role of protons is explained to be an environmental adaptation (24). For instance, *Thermoplasma acidophilum* grows in sulphuric acid ponds with a pH value of 2 at 59° C although its internal pH is 6.5 (25) and this internal conditions can only be maintained with a proton resistant membrane and an electron transport chain to protect the cytosol from irruption of protons (26). Hence, the proton pumping capacity of the membrane of aerobic thermophiles provides a high proton-motive force (27).

Unusual physical and chemical properties of tetraether lipids increase the stability of archaeal membranes. These properties which were sustained to TEL liposomes make them attractive for biotechnology applications.

High temperature stability enables heat sterilization of liposomes. However, most of the ester lipids cannot provide sufficient short and/or long term thermal stability. Thermal stability has been investigated by incubation of 5(6)-carboxyfluorescein (CF) and [^{14}C] loaded ester and ether lipid liposomes at different temperature values. Less CF leakage of tetraether lipid

liposomes from *Thermoplasma acidophilum* compared to all other ester and ether lipid liposomes attributed to phase transition at low temperatures.

For intravenous applications, stability of liposomes in serum and resistance against blood compartments is an important issue. In serum, bilayer-spanning and ether bonds of tetraether lipids provides better stability compared to other ester lipid liposomes (11).

For successful drug delivery, stability against macrophages and other bioactive species is expected. However, it is reported that tetraether lipid liposomes can be taken up by macrophages in 50 fold higher concentration than other conventional lipids. This may appear as a disadvantage at first, yet it can be very useful in several biotechnological applications, such as antigen entrapped liposomes that cause an immune response which is currently achieved by toxic Freund's adjuvant (28). As an option, radioisotope labelled liposomes can be used for macrophage targeting in nuclear medicine (29).

High membrane stability may also inhibit the drug release in targeted tissue. Consequently, it is important to consider the circumstances and the environmental properties of the targeting region to determine the reasonable balance between stability and release of the entrapped agent in liposomes.

1.4 Liposomal Drug Delivery Systems

In 1968 Bangham has introduced membrane models with phospholipids where he indicated that phospholipids suspended into excess aqueous solution tend to spontaneously form bilayer vesicles, "liposomes" (greek; "fat bodies"), and that their size and lamellar properties can be influenced by the preparation conditions (30). Since this discovery a number of liposomes were tailored with various lipids and lipid mixtures with modifications in size, physical, chemical and biological properties. In 1972, Gregoriadis and Ryman have introduced

liposomes as drug carriers (31). Liposomes began to be used as industrial products in medical, pharmaceutical, food, cosmetic and other industries. Liposomes became especially attractive for the pharmaceutical industry because of their biocompatibility, non-toxic, non-immunogenic and biodegradability properties and the scope of both hydrophilic and hydrophobic pharmaceutical incorporation, as well as the possibility of efficient delivery into cells and even into individual cellular compartments (32). Currently there are several drug incorporated liposome formulations available as pharmaceutical products. The main application range of these products lies within cancer treatment, reducing the serious toxicity and adverse side effects of anti-cancer drugs because the toxic drug can be entrapped into the liposome or incorporated to the lipid membrane. The liposome can even be targeted to the inflamed region to provide a local treatment. The first commercial liposome based drugs DAUNOXOME®, DOXIL® and AmBisome® introduced in 1995 were considered to be the mile stones of liposome technology which successfully combined the basic research and industrial implementation. When incorporating anti-cancer drugs, they reduce systemic toxicity, early degradation or inactivation of the drug (33, 34). Hydrophilic drugs can be loaded to vesicles in aqueous solution; hydrophobic drugs can be incorporated into the amphiphile layer. In both cases, charge of the particles and interactions of the active compound with the vesicle forming molecules play an important role in drug entrapment and delivery. (35, 36). Besides the liposome formulation, the site of the administration of liposomes is considered to have a severe impact on delivery. Surface charge, serum proteins, lipoproteins and phagocytic systems may disturb the drug-liposome composition (36-38). Tetraether lipid liposomes allow long term blood circulation. Furthermore, liposomes are not only used intravenously but also in dermatological, pulmonary and oral applications. In this thesis, the stability of tailored tetraether lipid liposomes was addressed. As a consequence of their chemical structure and special monolayer organization, tetraether lipids are very stable in

low pH environment. These properties make them an adequate candidate for oral drug delivery. The vesicles are able to pass through the stomach without being damaged and can carry the loaded agent to further sections of the oral system (39). Conventional lipid vesicles are not able to resist phospholipase degradation and pass through the callus during topical application. Tetraether lipid liposomes are relatively resistant against phospholipase degradation (40) which may provide a method of long-term drug release in the dermatological application.

1.5 Liposomal Drug Targeting Systems

The currently used anti-cancer drugs are not able to differenciate between cancer cells and healthy cells. This results in a systemic toxicity and serious side effects. Drug targeting systems offer a less invasive alternative to the traditional anticancer therapy. Drug targeting strategies are classified into two groups: passive targeting and active targeting. Besides systemic administration, passive targeting involves the administration of the anti-cancer drug to the tumor baring organ or environment. Such procedures can be highly invasive because of the necessity of injection or surgical procedure. Another alternative of passive drug targeting is spontaneous drug accumulation in “leaky” areas. Due to the increased permeability of the vascular endothelium of tumors, particles up to 500 nm can be accumulated into the interstial space (41, 42). Furthermore, systemic administration of liposomes causes limitations in applications because of rapid clearance from the bloodstream and uptake by reticuloendothelial system (RES) in liver and spleen (43). However, it is reported that, in comparison to free drug application, entrapped and modified liposomes exhibit significant changes in absorption, biodistribution and clearance (44, 45). Liposome size and surface modification such as PEG-liposomes reduces toxic effect of entrapped drug and prolongs drug

circulation time in the plasma (46). On the other hand, when a rapid response on a selective cell type within a tissue is necessary, an active delivery system can facilitate this aim. Active targeting strategies of liposomes are based on ligand-bearing liposome application. As ligands one can use antibodies, carbonhydrates, hormones, polypeptides, drugs, growth factors, glycoproteins, cytokines, toxins or lectins. (47). The best known ligand interactions can be classified as ligand-receptor interactions, antibody-antigen interactions and lectin-carbonhydrate interactions, protein-ligand interaction, metal-ligand interaction, integrin-ligand interaction (48). Lectins are nonimmunological proteins and liposomes can be modified effectively with these lectins and used to target cell surface carbonhydrates (49). In this respect, Concanavalin A is the first lectin to be purified on a large scale and available on a commercial basis; it was extracted from the jack bean *Canavalia ensiformis* and carries two metal binding sites, also it is one of the Mannose binding lectin (50, 51).

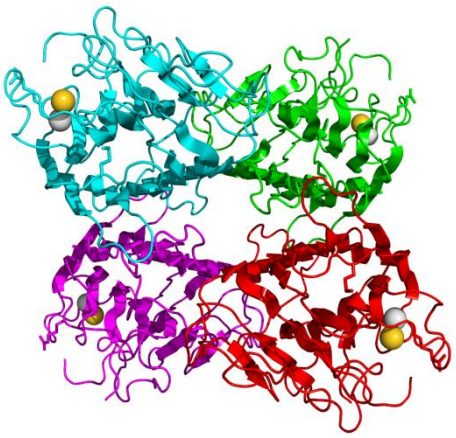

Figure 7. Concanavalin A (at neutral and alkaline pH, ConA exists as a tetramer of four identical subunits of approximately 26,000 daltons each. Below pH 5.6, ConA dissociates into active dimers of 52,000 daltons) (Ref: http://commons.wikimedia.org/wiki/File:3CNA_ Concanavalin_A.png)

One of the binding sites binds to sugar domains localized on inflamed tissues or tumors, the other binding side can be covalently bound to the liposome (52). Effective targeting of a drug carrier reduces adverse effects and provides higher impact on cancer therapy with a lower dose of drug.

The ligand conjugation of tetraether lipids serves this scope. In this thesis, covalent binding of ConA to the active lipid containing liposome was investigated. Tetraether lipids were activated with cyanuric chloride in the presence of chloroform and ConA was bound to the liposomes, prepared with the mixture of active and non-active tetraether lipids (52, 53).

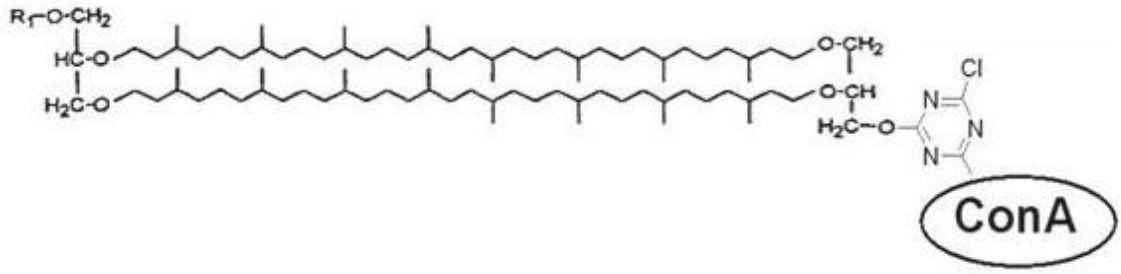

Figure 8. Concanavalin A conjugated tetraether lipid.

1.6 Liposome based drug delivery in Cancer Therapy

Since liposomes were discovered they have drawn the attention of researchers as potential carriers of various drugs and bioactive molecules in the therapeutical and diagnostical fields. The pharmaceuticals especially developed for cancer treatment are currently not able to specifically target inflamed cells. Liposomal drug targeting provides a better mode of cell recognition (54). Both hydrophilic and hydrophobic drugs can be associated with liposomes

by drug-lipid interactions of hydrophobic substances and drug trapping of hydrophilic drugs. Liposomal drug delivery provides the opportunity of longer systematic circulation of cytotoxic drugs and delivery to certain extravascular regions (55, 56). Recent studies showed that liposomes decrease the toxicity of several antitumor drugs due to the kidney uptake compared to the free drug. Also, by the encapsulation of drug, a much lower amount of drug is sufficient for effective therapy (57, 58). That also prevents the side effects caused by application of high doses of the drug. Liposomes also protect the drug from rapid degradation and exhibit higher efficiency compared to their free counterparts (59).

1.6.1 Angiogenesis

It is well known that for solid tumor growth, blood is essential for the suppliment of oxygen and nutrients. Under normal conditions, angiogenesis, the formation of new blood vessels, occurs in adults during the ovarian cycle, wound healing and other physiological processes during repair (60). Most of the tumors over a size of 1-2 mm^3 cannot survive without a blood vessel supply. Therefore in 1972 Folkman has explained the necessity of angiogenesis for tumor progression (61). At first view, angiogenesis seems to be the same as vasculogenesis. In fact, during vasculogenesis the blood vessel formation occurs by *de novo* production of endothelial cells. Angiogenesis on the other hand is a term to denote the formation of new blood vessels from pre-existing ones (62). It has been found that the tumor cells induce angiogenesis (63). It was also reported that angiogenesis plays a critical role not only in formation and maintainance of the primary tumor but also in its metastasis (64). Since then, anti-angiogenesis is regarded as a cancer therapy strategy. During the formation of a new blood vessel, the endothelial cell, the basement membrane and the extracellular matrix should be degraded and remodelled by matrix metalloproteinases (65). Then a new matrix should be

prepared by stromal cells. The proliferation and migration of endothelial cells is linked to growth factors. The endothelial cells then form a tube-like structure, where the blood flows through. Hence, studies of anti-angiogenesis were focused on the major factors that regulate angiogenesis such as the basic fibroblast growth factor (bFGF or FGF-2) and the vascular endothelial growth factor (VEGF). The VEGF family consists of sub-types such as VEGF-B, VEGF-C, VEGF-D and isoforms such as $VEGF_{121}$, $VEGF_{165}$ (66). Unlike bFGF, VEGF is expressed by the vast majority of cancers. In the case of blocking its activity, the tumor growth *in vivo* is inhibited (67). Beside bFGF and VEGF, the other factors and proteins effecting the angiogenesis are Platelet-derived growth factor (PDGF) which plays significant role in blood vessel formation, Transforming growth factor beta (TGF-β) which controls proliferation, and cellular differentiation, Angiopoietin 1 and integrins which are related with vascular development, Platelet Endothelial Cell Adhesion Molecule (PECAM-1) which is expressed in certain tumors for the tissue regeneration (68).

In this thesis, "imatinib (STI 571)" as an anti-angiogenic inhibitor is used. Besides cell proliferation, imatinib inhibits VEGF production. In the case of inhibition of VEGF expression, a large range of anti-tumor effects could be provided. Therefore VEGF expression is particularly investigated in this thesis.

VEGF is a disulfide-bonded dimeric glycoprotein. VEGF has various isoforms with a molecular mass of 34-45 kDa (69). These isoforms are responsible for identical biological activities (70). Dvorak and colleagues have discovered that VEGF has an important role in vascular permeability. It was reported that VEGF is normally expressed at low levels by most human and animal tissues during the growth process, and it is only under abnormal conditions, such as pregnancy and tumor existence, that the expression of VEGF is found to be increased (66). The receptors of these factors were described and afterwards numerous

angiogenic inhibitors were developed and tested over the years. Many of these drugs were already in use as anti-cancer drugs, but anti-angiogenic effect of these drugs were then described by Folkman, Klement and their colleagues (71, 72).

1.6.2 Tyrosine Kinase Inhibition

In cancer and benign proliferative disorders, protein-tyrosine kinases play a fundamental role in signal transduction (73). Their blocking by substances like the tyrosin kinase inhibitor imatinib can affect the tyrosine kinase signal cascade. Imatinib mesylate (Glivec® STI571, also known as imatinib) is a phenylaminopyrimidine analogue that binds to the ATP-binding site of a specific tyrosine-kinase (74). Although imatinib was first developed as a platelet-derived growth factor receptor- α inhibitor, it was later found that imatinib also inhibits the BCR-ABL, c-KIT (75-78). Imatinib is specific for the tyrosine kinase inhibitor domain in the *abl* (Abelson murine leukemia) gene. In diseases such as chronic myelogenous leukemia, the Philadelphia chromosome leads to a fusion protein of *abl* with *bcr* (breakpoint cluster region) gene which causes a constitutively active tyrosine kinase. Imatinib binds to the tyrosine kinase domain of this fusion protein competitively. Lately it was also reported that imatinib reduces the Bcr-Abl complex mediated secretion on VEGF. This thesis investigated the inhibitory effect of imatinib on VEFG secretion (79-81).

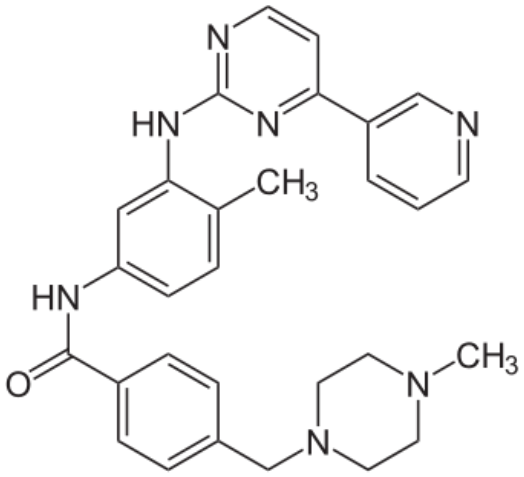

Figure 9. Imatinib (CGP57148B or STI-571). ($C_{29}H_{31}N_7O$) (Ref: http://de.wikipedia.org/ wiki/imatinib)

Currently imatinib is used for treatment of chronic myeloid leukemia (CML), malignant gastrointestinal tumors (GIST) and bone marrow (BM). Case studies reported that with most BM patients a significant improvement due to the imatinib-related effect was observed (82). Shortly after that, it was reported that the imatinib treatment reduces the VEGF expression. Hence, the improvement on BM can be explained with the anti-angiogenic property of imatinib, due to the significant correlation of BM cells and VEGF plasma levels in the patients (83). It has also been stated that the use of imatinib could induce anti-angiogenic and/or anti-vascular effects in GIST (84). It is clear that prevention of angiogenesis is essential to suppress tumor progression. Therefore imatinib is promising for the approach of anti-angiogenesis as a novel anti-cancer strategy (83, 85, 86). Like other anti-cancer pharmaceuticals, imatinib has also many serious side effects. Neutrophenia, thrombocytopenia, anemia, nausea and congestive cardiac failures are the most common side

effects of imatinib (81, 87). Therefore liposomal encapsulation is essential to reduce the side effects of anti-cancer drugs like imatinib (88).

1.7 The Chorioallantoic Membrane

For the screening of angiogenesis and anti-angiogenesis, an easy, reproducible, rapid and low cost assay was investigated by tissue engineers. For decades, in vivo assays such as rodent air sac, iris and vascular cornea as well as hamster check pouch and rabbit ear chamber have been used (89). Unfortunately these assays are relatively time consuming and expensive. When assessing alternative angiogenesis assays, the Chorioallantoic Membrane (CAM) Assay seems to be very appropriate for both angiogenesis and anti-angiogenesis studies (90). CAM is an extraembryonic membrane of the chicken egg, which mediates gas and nutrients exchange to the embryo and has a very dense capillary network. The immunocomponence of the chick is not fully developed during the embryo stage; this means the rejection system is not yet exerted (91). Besides real-time angiogenesis imaging, the CAM assay has an easy methodology, requires no sterility and is much cheaper than the other methods. Since 1976 various cell implantations such as melanoma, neuroblastoma, and carcinoma have been applied on CAM for the investigation of angiogenic responses (92-94).

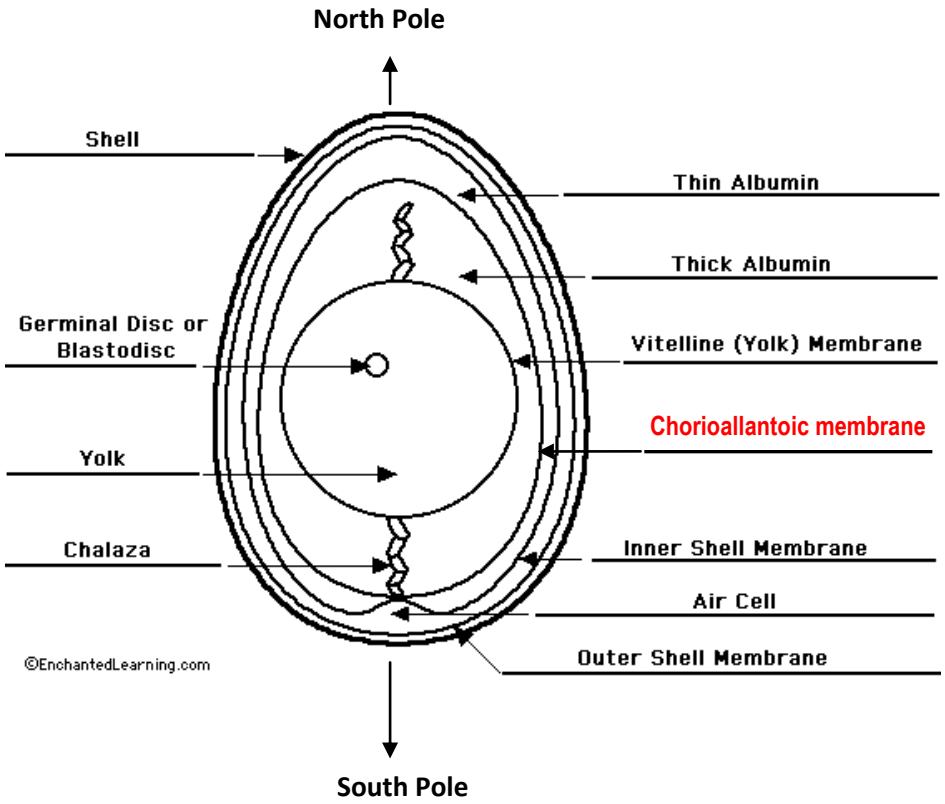

Figure 10. Chicken egg components (Ref: www.enchanedlearning.com)

It is known that solid tumors are not able to form blood vessels on their own, they need to elicit the production of these vessels from the host. The CAM assay provides a clear monitoring system that allows the observation of new vessels arising from the host and growing towards the tumor (95). The tumor can transfer this signal over a distance of up to 5 mm. If a micro vessel fails to penetrate the tumor until the 3rd day of implantation, the tumor remains pale (96). Tumor induced micro vessels are tiny and have short half-lifes. If the stimulus is turned off, they regress quickly (97). Therefore the anti-angiogenesis effect of an inhibitor can be determined very quickly on CAM. Hence in Chapter 5, the CAM model is

applied to determine the anti-angiogenic effect of a tyrosine kinase inhibitor. The effect of the inhibitor is assessed by counting the microvesses.

1.8 Objectives

The objectives of this thesis are the preparation and characterization of liposomal drug targeting and drug delivery models based on very stable tetraether lipids. Archaeal tetraether lipids are very promising to improve the stability of the current liposomal drugs in the pharmaceutical field. Thus, the initial objective of this thesis can be stated as "the investigation of stability properties of TEL liposomes under various conditions to reveal whether they meet the requirements of medical applications." It is known that conventional liposomes have several drawbacks such as low stability against high temperature, low pH values, biological media and high fusion tendency with biological barriers. Therefore extremely stabile liposomes were tailored with tetraether lipids. Tetraether lipids were isolated from archea species, which have extreme stable cell membranes stabile in low pH and high temperature mediums. The impact of the tetraether lipid in the composition of liposomes was investigated to overcome the drawbacks to provide stabile long-circulating liposomes to be used in oral and pulmonary systems.

Another objective of this thesis concerns the minimization of the damaging systemic side effect and toxic effect of drugs and provide rapid therapy with minimum dose of drug. Therefore surface modified TEL liposomes were investigated to serve as ligand-carbohydrate interaction model for site specific targeting of stabile TEL liposomes. This model simulates the interaction of lectin modified TEL liposomes with sugar residues surrounding the cells. Binding efficiency of the lectin conjugated TEL liposome was discussed. Subsequently, a protein-tyrosine kinase inhibitor „Imatinib"(Glivec®- STI 571) was entrapped into tetraether lipid to investigate the comparative efficiency of imatinib encapsulated TEL liposomes.

Thereby, the anti-angiogenesis effect of the inhibitor can be provided with less drug dose compared to free drug.

Lately it was reported that imatinib could also induce antiangiogenic and/or antivascular effect. For this purpose, imatinib encapsulated TEL liposomes were investigated on a very effective and simple angiogenesis model, known as “Chorioallantoic membrane model”. Consequently, to determine the anti-angiogenic effect of imatinib entrapped TEL liposomes the further analytic investigations were subsequently applied.

1.9 References

1. Sprott, G. D. (1992) Structures of Archaebacterial Membrane Lipids. Vol. 24 pp. 555-566, J Bioenerg Biomembr
2. Grogan, D. W. (1989) Phenotypic characterization of the archaebacterial genus Sulfolobus: comparison of five wildtype strains. Vol. 171 pp. 6710-6719, J Bacterial
3. Darland, G., Brock, T. D., Samsonoff, W., and Conti, S. F. (1970) A thermophilic, acidophilic mycoplasm isolated from a coal refuse pile. Vol. 170 pp. 1416-1418, Science
4. Shi-Lung, L., and Chang, E. L. (1990) Purification and characterization of a liposomal-forming tetraether lipid fraction. Vol. 167 pp. 238-243, Biochem Biophy Res Comm
5. Sprott, G. D., Meloche, M., and Richards, J. C. (1991) Proportions of diether, macrocyclic diether, and tetraether lipids in Methanococcus jannaschii grown at different temperatures. Vol. 173 pp. 3907-3910, J Bacteriol
6. Benvegnu, T., Lemiègre, L., and Cammas-Marion, S. (2009) New Generation of Liposomes Called Archaeosomes Based on Natural or Synthetic Archaeal Lipids as Innovative Formulations for Drug Delivery. Vol. 3 pp. 206-220, Recent Patents on Drug Delivery & Formulation
7. Patel, G. B., and Sprott, G. D. (2005) Archaeal Membrane Lipids. DOI: 10.1038/npg.els.0004316, Encyclopedia of Life Sciences-Wiley Online Library
8. Langworthy, T. A., Woese, C. R. (Ed), and Wolfe, R. S. (Ed) (1985) Lipids of archaebacteria in The Bacteria. Vol. 8 pp. 459-497, Academic Press, New York

9. Bode, M. L., Buddoo, S. R., Minnaar, S. H., and du Plessis, C. (2008) Extraction, isolation and NMR data of the tetraether lipid calditoglycerocaldarchaeol (GDNT) from Sulfolobus metallicus harvested from a bioleaching reactor. Vol. 154 pp. 94-104, Chem Phys Lip

10. Bligh, E. G., and Dyer, W. J. (1992) A rapid method for total lipid extraction and purification. Vol. 37 pp. 911-917, Can J Biochem Physiol

11. Choquet, C. G., Patel, G. B., Beveridge, T. J., and Sprott, G. D. (1994) Stability of pressure-extruded liposomes made from arhaeobacterial ether lipids. Vol. 42 pp. 375-384, Appl Microbiol Biotechnol.

12. De Rosa, M., De Rosa, S., Gambocarta, A., and Bu'Lock, J. D. (1977) Lipid Structures in the Caldariella Group of extreme Thermoacidophile Bacteria. Vol. 1977 pp. 514-515, J Chem Soc Chem Commun.

13. Bakowsky, U., Rothe, U., Antonopoulos, E., Martini, T., Henkel, L., and H-J, F. (2000) Monomolecular organization of the main tetraether lipid from *Thermoplasma acidophilum* at the water-air interface. Vol. 105 pp. 31-42, Chem Phys Lip

14. Kirby, C., Clarke, J., and Gregoriadis, G. (1980) Effect of the cholesterol content of small unilamellar liposomes on their stability *in vivo* and *in vitro*. Vol. 186 pp. 591–598., Biochem J

15. Okada, J. I., Cohen, S., and Langer, R. (1995) In *vitro* evaluation of polymerized liposomes as an oral drug delivery system. Vol. 12 pp. 576-582, Pharm Res

16. Ravily, V., Santaella, C., and Vierling, P. (1996) Membrane permeability and stability in buffer and in human serum of fluorinated di-O-alkylglycerophosphocholine-based liposomes. Vol. 1285 pp. 79-90, Biochim Biophys Acta

17. Woodley, J. F. (1984) Liposomes for oral administration of drugs. Vol. 2 pp. 2-18, CRC Crit Rev Ther Drug Carrier Syst

18. Kozumplik, V., Staffa, F., and Hoffmann, G. E. (1989) Purification of pancreatic phospholipase A_2 from human duodenal juice. Vol. 1002 pp. 395-397, Biochim Biophys Acta

19. Patel, G. B., Agnew, B. J., Deschatelets, L., Fleming, P. L., and Sprott, D. G. (2000) In vitro assessment of archaeosome stability for developing oral delivery systems. Vol. 194 pp. 39-49, Int J Pharm

20. De Rosa, M. (1996) Archaeal lipids: structural features and supramolecular organization. Vol. 284-285 pp. 13-17, Thin Solid Films

21. Diamond, J. M., and Wright, E. M. (1969) Biological Membranes: the Physical Basis of ion and Nonelectrolyte Selectivity. Vol. 31 pp. 581-646, Annu Rev Physiol

22. van de Vossenberg, J. L. C. M., Ubbink-Kok, T., Elfering, M. G. L., Driessen, A. J. M., and Konings, W. N. (1995) Ion permeability of the cytoplasmic membrane limits the macimum growth temperature of bacteria and achaea. Vol. 18(5) pp. 925-932, Mol microbiol

23. Hauser, H., Oldani, D., and Phillips, M. C. (1973) Mechanism of ion escape from phosphatidylcholine and phosphatidyl serine single bilayer vesicles. Vol. 12 pp. 4507-4517, Biochem

24. Skulachev, V. P. (1994) The latest news from the sodium world. Vol. 1187 (2) pp. 216-221, Biochim Biophys Acta -Bioenergetics

25. Freisleben, H. J., Henkel, L., Gutermann, R., Rudolph, P., John, G., Sternberg, B., Winter, S., and Ring, K. (1994) Fermentor cultivation of *Thermoplasma acidophilum* for the production of cell mass and of the main phospholipid fraction. Vol. 40 pp. 745-752, Appl Microbiol Biotechnol

26. Schäfer, G., Anemüller, *S.*, Moll, R., Meyer, W., and Lübben, M. (1990) Electron transport and energy conservation in the archaebacterium *Sulfolobus acidocaldarius*. Vol. 75 pp. 335-348, FEMS Microbiol Revs

27. De Vrij, W., Bulthuis, R. A., and Konings, W. N. (1988) Comparative study of energy-transducing properties of cytoplasmic membranes from mesophilic and thermophilic Bacillus species. Vol. 170 pp. 2359-2366, J Bacteriol

28. Patel, G. B., and Sprott, D. G. (1999) Archaeobacterial Ether Lipid Liposomes (Archaeosomes) as Novel Vassine and Drug Delivery Systems. Vol. 19(4), Crit Rev Biotechnol

29. Goupille, P., Chevalier, X., Valat, J.-P., Garaud, P., Perin, F., and Le Pape, A. (1997) Macrophage Targeting with ^{88m}Tc-Labeled J001 For Scintigraphic assessment of Experimental Osteoarthitis in the Rabbit. Vol. 36, Br J Rheumatol

30. Bangham, A. D. (1968) Membrane models with phospholipids. Vol. 18 pp. 31-95, Prog Biophys Mol Biol

31. Gregoriadis, G., Ryman, B. E. (1972) Lysosomal localization of fructofuranoside-containing liposomes injected into rats. Vol. 129 pp.123-133, Biochem J

32. Gregoriadis, G. (1991) Overview of Liposomes. Vol. 28B, J Antimicrob Chemother

33. Allen, T. M. (1997) Liposomes: Opportunities in drug delivery. Vol. 54 pp. 8-14, Drugs

34. Allen, T. M., and Moase, E. H. (1996) Therapeutic opportunities for targeted liposomal drug delivery. Vol. 21 pp. 117-133, Adv Drug Deliv Rev

35. Bajoria, R., and Contractor, S. F. (1997) Effect of surface charge of small unilamellar liposomes on uptake and transfer of carboxyfluorescein across the perfused human term placenta. Vol. 42 pp. 520-527, Pediatr Res

36. Miller, C. R., Bondurant, B., McLean, S. D., McGovern, K. A., and O'Brien, D. F. (1998) Liposome-cell interactions in vitro: Effect of liposome surface charge on the binding and endocytosis of conventional and sterically stabilized liposomes. Vol. 37 pp. 12875-12883, Biochem

37. Bakker, J., Sanders, A., and Van Rooijen, N. (1998) Effects of liposome-encapsulated drugs on macrophages: Comparative activity of the diamidine 4',6-diamidino-2-phenylindole and the phenanthridinium salts ethidium bromide and propidium iodide. Vol. 1373 pp. 93-100, Biochim Biophys Acta

38. Papisov, M. I. (1998) Theoretical considerations of RES-avoiding liposomes: Molecular mechanics and chemistry of liposome interactions. Vol. 32 pp. 119-138, Adv Drug Deliv Rev

39. Elferink, M. G. L., de Wit, J. G., Driessen, A. J. M., and Konings, W. N. (1994) Stability and proton-permeability of liposomes composed of archaeal tetraether lipids. Vol. 1193 pp. 247-254, Biochim Biophys Acta

40. Lasch, J., and Wohlrab, W. (1986) Liposome-bound cortisol: a new approach to cutaneous therapy. Vol. 45 pp. 1295-1299, Biomed Biochim Acta

41. Jain, R. K. (1987) Transport of molecules across tumor vasculature. Vol. 6, Cancer Metastasis Rev

42. Torchilin, V. P. (2000) Drug targeting. Vol. 11(2) pp. 81-91, Eur J Pharm Sci

43. Alving C, and N., W. (1992) Complement-dependent phagocytosis of liposomes: Supression by `stealth' lipids. Vol. 2 pp. 383-395, J Liposome Res

44. Bethune, C., Blum, A., Geyer, J. R., Silber, J. R., and Ho, R. J. (1999) Lipid association increases the potency against primary medulloblastoma cells and systemic exposure of 1-(2-chloroethyl)-3-cyclohexyl-1-nitrosourea (CCNU) in rats. Vol. 16 pp. 896-903, Pharm Res

45. Gabizon, A. (1995) Liposome circulation time and tumor targeting: Implications for cancer chemotherapy. Vol. 16 pp. 285-294, Adv Drug Del Rev

46. Papahadjopoulos, D., Allen, T. M., Gabizon, A., Mayhew, E., Matthay, K., Huang, S. K., Lee, K. D., Woodle, M. C., Lasic, D. D., and Redemann, C. (1991) Sterically stabilized liposomes: improvements in pharmacokinetics and antitumor therapeutic efficacy. Vol. 88 (24) pp. 11460-11464, PNAS

47. Papahadjopoulos, D., and Gabizon, A. (1987) Targeting of liposomes to tumor cells in vivo. Vol. 507 pp. 64-74, Ann N.Y Acad Sci

48. Kim, G. J. and Nie, S. (2005) Targeted cancer nanotherapy. Vol. 8-8(1) pp. 28-33, Materials Today

49. Kannagi, N. (2004) Carbohydrate-mediated cell adhesion in cancer metastasis and angiogenesis. Vol. 95(5) pp. 377-384, Cancer Sci

50. Read, B. D., Demel, R. A., Wiegandt, H., and Deenen, L. L. M. (1977) Specific interactions of Concanavalin A with glycolipid monolayers. Vol. 470 pp. 325-330 Biochem Biophys Acta

51. Goeffrey, H., McKenzie, W. H. and Sawyer, J. (1973) The binding properties of dimeric and tetrameric Concanavalin A, Binding of ligands to noninteracting macromolecular acceptors. Vol. 248(2) pp. 549-556, J Bio Chem

52. Kneuer, C., Ehrhardt, C., Radomski, M. W., and Bakowsky, U. (2006) Selectins-potential pharmacological targets? Vol. 21-22 pp. 1034-1040, Drug Dis Today

53. Gosk, S., Moos, T., Gottstein, C., and Bendas, G. (2008) VCAM-1 directed immunoliposomes selectively target tumor vasculature *in vivo*. Vol. 1778 pp. 854-863, Biochim Biophys Acta,

54. Crommelin, D. J. A., and Storm, G. (1990) Review of progress in drug targeting, in Comprehensive Medicinal Chemistry. Vol. 5 pp. 601-701, Pergamon Press

55. Cabizon, A. and Papahadjopoulos, D. (1988) Liposome formulations with prolonged circulation time in blood and enhanced uptake by tumors. pp. 856949-856953, Proc Nat1 Acad Sci USA

56. Klibanov, A. L., Maruyama, K., Torchilin, V. P., and Huang, L. (1990) Amphipathic polyethyleneglycols effectiveiy prolong the circulation time of liposomes. Vol. 53 pp. 235-237, FfBS Len

57. Kline, S., Larsen, T. A., Fieber, L., Fishbach, R., Greenwood, M., Harris, R., Kline, M. W., Tennican, P. O., and Janoff, E. N. (1995) Limited toxicity of prolonged therapy with high doses of amphotericin B lipid complex. Vol. 21 pp. 1154-1158, Clin Infect Dis

58. Amantea, M. A., Bowden, R. A., Forrest, A., Working, P. K., Newman, M. S., and Manielok, R. D. (1995) Population pharmacokinetics and renal functionsparing effects of amphotericin B colloidal dispersion in patients receiving bone marrow transplants. Vol. 39 pp. 2024-2047, Antimicrob Agent Chemother

59. Allen, T. M. (1996) Liposomal Drug Delivery. Vol. 1(5) pp. 645-651, Curr Opin Coll Int Sci

60. Klagsbrun, M., and D'Amore, P. (1991) Regulators of angiogenesis. Vol. 53 pp. 217-239, Annu Rev Physiol

61. Folkman, J. (1972) Anti-angiogenesis: new concept for therapy of solid tumors. Vol. 175 pp. 409-416, Ann Surg

62. Penn, J. S. (2008) Retinal and Choroidal Angiogenesis. Vol. 6. pp. 119–138, Springer

63. Haas, T. L., Milkiewicz, M., Davis, S. J., Zhou, A. L., Egginton, S., Brown, M. D., Madri, J. A., and Hudlicka, O. (2000) Matrix metalloproteinase activity is required for activity-induced angiogenesis in rat skeletal muscle. Vol. 279(4) pp. H1540–1547, American Journal of Physiology. Heart Circu Physiol

64. Holmgren, L., O'Reilly, M. S., and Folkman, J. (1995) Dormancy of micrometastases: balanced proliferation and apoptosis in the presence of angiogenesis suppression. Vol. 1 pp. 149-153, Nat Med

65. Moses, M. A. (1997) The regulation of neovascularization of matrix metalloproteinases and their inhibitors. Vol. 15 pp. 180-189 Stem Cells

66. Dvorak, H. F., Brown, L. F., Detmar, M., and Dvorak, A. M. (1995) Review: Vascular permeability factor/vascular endothelial growth factor, microvascular hyperpermeability and angiogenesis. Vol. 146 pp. 1029-1039, Am J Pathol

67. Kim, K. J., Li, B., Winer, J., Armanini, M., Gillett, N., Philips, H. S., and Ferrar, N., (1993) Inhibition of vascular endothelial growth factor-induces angiogenesis suppresses tumor growth in vivo. Vol. 362 pp. 841-844, Nature

68. Chizea, J. P., Dailey, V. K., Williams, E., Johnson, M. D., Pestell, R. G., and Ojeifo, J. O. (2008) Endothelial Progenitor Cells Significantly Contribute to Vasculatures in Human and Mouse Breast Tumors. Vol. 1 pp. 30-62, The Open Hematol J

69. Conn, G., Soderman., D. D., Schaeffer, M. T., Wile, M., Hatcher, V. B., and Thomas, K. A. (1990) Purification of a glycoprotein vascular endothelial cell mitogen from a rat glioma-derived cell line. Vol. 87 pp. 1323-1327, Proc Natl Acad Sci USA

70. Houck, K. A., Leung, D. W., Rowland, A. M., Winer, J., and Ferrara, N. (1992) Dual regulation of vascular endothelial growth factor availability by genetic and proteolytic mechanisms. Vol. 267 pp. 26031–26037, J Biol Chem

71. Klement, G., Baruchel, S., Rak, J., Man, S., Clark, K., Hickli, D. J., Bohlen, P., and Kerbel, R. S. (2000) Chronically sustained regressions of human tumor xenografts in the absence of overt toxicity by continuous low-dose vinblastine and anti-VEGF Receptor-2 antibody therapy. Vol. 105 pp. R15-24, J Clin Invest

72. Browder, T., Butterfield, C. E., Kraling, B. M., Marshall, B., O'Reilly, M. S., and Folkman, J. (2000) Antiangiogenic scheduling of chemotherapy improves efficacy against experimental drug-resistant cancer. Vol. 60 pp. 1878-1886, Cancer Res

73. Lugo, T. G., Pendergast, A. M., Muller, A. J., and Witte, O. N. (1990) Tyrosine kinase activity and transformation potency of bcr-abl oncogene products. Vol. 247 pp. 1079-1082, Science

74. Buchdunger, E., O'Reilly, T., and J., W. (2002) Pharmacology of Imatinib (STI571). Vol. 38(5) pp. 28-36, Eur J Cancer

75. Jones, R. L., and Judson, I. R. (2005) The development and application of imatinib. Vol. 4(2) pp. 183-191, Expert Opin Drug Saf

76. Buchdunger, E., Cioffi, C. L., Law, N., Stover, D., Ohno-Jones, S., Druker, B. J., and N.B., L. (2000) Abl protein-tyrosine kinase inhibitor STI571 inhibits in vitro signal transduction mediated by c-Kit and platelet-derived growth factor receptors. Vol. 295 pp. 139-145, J Pharmacol Exper Ther

77. Joensuu, H., Roberts, P. J., Sarlomo-Rikala, M., Andersson, L. C., Tervahartiala, P., Tuveson, D., Silberman, S., Capdeville, R., Dimitrijevic, S., Druker, *B.*, and Demetri, G. D. (2001) Effect of the tyrosine kinase inhibitor STI571 in a patient with a metastatic gastrointestinal stromal tumor. Vol. 344 pp. 1052-1056, N Engl J Med

78. Sjöblom, T., Shimizu, A., O'Brien, K. P., Pietras, K., Dal Cin, P., Buchdunger, E., Dumanski, J. P., Ostman, A., and Heldin, C. H. (2001) Growth inhibition of dermatofibrosarcoma protuberans tumors by the platelet-derived growth factor receptor antagonist STI571 through induction of apoptosis. Vol. 61 pp. 5778-5783, Cancer Res

79. Ebos, M. L., Tran, J., Master, Z., Dumont., D., Melo, J. V., Buchdunger, E., and Kerbel, R. S. (2002) Imatinib mesylate (STI571) reduces Bcr-Abl-mediated vascular

endothelial growth factor secretion in chronic myelogenous leukemia. Vol. 1 pp. 89-95, Mol Cancer Res

80. Scheinfeld, N., (2006) A comprehensive review of imatinib mesylate (Gleevec) for dermatological diseases. Vol. 5(2) pp. 117-122, J Drugs Dermatol

81. Kerkelä, R., Grazette, L., Yacobi, R., Iliescu, C., Patten, R., Beahm, C., Walters, B., Shevtsov, S., Pesant, S., Clubb, F. J., Rosenzweig, A., Salomon, R. N., Van Etten, R. A., Alroy, J., Durand, J. B., and Force, T. (2006) Cardiotoxicity of the cancer therapeutic agent imatinib mesylate. Vol. 12(8) pp. 908-916, Nat Med

82. Thiele, J., Kvasnicka, H. M., Schmitt-Graeff, A., Bundschuh, S., Biermann, T., Roessler, G., Wasmus, M., Diehl, V., Zankovich, R., and Schaefer, H. E. (2000) Effects of chemotherapy (busulfan-hyroxyurea) and interferon-alfa on bone marrow morphologic features in chronic myelogenous leukemia: histochemical and morphometric study on sequential trephine biopsy specimens with special emphasis on dynamic features. Vol. 114 pp. 57-65, J Clin Pathol

83. Kvasnicka, H. M., Thiele, J., Staib, P., Schmitt-Graeff, A., Griesshammer, M., Klose, J., Engels, K., and Kriener, S. (2004) Reversal of bone marrow angiogenesis in chronic myeloid leukemia following imatinib mesylate (STI571) therapy. Vol. 103 (9) pp. 3549-3551, Blood

84. De Giorgi, U., Aliberti, C., Benea, G., Conti, M., and Marangolo, M. (2005) Effect of Angiosonography to Monitor Response During Imatinib Treatment in Patients with Metastatic Gastrointestinal Stromal Tumors. Vol. 11 (6171) pp. 158-162, Clin Cancer Res

85. Rocha, A., Azevedo, I., and Soares, R. (2007) Anti-angiogenic effects of imatinib target smooth muscle cells but not endothelial cells. Vol. 10 pp. 279-286, Angiogenesis

86. Folkman, J. (1971) Tumor angiogenesis: therapeutic implications. Vol. 285 pp. 1182-1186, N. Engl J Med

87. Tefferi, A., Mesa, R. A., Gray, L. A., Steensma, D. P., Camoriano, J. K., Elliott, M. A., Pardanani, A., Ansell, S. M., Call, T. G., Colon-Otero, G., Schroeder, G., Hanson, C. A., Dewald, G. W., and Kaufmann, S. H. (2002) Phase 2 trial of imatinib mesylate in myelofibrosis with myeloid metaplasia. Vol. 99(10) pp. 3854-3856, Blood

88. Harata, M., Soda, Y., Tani, K., Ooi, J., Takizawa, T., Chen, M., Bai, Y., Izawa, K., Kobayashi, S., Tomonari, A., Nagamura, F., Takahashi, S., Uchimaru, K., Iseki, T., Tsuji, T., Takahashi, T. A., Sugita, K., Nakazawa, S., Tojo, A., Maruyama, K., and Asano, S. (2004) CD19-targeting liposomes containing imatinib efficiently kill Philadelphia chromosome–positive acute lymphoblastic leukemia cells. Vol. 104 (5) pp. 1442-1449, Blood

89. Ribatti, D., and Vacca, A. (1999) Models for studying angiogenesis in vivo. Vol. 14 pp. 207–213, Int J Biol Markers

90. Ribatti, D. (2009) Chick embryo chorioallantoic membrane as a useful tool to study angiogenesis. Vol. 270 pp. 181-224, Int Rev Cell Mol Biol

91. Leene, W., Duyzings, M. J. M., and Von Steeg, C. (1973) Lymphoid stem cell identification in the developing thymus and bursa of Fabricius of the chick. Vol. 136 pp. 521–533, Z Zellforsch

92. Takigawa, M., Enomoto, M., Nishida, Y., Pan, H. O., Kinishita, A., and Suzuki, F. (1990) Tumor angiogenesis and polyamines, α-difluoromethylornithine, an irreversible inhibitor of ornithine decaboxylase, inhibit B16 melanoma-induced angiogenesis in ovo and the proliferation of vascular endothelial cells in vitro. Vol. 50 pp. 4131-4138, Cancer Res

93. Klasbrun, M., D., K., and Folkman, J. (1976) Tumor angiogenesis activity in cell grown in tissue culture. Vol. 36 pp. 110-114, Cancer Res

94. Ribatti, D., Raffaghello, L., Pastorino, F., Nico, B., Vacca, A., and Dammacco, F. (2001) Mast cells and their secretory granules are angiogenic in the chick embryo chorioallantoic membrane. Vol. 31 pp. 6002-6008, Clin Exp Allergy

95. Cavallo, T., Sade, R., Folkman, J., and Cotran, R. S. (1972) Tumor Angiogenesis: Rapid Induction of Endothelial Mitoses Demonstrated by Autoradiography. Vol. 54 pp. 408-420, J Cell Biol

96. Merwin, R. M., and Algire, G. H. (1956) The Role of Graft and Host Vessels in the Vascularization of Grafts of Normal and Neoplastic Tissue. Vol. 17 pp. 23-33, J Nat Cancer Inst

97. Folkman, J. (1974) Tumor angiogenesis Factor. Vol. 34 pp. 2109-2113, Cancer Res

2 Archaebacterial Tetraetherlipid Liposomes

Published in Springer Protocols “Liposomes : Methods and Protocols”,

Volume 1: Pharmaceutical Nanocarriers

Series: Methods in Molecular Biology

Volume No.: 605

DOI: 10.1007/978-1-60327-360-2_1

2.1 Abstract

Liposomes are widely investigated for their applicability as drug delivery systems. However, the unstable liposomal constitution is one of the greatest limitations, because the liposomes undergo fast elimination after application to the human body. In the presented study, novel archeal lipids were used to prepare liposomal formulations which were tested for their stability at elevated temperatures, at different pH-values and after heat sterilization.

Key words: AFM, GDNT, Tetraether lipids, Liposome, Sulfolobus acidocaldarius, Archae

2.2 Introduction

Liposomes are bilayered spherical membrane structures which are promising for pharmaceutical and diagnostic use (1). However, there are limitations of the usage of liposomes which is mainly caused by their low stability (2). To reduce this problem, in this study an archael lipid, Glycerol Dialkyl Nonitol Tetraether lipid (GDNT) (see Fig. 1) is chosen to prepare highly stable liposomes. The GDNT is isolated from *Sulfolobus acidocaldarius* (3). Archaea are one of the three major domains of life (4). The major difference of these archaea from bacterial and eukaryotic cells is their membrane lipids (5). Archaea do not have any cell wall nevertheless the properties of the cell membrane lipid provide a remarkable long-term stability (6). The archaea are divided into phenotypes of methanogens, halophiles and thermophiles. The lipid used in this study is from a type of thermophilic archaea. *Sulfolobus acidocaldarius* is a well studied extremely thermophilic archae with the optimal growth conditions of 70–80° C and pH 3 (7, 8). These archael membrane lipids consist of monopolar ether head groups and saturated, branched phytanyl chains which are mainly attached to the glycerol backbone carbons through ether bonds. This chemical structure provides high stability due to low oxidation capacity and hydrolytic resistance (9). Liposomes can incorporate hydrophilic and lipophilic drugs and reduce the overall dose and amount of side effects by specific targeting. Also, the relatively stable structure of GDNT liposome offers new range of applications. Liposomal formulations made of GDNT are able to protect the pharmaceuticals from biochemical degradation or metabolism. Therefore, they are interesting for oral applications. Kimura reviewed that a significant quantity of drug entrapped into liposomes can be absorbed by the small-intestinal mucosa (10). However, for oral drug delivery, there are still some questions concerning the

stability of liposomes in the acidic milieu of the gastrointestinal tract and their absorption therein (11). Pulmonary drug delivery is also applicable using liposomes, because they are absorbed through the thin layer of alveolar epithelial cells (vast surface for an adult is 43–102 m^2) (12–14) and transported into the systemic circulation (15–17). However, the inhaled objects can be eliminated by macrophages from the alveoli surface when they are bigger than 260 nm (18). For the future aspects of tetraetherlipid liposomes, there are still some details to be clarified. This article is concerned with the stability of GDNT liposomes which certainly plays a fundamental role in liposomal delivery.

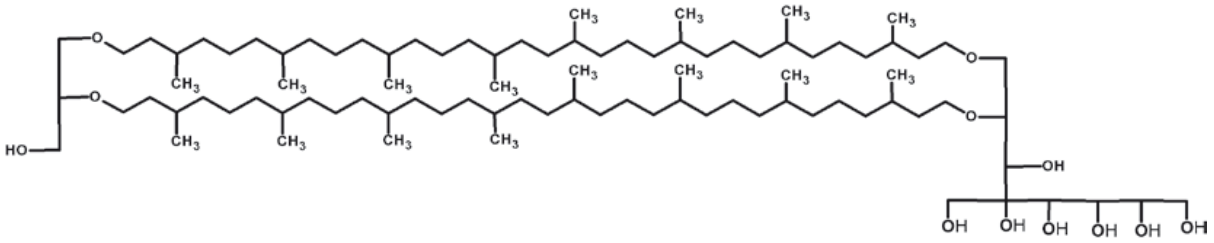

Figure 1. *GDNT* Glycerol Dialkyl Nonitol Tetraetherlipid. (Ref: Lo, S.-L. Montague, C. E., Chang, E. L. (1989) Purfication of glycerol dialkyl nonitol tetraether from *Sulfolobus acidocaldarius*, Vol:30 J Lip Res)

2.3 Materials

2.3.1 Extraction and Hydrolysis of the Tetraether Lipids

1. 25 g Freeze-dried biomass from *Sulfolobus acidocaldarius* (BHP Billiton, Global Technology, Perth Technology Centre, Australia), store at –20° C.

2. Chloroform ($CHCl_3$): methanol (MeOH) : 5 % trichloroacetic acid (TCA) mixture (1:2:1 v/v). Store at RT.

3. MeOH:H_2O mixture (1:1 v/v). Store at RT.

4. 100 ml 1 M methanolic hydrochloric acid. Store at RT.

5. 8 M KOH is prepared to adjust the pH level to pH 14 and to adjust the pH level to pH 3 32 % HCl is prepared. Store at RT.

2.3.2 Separation of the GDNT

1. A chromatography column with a diameter of 4 cm (conventional glass) is filled with 300 g silica gel 60 (Merck, Germany) for separation of lipid fractions.

2. The eluents used are $CHCl_3$ followed by $CHCl_3$:diethyl ether (8:2 v/v) and $CHCl_3$: MeOH (8:2 v/v), according to Lo et al. (19).

3. $CHCl_3$: MeOH, (9:1 v:v) is prepared for thin layer chromatography.

2.3.3 Liposome Formulations

1. Phospholipon 90 G (Lipoid, Germany) is dissolved in $CHCl_3$:MeOH (3:1 v/v) to achieve a final concentration of 10 mg/ml solution.

2. For hydrolysis, ultrapure, bidistilled water (pH 5.5) is used.

3. Nylon syringe filters with the pore size of 0.45 μm are supplied from Rotilabo Roth (Carl Roth Karlsruhe Germany).

4. The Extruder is supplied from Avestin Europa GmbH with polycarbonate membranes of 19 mm diameter and 100 nm pore diameter.

2.3.4 Stability Tests of Liposomes

1. For the pH stability studies pH 2.0 solution (50 ml 0.2 M KCl is adjusted with 0.1 M HCl), pH 4.0 solution, (100 ml 0.1 M potassium hydrogen phthalate is adjusted with 0.1 M HCl) pH 7.4 buffer (129 mM NaCl, 2.5 mM KCl, 7.4 mM Na_2HPO_4, 1.3 mM KH_2PO_4) and pH 9.0 (100 ml 0.025 M NaB_4O_7, 9.2 ml 0.1 M HCl) are prepared.

2.3.5 Atomic Force Microscopy

1. As substrate for the sample preparation, silicon wafers from Wacker Chemie AG (Munich, Germany) with a natural silicon oxide layer (thickness 3.8 nm) and a surface roughness of 0.3 nm is used. The wafers are split into small pieces of about 1 × 1 cm. The pieces are cleaned in a bath sonicator for 20 min in $CHCl_3$:MeOH (2:1, v:v), then they are dried in a air stream and stored in a dust free atmosphere.

2. NSC 16/Cr-Au cantilevers from Anfatec Instruments AG (Oelsnitz, Germany) with a nominal force constant of 45 N/m, resonant frequency of 170 kHz and a length of 230 μm are used. The sharpness of the tip is less than 10 nm.

2.4 Methods

2.4.1 Extraction and Hydrolysis of the GDNT Lipids

1. Different methods for the extraction and purification of the GDNT are established. We used the combined extraction and hydrolysis method according to Bode et al. (20)

2. 25 g freeze-dried biomass from Sulfolobus acidocaldarius grown at 68° C, is transferred into a 1 l flask and into this flask 400 ml of a $CHCl_3$:MeOH:TCA mixture is added.

3. The mixture is heated to a gentle reflux temperature of 60° C for 2 h.

4. After cooling down to room temperature, the mixture is filtered. The filter cake is transferred back to the flask and kept at 60° C in the same solvent mixture as before. This procedure is continued for three more cycles.

5. The collected extractions (upper green layer of precipitate and a clear brown colored solution) are washed with a mixture of MeOH:H_2O (1:1, 800 ml).

6. From the combined chloroform extracts, the solvent is evaporated in vacuum at elevated temperatures.

7. 100 ml 1 M methanolic HCl is added to the residue and this is heated at 80° C for 16 h.

8. Then the reaction mixture is cooled down to room temperature and 100 ml water is added. The pH of the resultant mixture is adjusted to 14 using 8 M KOH.

9. The mixture is subjected to base hydrolysis at 80° C for 1 h, and cooled down to room temperature. Subsequent to this, the mixture is adjusted to pH 3 with 32 % HCl.

10. The resultant mixture is extracted with $CHCl_3$ (3 × 200 ml). The chloroform extract is separated, dried with magnesium sulfate and solvent evaporation under vacuum to yield a brown lipid residue.

2.4.2 Separation of the GDNT

1. The separation of 8 g of the hydrolysed lipid fraction from the total lipid extraction is done via silica gel 60 column chromatography.

2. The samples are collected (50 ml fractions) and their lipid composition is analyzed by thin layer chromatography. The lipids are stained by the use of methanolic sulfuric acid followed by an ashing process. The lipid is visible as dark spots. GDNT shows a *R*f value of 0.45 ($CHCl_3$: MeOH, 9:1, v:v) in accordance to literature (0.45 (19) and 0.35 (20)).

3. The fractions containing GDNT are collected and the solvents are evaporated at elevated temperature. The purified lipid is stored at –20° C before use.

2.4.3 Preparation of Liposomes

1. Preparation of liposomes conducted with different molar ratios of GDNT and Phospholipon. As a stock solution, Phospholipon is dissolved in chloform:methanol (2:1, v/v) and 10 mg/ml solution is prepared.

2. Different liposome compositions are prepared (see Fig. 2)

3. The liposome preparation procedure is based on film formation and hydration. After transferring the mixture of Phospholipon and GDNT solutions into 10 ml round bottom flasks, the chloroform-methanol solution is removed by evaporation at 300 mbar and 45° C to obtain a lipid film.

4. For hydration, bidistilled water is used to prepare the liposomes in the concentration of 10 mg/ml. To form the lipid vesicles, a bath sonicator at 45° C is used. After obtaining a dispersion of the lipid in water, sonication is continued with a probe type sonicator to increase the energy input. For the following processes, the sample is transferred into a 50 ml plastic tube.

5. Sonication is continued for 8 min (30 s sonication followed by 30 s rest). The power was set to level 6. (see Notes 1 and 2). If a clear dispersion is not achieved, the sonication can be continued.

6. After sonication the samples are filtered by syringe filters with the pore size of 0.45 μm to separate large vesicles that may blockade the extruder membrane (see Note 3).

7. For the preparation of ~100 nm liposomes, the formulations are extruded through a 0.1 μm polycarbonate membrane. Preheating of the extruder above the main phase transition of the lipid mixture (40° C) is essential to provide an effective liposome extrusion (see Note 4). The extrusion is conducted 21 times to each sample. The achieved liposomes have a diameter of 100–150 nm. If the initial size measurements verify larger diameters, the extrusion can be repeated 11 times more.

8. All the size measurements in this study are performed on a Zeta Sizer (Malvern instruments GmbH, Germany). The diluted liposomal formulations (10:60, v:v, bidistilled water) are measured in a micro cuvette (Malvern instruments GmbH, Germany).

9. Zeta potential measurements are also performed on the Zeta Sizer. All samples are diluted 1:10 (v:v) with water. A folded electrophoresis cell is used (Malvern instruments GmbH, Germany) for Laser Doppler Anemometry (LDA) measurements.

10. The cuvette or electrophoresis cell is placed in the Zeta Sizer and allowed to equilibrate to the pre-set temperature (25° C).

11. The manufacturer's software automatically adjusts the Laser attenuation and measurement position. For each size and zeta potential determination, 3 measurements consisting of 6 sub runs with duration of 10 s are averaged.

12. In Fig. 2, the initial diameter and zeta potential values of liposome formulations are presented.

2.5 Stability Testing

2.5.1 ThermostabilityTesting

1. After measuring the initial diameters and the zeta potentials of liposomes, from each composition, 100 μl aliquots are mixed with 600 μl bidistilled water, in a glass tube.

2. The samples are transferred into a metal tube holder and incubated at 36° C, 60° C, and 100° C for 4 h in a cabinet heater.

3. After incubation, when the samples are at room temperature, the diameter values are determined with Zeta Sizer.

4. The results of thermostability tests are presented in Fig. 2.

2.5.2 Stability During Autoclavation

1. The autoclavation is performed on a standard autoclave 3850 ELC (Systec GmbH, Germany).

2. Due to the properties of high thermostability the autoclavation of liposomes were considered to be applicable, which brings large sterilization possibilities along with.

3. Before autoclavation, the liposome samples were diluted with bidestilled water in the ratio of 10:60 which is the same dilution value to be used in zeta-size measurements.

4. The samples were loaded into the autoclave and treated with a standard autoclave procedure for solutions (15 min at 121° C, 29 psi pressure, saturated steam).

5. The size measurements in Fig. 2. It could be shown that the liposomal formulations containing GDNT can be autoclaved. The diameter is relatively constant.

2.5.3 pH Stability

As a first test for the stability of the formulations in the gastrointestinal tract, liposomes are incubated in solutions of different pH-values mimicking the gastrointestinal environment.

1. pH stability tests are performed by incubating the liposomes in different solutions. From each liposomal formulation, 100 µl aliquots are incubated in 600 µl of pH 2.0, pH 4.0, pH 7.4, pH 9.0 buffer solutions.

2. The initial diameters and zeta potentials are measured with a Zeta Sizer (Malvern Instruments, Germany, HeNe Laser 633 nm, 173° C scattering angle, 25° C) right after mixing the liposomes with buffer solutions.

3. After 4 days of incubation, hydrodynamic diameters are determined as it is explained in Chap. 2.4.3.

4. With the size measurements, the effect of GDNT stabilizing effect is shown. The results are presented in Fig. 2. With the increase of GDNT molar ratio, the liposome size is much more stable compared to the low molar content of GDNT.

Formulation (molar ratio)	Mean Diameter [nm] (PDI)	Zeta-Potential
1:9 GDNT:Phospholipon	96.6 (0.197)	-14.6±0.285
5:5 GDNT: Phospholipon	88.2 (0.224)	-11.2±0.127
9:1 GDNT: Phospholipon	69.0 (0.223)	-5.28±0.079
10:0 GDNT:Phospholipon	137.5 (0.295)	-15.3±0.60

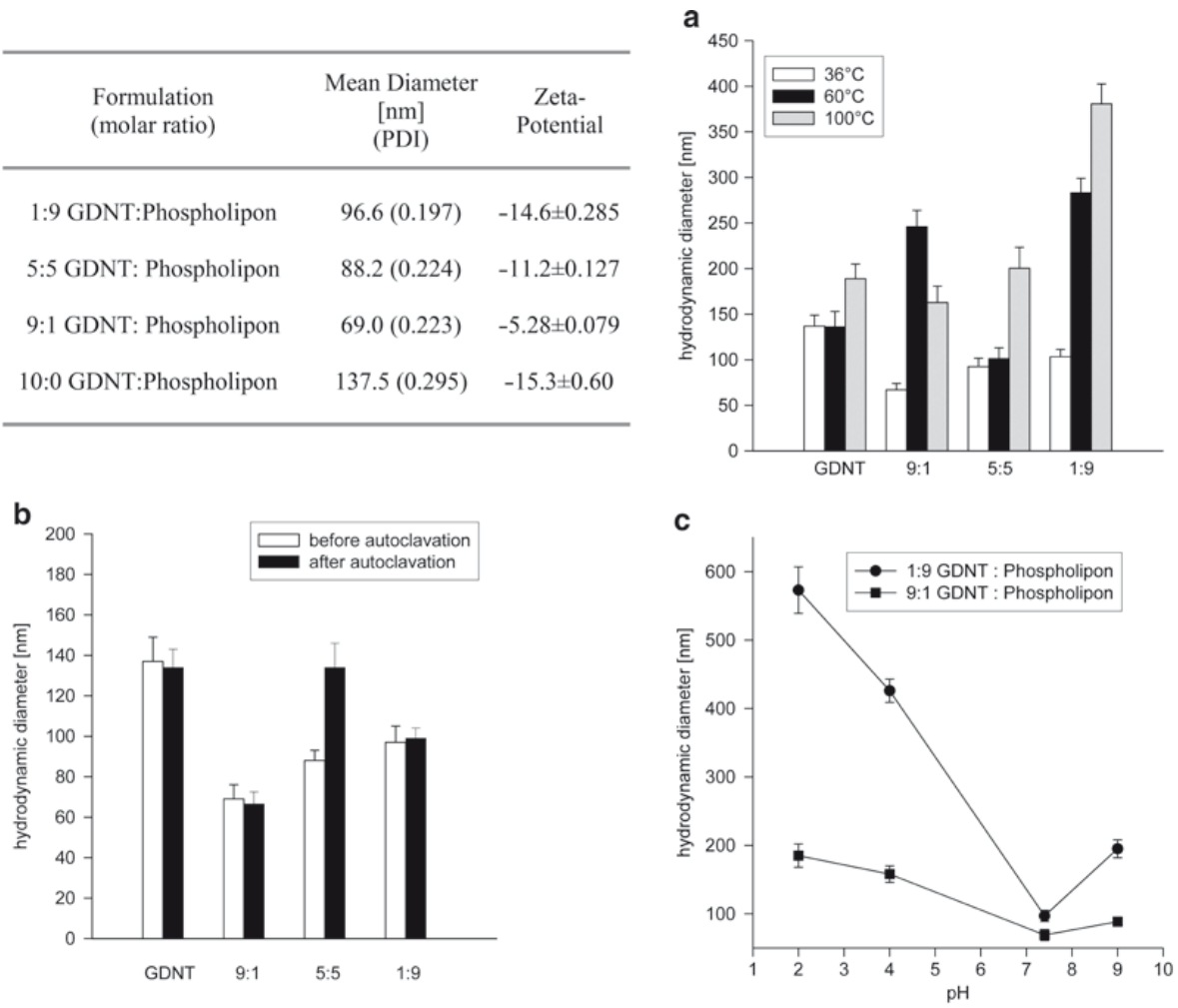

Figure 2. Different liposomal formulations containing the tetraether lipid GDNT are characterized regarding their stability. The initial diameter ranged from 69 nm for the mixture 9:1 GDNT:Phospholipon to 137.5 nm for the pure GDNT. The negative zeta potential is representative for all liposomal formulations. (a) The stability according to the liposomal size of the liposomes iss tested at different temperatures. The measurements are done after incubating 40 µl liposome solutions in 240 µl bidestilled water for 4 h. The results show the stabilizing effect of GDNT content in the liposome structure. (b) The diagram represents the stability of particles after autoclavation. The samples are incubated 15 min at 121° C and 29 psi for sterilization. (c) Both of the samples are investigated after incubating 4 days in

different pH solutions. Standard deviations are calculated from three independent measurements.

2.6 Atomic Force Microscopy

1. Atomic force microscopy (AFM) is performed on a Digital Nanoscope IV Bioscope (Veeco Instruments, Santa Barbara, CA). The AFM is vibration and acoustically damped (21). All measurements are performed in tapping mode. The applied force to the sample surface is adjusted to a minimum to avoid the damage of the sample. The sample is investigated and scanned under constant force. The scan speed is proportional to the scan size and the scan frequency is between 0.5 and 1.5 Hz. Images are obtained by displaying the amplitude signal of the cantilever in the trace direction, and the height signal in the retrace direction, both signals being simultaneously recorded. The results are visualized either in height (the real height of the sample in a resolution on 0.3 nm) or in amplitude mode (the damping of the frequency signal).

2. Various methods are available for sample preparation. A very convenient procedure for the preparation of liposomes is the self-assembly technique (22). Small pieces of silicon wafers (about 1 × 1 cm) as substrate material are placed into the sample dispersion for 20 min at room temperature and the liposomes are allowed to adsorb to the surface under equilibrium conditions. The silicon substrates are removed from the dispersions. The samples are dried at room temperature and investigated within 2 h.

3. The liposomes containing GDNT are stable against the substrate surface, while conventional liposomes tend to spread to the surface and form a supported lipid bilayer as shown in Fig. 3.

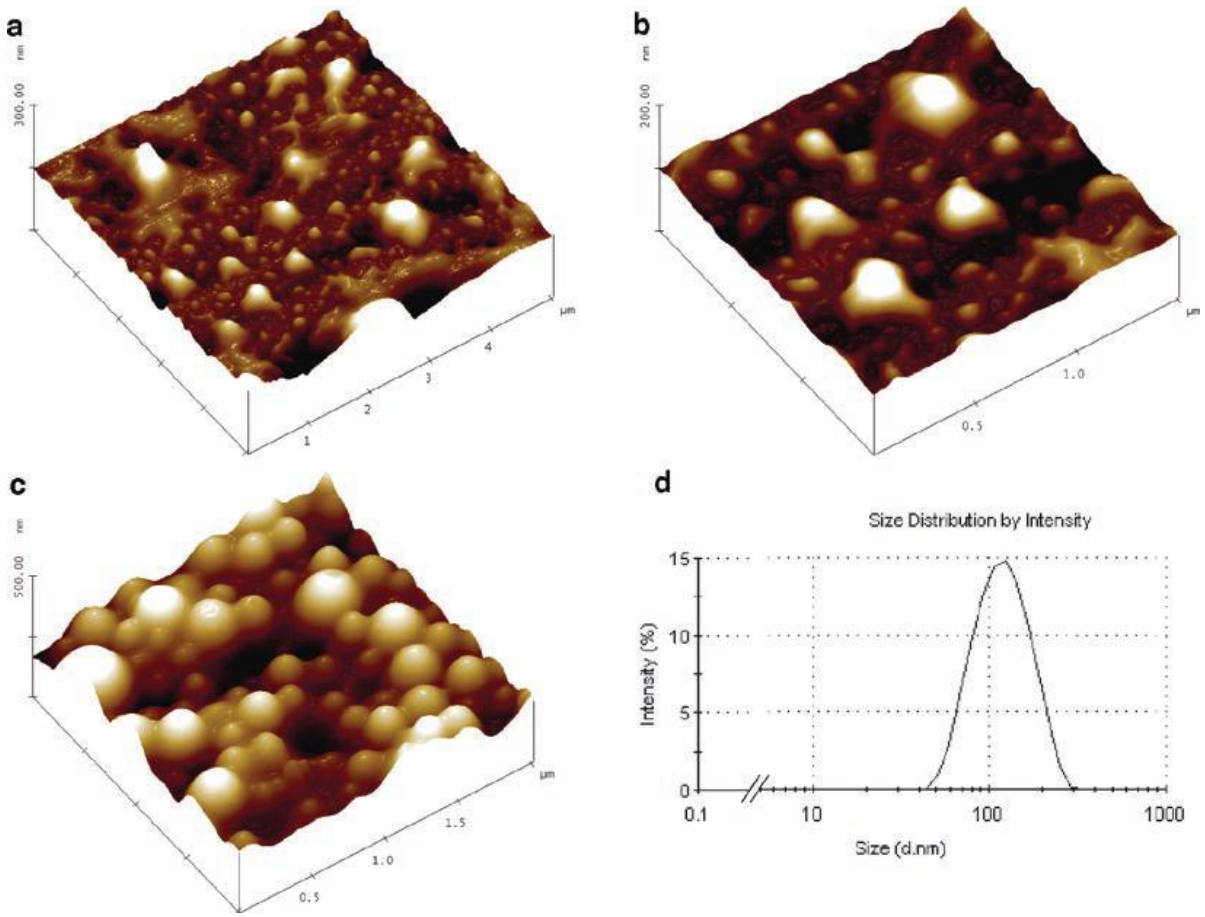

Figure 3. Visualization of the liposome morphology and size distribution determined with AFM and Zeta Sizer. (a, b) Pure phospholipon liposomes adhered on silicon wafer as substrate. The liposomes have diameters between 80 and 250 nm with an average diameter of 178 ± 12 nm. The liposomes tend to spread to the surface, because of the low membrane stability. (c) Pure GDNT liposomes with an average diameter of 137 ± 8 nm (PDI 0.295 ± 0.017) and a zeta potential of –15.3 ± 0.60 mV. The liposomes are stable and show a spherically, round shape. (d) Size distribution of the pure GDNT liposomes measured with Zeta Sizer.

2.7 Notes

1. The container should be small enough so that the sonicator probe can immerse deeply (1–2 cm) in the sample but large enough so that the probe does not touch the sides or bottom of the container. 50 ml plastic tubes with round bottoms are used.

2. Probe type sonication heats the solution very quickly; to avoid damage of lipids and liposomes, an ice bath in a beaker is prepared and placed securely on a ring stand in the sound proof box of the sonicator.

3. For the filtration of liposome solutions the whole sample is transferred through the filter into plastic tubes.

4. When working with an extruder, it is important to assure that the retainer nuts are tight to avoid the leaking of the liposome solutions.

2.8 References

1. Torchilin, V. P. (2005) Recent advances with liposomes as pharmaceutical carriers. Vol.4 pp.145–160, Nat Rev Drug Discov
2. Sharma, A., and Sharma, U. S. (1997) Liposomes in drug delivery: progress and limitations. Vol. 154 pp.123–140, Int J Pharm
3. Brock, T., Brock, K., Belly, R., and Weiss, R. (1972) Sulfolobus: a new genus of sulfur-oxidizing bacteria living at low pH and high temperature. Vol. 84 pp. 54–68, Arch Microbiol
4. Woese, C. R., Kandler, O., and Wheelis, L. L. (1990) Towards a natural system of organisms: proposal for the domains archaea, bacteria and eucarya. Vol. 87 pp. 4576–4579, Proc Natl Acad Sci
5. De Rosa, M., and Gambacorta, A. (1988) The lipids of archaebacteria. Vol. 27 pp. 153, Prog Lipid Res
6. Gambacorta, A., Gliozzi, A., and De Rosa, M. (1995) Archaeal lipids and their biotechnological application. Vol. 11 pp. 115–131, World J Microbiol Biotechnol
7. Brock, T. D., Brock, K. M., Belly, R. T., and Weiss, R. L. (1972) *Sulfolobus*: A new genus of sulfur-oxidizing bacteria living at low pH and high temperature. Vol. 84 pp. 54–68, Arch Microbiol
8. Grogan, D. W. (1989) Phenotypic characterization of the archeabacterial genus *Sulfolobus*: comparison of five wild-type strains. Vol. 171 pp. 6710–6719, J Bacteriol
9. Kates, M. (1978) The phytanyl ether-linked polar lipids and isoprenoid neutral lipids of extremely halophilic bacteria. Vol. 15 pp. 301–342, Prog Chem Fats Other Lipids

10. Kimura, T., and Gregoriadis, G. (ed) (1988) Transmucosal passage to liposomal drugs. Liposomes as drug carriers. pp. 635–647, Wiley, Chichester

11. Gilligan, C. A., and Li Wan Po, A. (1991) Oral vaccines: design and delivery. Vol. 75 pp. 1–24, Int J Pharma

12. Weibel, E. R. (1973) Morphological basis of alveolar–capillary gas exchange.Vol. 53 pp. 419–495, Physiol Rev

13. Gehr, P., Bachofen, M., and Weibel, E. R. (1978) The normal human lung: ultrastructure and morphometric estimation of diffusion capacity. Vol. 32pp. 121–140, Respir Physiol

14. Stone, K. C., Mercer, P. R., and Gehr, P. (1992) Allometric relationships of cell numbers and size in the mammalian lung. Vol. 6 pp. 235–243, Am J Respir Cell Mol Biol

15. Kellaway, I. W., and Farr, S. J. (1990) Liposomes as drug delivery systems to the lung. Vol. 5 pp. 149–161, Adv Drug Del Rev

16. Patton, J. S., Fishburn, C. S., and Weers, J. G. (2004) The lung as a portal of entry for systemic drug delivery. Vol. 1 pp. 338–344, Proc Am Thorac Soc

17. Patton, J. S., and Byron, P. R. (2007) Inhaling medicines delivering drugs to the body through the lungs. Vol. 6 pp. 67–74, Nat Rev Drug Discov

18. Niven, R. W. (1995) Delivery of biotherapeutics by inhalation aerosol. Vol. 12 pp. 151–231, Crit Rev Ther Drug Carrier Syst

19. Lo, S. L., Montague, C. E., and Chang, E. L. (1989) Purification of glycerol dialkyl nonitol tetraether from Sulfolobus acidocaldarius. Vol. 6 pp. 944–949, J Lipid Res

20. Bode, M. L., Buddoo, S. R., Minnaar, S. H., and du Plessis, C. A. (2008) Extraction, isolation and NMR data of the tetraether lipid calditoglycerocaldarchaeol (GDNT)

from Sulfolobus metallicus harvested from a bioleaching reactor. Vol. 154(2) pp. 94–104, Chem Phys Lipids

21. Oberle, V., Bakowsky, U., Zuhorn, I. S., and Hoekstra, D. (2000) Lipoplex formation under equilibrium conditions reveals a three-step mechanism. Vol. 79 pp. 1447–1454, Biophys J

22. Kneuer, C., Ehrhardt, C., Radomski, M. W., and Bakowsky, U. (2006) Selectins-potential pharmacological targets? Vol. 11 (21–22) pp. 1034–1040, Drug Discov Today

3 New Highly Stable Liposomal Formulations Based On Tetraetherlipids From The Archaeon *Thermoplasma Acidophilum*

3.1 Abstract

Background: Liposomes prepared with tetraether lipids (TEL) are considered to be more stable than conventional liposomes. In this study, the stability of tetraether lipid liposomes from *Thermoplasma acidophilum* was investigated under conditions simulating the pulmonary system and gastrointestinal tract. A number of molar ratio formulations of TEL:Phospholipon 100H (Ph) were compared in each condition.

Materials and Methods: The liposomes were exposed to various temperature and pH conditions. The effect of these conditions on the stability of liposomes was investigated by zeta size, zeta potential and morphological assessments. The effect of autoclaving on liposome stability was observed. Moreover, 5(6)-Carboxyfluorescein (CF) release was measured after the incubation in Fetal Calf Serum (FCS) and Alveolar Surfactant medium.

Results: According to the analysis of different TEL:Ph liposome formulations, it was indicated that TELs endow improved physical properties. The contribution of TELs to liposome properties was shown to have a significant impact on stability against low pH and sterilization by autoclavation. The stability of 10:0 molar ratio Tetraether:Phospholipon 100H (TEL:Ph) liposomes was confirmed with AFM before and after FCS incubation according to their size and morphology.

Conclusion: It could be concluded that the contribution of TEL with increasing molar ratio in the TEL:Ph liposome formulations resulted in increasing structural stability under high temperature, low pH, autoclave and lung surfactant conditions.

Keywords: Tetraether lipid liposomes, Stability, Pulmonary Drug Delivery, Oral Drug Delivery

3.2 Introduction

Liposomes are spherical lipid membranes consisting of one or more lipid layers. These lipid layers have hydrophilic and hydrophobic compartments (1). Conventional liposomes have an attractive potential for constructing tailor-made vehicles because of their enormous versatility in particle size and other physical parameters. Biocompatible properties allow them to be used as delivery systems for drugs, proteins, plasmid DNAs, antisense oligonucleotides or ribosomes, as well as for biochemical, pharmaceutical and cosmetic purposes. Besides the non-pathogenic and non-immunogenic features, their production is of relatively low cost; therefore they are appropriate for drug delivery on medical applications such as parenteral, transdermal, and pulmonary application.

However, some drawbacks are observed especially in case of liposomes composed of distearoylphosphatidylcholine or dipalmitoylphosphatidylcholine, phosphatidylserine and cholesterol. These drawbacks are (i) low stability at low pH values, (ii) low stability against biological media (such as FCS or surfactant), (iii) high fusion tendency with biological barriers and (iv) their rapid clearance by the reticulo-endothelial system (RES) or fast metabolism (2).

It is known that archaeal liposomes which include saturated bipolar tetraether lipids are more stable than liposomes formed of bacterial or eukaryotic lipids (3, 4). To overcome the stability drawbacks of classical liposomes, liposomes with tetraether lipids from *Thermoplasma acidophilum* were prepared and the impact on stability was investigated (5).

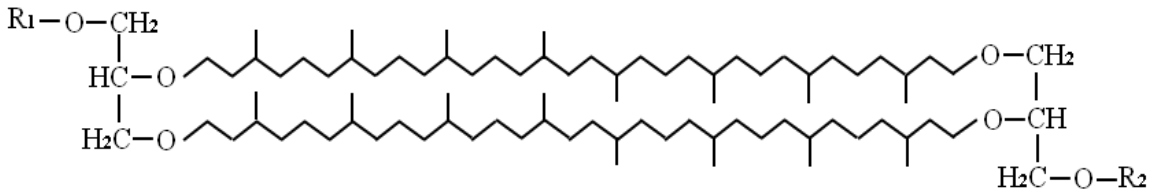

Figure 1. Tetraether lipids general structure. (Ref: Albers, S.-V., van de Vossenberg, J.L.C.M., Driessen, A. J.M. Konings,W.N. (2000) Adaptation of the archaeal cell membrane to heat stress, Vol. 5, pp. 796-803 Front Biosci)

Thermoplasma acidophilum is a thermoacidophilic archaeon, first isolated in 1970 by Darland *et al*. (6). The optimal living conditions for *Thermoplasma acidophilum* are at pH 2 and at a temperature of 59° C. The specific structure of lipids composing the cytoplasmic membrane of these archaea allows them to sustain the extreme environmental conditions. The lipid constitution of archaeal membranes contain ether bonds and varying numbers of cyclopentanes in the hydrocarbon chains providing thus a higher aqueous dispersity and expanded bilayer membrane (3, 4). Furthermore archaeal lipids do not contain double bonds. These properties distinguish archaea species like *Thermoplasma acidophilum* from bacterial species (7).

Liposomes prepared with archaeal lipids offer a wide range of medical and pharmaceutical applications due to their enhanced stability properties. When incorporating a hydrophilic and lipophilic drug, liposomes become an attractive tool for reducing overall drug dose and decreasing side effects. According to Kimura, a significant quantity of drug entrapped liposomes can be taken up by small-intestinal mucosa (8). In this context, further

investigations are necessary for characterization of liposome stability properties in acidic milieu of the gastrointestinal tract and their absorption therein (9). Certainly the most important criterion of a well-designed vesicle to be used in oral delivery is the ability to survive in the environment of the gastrointestinal tract. As a result of low pH values most conventional lipid liposomes undergo complete disintegration forming a mixture of soluble micelles (10, 11).

The pulmonary system is attractive for a liposomal drug delivery system too. When smaller than 260 nm, liposomes can be absorbed on a large surface of alveolar epithelium. Particles larger than 260 nm are likely to be destroyed by the macrophage system of the lung (12). Another criterion that affects stability in the pulmonary system is the influence of the natural surface surfactant of the lung. Hence, in this study, liposome stability was investigated during exposure to the commercial lung surfactant Alveofact (13).

This study addresses the stability properties of tetraether lipid liposomes in comparison to phospholipid liposomes, which provides a perspective on further usage of tetraether lipid liposomes as drug carriers in the gastrointestinal tract and pulmonary system.

3.3 Materials and Methods

3.3.1 *Materials*

Freeze-dried biomass from *Thermoplasma acidophilum* was a kind gift from SIT GmbH and Interface Technologies (Rosenhof/Heiligenstadt, Germany), it was stored at –20° C until usage. Phospholipon 100 H (Ph; commercial phosphatidylcholine including stearic and palmitic acid) and 5(6)-Carboxyfluorescein (CF) were purchased from Lipoid GmbH (Ludwigshafen, Germany) and Fluka, (Buchs, Switzerland), respectively. Fetal Calf Serum (FCS) was obtained from PAA (Coelbe, Germany), Triton X-100 was provided by Carl Roth (Karlsruhe, Germany). Chloroform ($CHCl_3$) and methanol (MeOH) were both purchased from Carl Roth (Karlsruhe, Germany) and the Chloroform:Methanol ($CHCl_3$:MeOH) (2:1 v/v) mixture was stored at room temperature until it was used.

HEPES buffer solution (HBS) was prepared with 40 mM HEPES (4-(2-hydroxyethyl)-1-piperazineethanesulfonic acid), 5 mM Glucose (Dextrose) and 120 mM NaCl and adjusted to pH 7.4. Phosphate buffer solution pH 7.4 had the composition of 1.3 mM KH_2PO_4, 7.4 mM Na_2HPO_4 x $2H_2O$, 129 mM NaCl, 2.5 mM KCl and dissolved in bi-distilled water. The rest of the chemicals not mentioned separately were purchased from Thermo Fischer Scientific (Schwerte, Germany) and Carl Roth (Karlsruhe, Germany).

All chemicals and solvents used in our experiments were of analytical grade.

3.3.2 Extraction of the tetraether lipids

Tetraether lipids (TEL) were extracted from 10 g freeze-dried biomass of *Thermoplasma acidophilum* according to a modified method of Bode *et al*. (14). The biomass was transferred into a 1 L flask and mixed with 500 mL $CHCl_3$:MeOH (2:1 v/v). The mixture was heated to a reflux temperature of 60° C for 12 hours. After cooling down to room temperature, the mixture was filtered through 300 g silica 60 (Merck, Germany). The filter cake was transferred to the flask and refluxed for another 12 hours. After filtration, the solvent from the resultant mixture was evaporated under vacuum to yield a lipid residue. This residue consists of total lipid fraction. From this total lipid fraction, 10 mg/mL tetraether lipid solution in $CHCl_3$:MeOH (2:1 v/v) was prepared.

3.3.3 Preparation of liposomes

Phospolipon 100 H (100 % saturated phosphatidylcholine) was dissolved in $CHCl_3$:MeOH (2:1 v/v) to prepare a 10 mg/mL stock solution. Liposome suspensions were prepared in molar ratios of 10:0, 7:3, 5:5, 0:10 Tetraether lipid: Phospholipon 100 H (TEL:Ph). These suspensions were transferred to 10 mL round bottom flasks and evaporated at 45° C 300 mbar with a rotary evaporator (Heidolph, Laborota 400, Schwabach, Germany) to obtain a lipid film. First the thin film was hydrated with bi-distilled water containing 0.9 % NaCl. To obtain a homogeneous suspension of the liposomes in water, the solution was sonicated with a probe type sonicator with an increased energy input. (G. Heinemann Ultraschall und Labortechnik Schwöbosch, Germany) sonication was applied (for 8 min, 30 sec sonication followed by 30 sec rest). After sonication, liposomes were filtered with syringe filters

through a pore size of 0.2 µm. Finally all the liposome suspensions were extruded 21 times through a 0.1 µm polycarbonate membrane filters by a mini extruder device. (Avanti, Hamburg, Germany)

3.3.4 Preparation of 5(6)-Carboxyfluorescein encapsulated liposomes

CF liposomes were also prepared according to the solvent evaporation method. The related liposome compositions with the same molar ratios were rotary evaporated at 45° C, 300 mbar with a rotary evaporator. The liposomes were hydrated with PBS, pH 7.4 which contained 50 mM CF. After hydration the same procedure was applied as mentioned above. The % encapsulation efficiency (% EE) was calculated with the equation of:

$$\text{Encapsulation efficiency (\%)} = \frac{C_{total} - C_{out}}{C_{total}} \times 100$$

where C_{out} defines the fluorescence intensity not encapsulated in liposomes, and C_{total} is corresponding the value after adding Triton X-100 in order to disturb the liposomes to find out the total liposome concentration. Additional to that, % CF leakage was also determined from the equation described by Ishii *et al.* (15). These calculations were applied after Alveofact and FCS incubations.

3.3.5 Vesicle size and zeta-potential determination

Mean diameters and polydispersity index (PDI) of liposomes were determined by photon correlation spectroscopy (PCS) by using a ZetaSizer (Nano Series; Malvern instruments GmbH, Germany), with a scattering angle of 90° at a temperature of 25° C. Before all the measurements, 10 µl liposome suspensions were diluted with bidistilled water in the ratio of 1:6 (v/v). The zeta potentials of the particles were determined by Laser Doppler Anemometry (LDA) on using a ZetaSizer (Nano Series; Malvern instruments GmbH, Germany) and the measurements were performed in a folded electrophoresis cell with 633 nm He-Ne Laser, scattering angle of 173°, at 25° C. 70 µl of liposome suspension were diluted with 730 µl bi-distilled water and measured in triplicates. The results were expressed as mean ± standard deviation of mean (S.D.).

3.3.6 Atomic Force Microscopy

The stability against FCS was determined by using Atomic Force Microscopy (AFM). Morphology of the liposomes was observed before and after incubation in FCS by AFM which was performed on a JPK NanoWizard™ (Berlin, Germany). The AFM was tuned to provide acoustic and vibrational damping. The samples were treated with silicon cantilevers with ultra sharp tips (radius of the tip curvature <10 nm). The resonance frequency was kept at ~170 kHz, and the scan speed was proportional to the scan size. To avoid damaging of the surfaces, intermittent contact (air) mode was chosen and 5 x 5 µm AFM images were captured.

3.3.7 Thermostability

Each liposomal formulation were diluted with bi-distilled water containing 0.9 % NaCl (1:6 v/v) incubated for 4 hours at 25° C, 36° C, and 60° C. After incubation, the samples were cooled down to room temperature and the mean diameters and polydispersity index (PDI) of liposomes were determined by using PCS.

3.3.8 Stability during Autoclavation

The samples were autoclaved to evaluate sterilization potential. Autoclavation was performed on a standard autoclave 3850 ELC (Systec GmbH, Wettenberg Germany). Samples were diluted with bi-distilled water containing 0.9 % NaCl (1:6 v/v) and were treated with a standard autoclavation procedure for solutions (15 min at 121° C, 29 psi pressure and saturated steam). After cooling down, the mean diameters and PDI of liposomes were determined by using PCS as mentioned above.

3.3.9 pH Stability

To observe the pH effect on the mean diameter of the liposomes, the measurements were done with different pH-values mimicking the gastrointestinal environment. 100 µl aliquots of liposome formulations were incubated in 600 µl of various pH buffer solutions; pH 2.0 (50 ml of 0.2M KCl, 13 ml 0.2 M HCl), pH 4.0 (100 ml 0.1 M $KHC_8H_4O_4$, 0.2 ml 0.1 M HCl), pH 7.4 (100 ml 0.1 M KH_2PO_4, 78.2 ml 0.1 M NaOH), pH 9.0 (100 ml 0.1 M $C_4H_{11}NO_3$ and 11.4 ml 0.1 M HCl). After 4 days of incubation the mean diameters and PDI were determined.

3.3.10 Stability in lung surfactant

The lung surfactant Alveofact was obtained from Lyomark Pharma (Oberhaching, Germany). The structural integrity of liposomes was measured whilst incubation with Alveofact, mimicking the conditions in the human respiratory system. 1 ml of total lipid solution was treated with 60 mg of Alveofact vial and 1ml HBS mixture (16). CF liposome solutions containing 50 mM CF were incubated in Alveofact solution with a ratio of 1:9 (v/v) (13). To determine the CF leakage due to liposome disruption induced by Alveofact incubation, the samples were placed into 96-well plates and fluorescence measurements were performed by using an excitation wavelength of 480 nm and emission was detected at 530 nm. The system was set for the liposomal amounts to give a total fluorescence between 3000 and 6500 arbitrary fluorescence units (FU) at a gain of 55 FU to avoid quenching effects. (Tecan Saphire 2, Tecan, Austria)

The initial fluorescence was determined right after starting the incubation. To determine the total fluorescence, after 4 hours of incubation at 37° C, Triton X-100 (1.0 % v/v concentration) was added to the CF liposomes in the volume ratio of 1:20 to disrupt CF liposomes (17).

3.3.11 Stability against FCS

Resistance against FCS incubation was observed using commercial FCS. % CF leakage was investigated for each one of the liposome formulations. The liposome formulations were diluted with FCS in a ratio of 1:2.5 (v/v) and incubated at 37° C for 4 hours. Right after

starting incubation, the initial values were measured. The same fluorescence settings were used as explained above. The % CF leakage was calculated with the equation of:

$$\% \text{ CF Leakage} = \frac{F - F_i}{F_f - F_i} \times 100$$

where, F_i denotes initial fluorescence intensity, F is the intensity after 4 hours incubation in related mediums and F_f is the final intensity in the absence of Triton X-100 (18). The same calculations were repeated as before with the values of Alveofact incubation.

3.4 Results

3.4.1 Characteristics of liposomes

Liposomes were prepared with the compositions of 0:10, 5:5, 7:3, 0:10 TEL:Ph (molar ratio). The mean size, zeta potential and polydispersity indexes (PDI) were compared according to the TEL proportion. This data is presented in Table 1. To prepare unilamellar liposomes, the liposome solutions were extruded for 21 times through a 100 nm extrution filter (19).

The initial diameters of the liposomes vary from 34.5 nm to 135.6 nm. The PDI values were between 0.120 and 0.240, and all the liposomes were negatively charged. This negative charge increases with ascending tetraether lipid content. The potentials vary from -19.40 to -49.90 mV. With the increase of TEL proportion, the size of the unilamellar liposome increases as well. Initial mean diameter, PDI and zeta potential of the different formulations of the liposomes are listed in Table 1. % CF encapsulation efficiencies of the formulations measured as it explained in Material Method Section. The results were 9.4 mM (18.8±3,81 %)

for 0:10 TEL:Ph, 11.36 mM (22.73±0.21 %) for 5:5 TEL:Ph, 10.21 mM (20.43±5.71 %) for 7:3 TEL:Ph, 10.24 mM (20.48±4.94 %) for 10:0 TEL:Ph.

Table. 1. Initial properties of liposomes were measured 1 day after preparation. Mean diameters (nm) and polydispersity index (PDI) of liposomes were determined by photon correlation spectroscopy (PCS) and the zeta potentials (mV) of the particles were determined by Laser Doppler Anemometry (LDA) by using a ZetaSizer.

Formulation (Molar Ratio)	Mean Diameter ± S.D. [nm]	PDI ± S.D.	ζ-potential ±S.D. [mV]
10:0 TEL : Phospholipon 100H	135.60±0.03	0.160±0.03	-49.90±0.91
7:3 TEL : Phospholipon 100H	107.00±0.53	0.120±0.02	-45.50±0.63
5:5 TEL : Phospholipon 100H	99.64±1.04	0.190±0.02	-42.50±1.41
0:10 TEL : Phospholipon 100H	34.50±0.77	0.240±0.01	-19.40±0.03

3.4.2 Thermostability of the liposomes

Liposomes were incubated at different temperatures. The relative thermostability of the liposomes was investigated with mean size and the polydispersity index measurements after 4 hours of incubation at various temperature conditions. At room temperature and at 36° C no significant difference was observed. However, at 60° C, the size of the formulation 0:10 TEL:Ph was found to be 149.2±1.39 nm and an increase of the PDI value could be observed which was 0.44±0.11 nm. The other formulations with TEL content demonstrate a better

stability at higher temperature conditions. Hydrodynamic diameters are illustrated in Figure 2 and the PDI results after incubation are listed in Table 2.

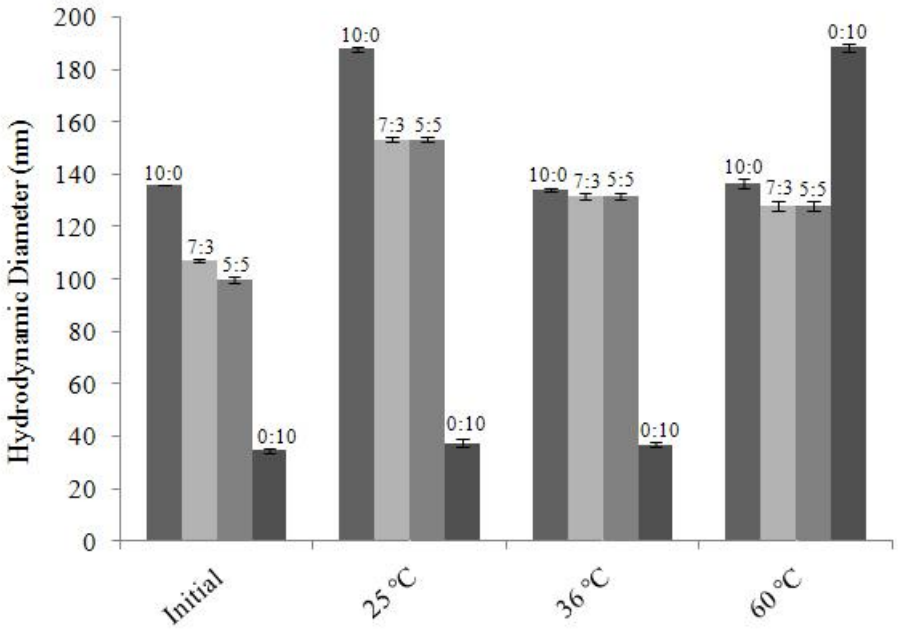

Figure 2. The hydrodynamic diameters of liposomes were determined after 4 hours incubation in related temperature conditions.

Table. 2. The PDI measurements were evaluated after 4 hours incubation in related temperature conditions.

Formulation (Molar Ratio)	PDI ± S.D. 25° C	36° C	60° C
10:0 TEL : Phospholipon 100H	0.150±0.03	0.170±0.04	0.170±0.05
7:3 TEL : Phospholipon 100H	0.120±0.02	0.130±0.01	0.140±0.02
5:5 TEL : Phospholipon 100H	0.156±0.01	0.148±0.06	0.176±0.01
0:10 TEL : Phospholipon 100H	0.240±0.04	0.250±0.08	0.440±0.11

3.4.3 Stability during Autoclavation

Clinical applications of liposomal vesicles require absolute sterility. Since conventional lipids mostly degrade during heating or radiation, structural improvements are necessary to overcome this drawback are necessary (20, 21).

As an alternative, 0.2 µm bacterial filters were also reported to have a limited scope because the sterilization of the liposomes with these bacterial filters is only suitable for liposomes smaller than 300 nm mean diameter (22). This proves to be a severe drawback for the clinical use of liposomes. Therefore, stability of TEL liposomes was investigated under autoclavation conditions according to Bode *et al.* (14). Previously, we have reported the autoclavation data for Glycerol Dialkyl Nonitol Tetraether (GDNT) liposomes (5). Due to the high stability properties of TEL, in this study we investigated the total polar lipids and different TEL

formulations were compared after autoclavation. Size and PDI values were determined (Fig. 3). The liposome solutions were autoclaved (121° C) for 15 min. 10:0 TEL:Ph liposome formulations were intact and it was indicated that they have high stability even at this temperature. The PDI values were observed to be under 0.200 and no significant difference was observed between the hydrodynamic sizes of liposomes before and after autoclavation. The 0:10 TEL:Ph formulation was used as a negative control in this study. In the comparison of the hydrodynamic size and PDI values before and after autoclavation, high increase of both parameters was observed for this formulation.

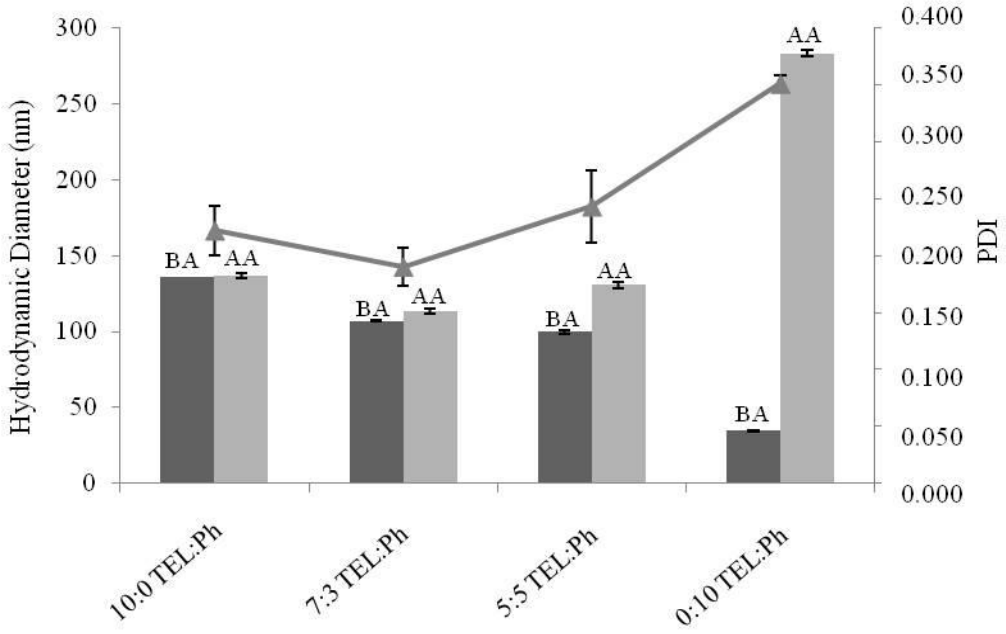

Figure 3. Stability of TEL:Ph formulations under BA: Before Autoclavation, AA: After Autoclavation. The measurements were conducted in triplicates. Bars represent the hydrodynamic diameter (nm), the line represents the PDI after autoclavation. The initial PDI values before autoclavation are 0.160±0.030, 0.122±0.015, 0.192±0.022, 0.236±0.014 for 10:0, 7:3, 5:5, 0:10 TEL:Ph respectively. (Mean ± S.D)

3.4.4 pH stability

After incubation in different pH media, the effect of the TEL proportion on the liposomes was observed. As it was reviewed elsewhere, with increase of pH, permeability of phospholipid membrane increases and liposomes swell in an attempt to compensate the pH imbalance across the inside and outside of the membrane (23, 24). In Figure 4 it is shown that the 0:10 TEL:Ph liposome size increases by more than 4 times of its initial size. Also mean diameter for this formulation was doubled. TELs provide osmotic resistance to the liposomal membrane by their specific chemical properties as reported previously (5). Besides, the other formulations with different proportions of TEL show no significant change of size and PDI after incubation of pH 2.0 to pH 9.0 buffers.

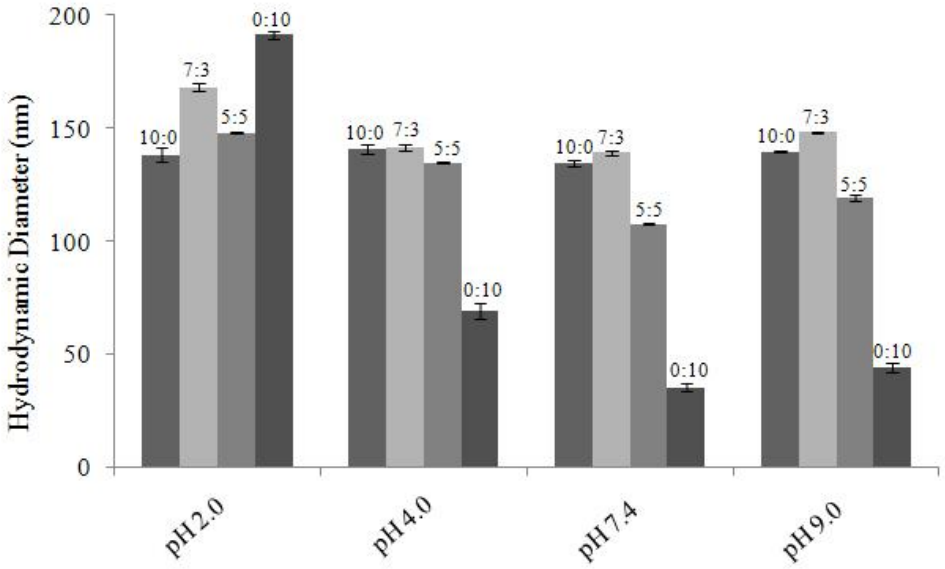

Figure 4. Hydrodynamic diameters were presented after 4 days of incubation in pH buffers mentioned in Material and Method section. For 10:0 TEL:Ph PDI varies between 0.14±0.02 to 0.24±0.03, for 7:3 TEL:Ph between 0.06±0.05 to 0.15±0.07, for 5:5 TEL:Ph between 0.22±0.09 to 0.14±0.02. But for 0:10 TEL:Ph at pH 9.0; 0.28±0.04, at pH 7.4 0.20±0.11, at pH 4.0; 0.31±0.15; at pH 2.0; 0.43±0.12 (Mean±S.D).

3.4.5 Stability against Alveofact and FCS

The same liposome formulations as mentioned above were investigated to observe the ability of survival in the lung surfactant. % CF encapsulation efficiency was measured right after the incubation as explained in Material Method section. The initial % CF encapsulation efficiencies of the formulations were 18.8±3.81 % for 0:10 TEL:Ph, 22.73±0.21 % for 5:5 TEL:Ph, 20.43±5.71 % for 7:3 TEL:Ph, 10.24 mM (20.48±4.94 %) for 10:0 TEL:Ph. Figure 5 illustrates the % CF leakage after 4 hours of FCS and Alveofact incubations. The results were 95.50±0.86 % (0:10 TEL:Ph), 96.01±0.11 % (5:5 TEL:Ph), 96.18±2.45 % (7:3 TEL:Ph), 94.79±0.60 % (10:0 TEL:Ph), and 91.99±1.54 % (0:10 TEL:Ph),

93.91±0.48 % (5:5 TEL:Ph), 92.62±1.27 % (7:3 TEL:Ph), 89.81±0.60 % (10:0 TEL:Ph). Liposomes incubated in FCS and Alveofact solution showed similar leakage behaviour. With increasing ratio of TEL in the liposome formulations, the integrity of the liposome structures was preserved. After 4 hours of incubation, the release of CF was kept under 10 % for all formulations. Also, AFM images in Figure 6a and 6b show the comparison of liposomes before and after 4 hours incubation in FCS. 0:10 TEL:Ph liposomes were the least stable of all tested formulations and released 8.28±06 % CF during Alveofact incubation, and 5.04±0.17 % CF during FCS incubation. After 5 hours incubation of liposomes prepared with *Thermoplasma acidophilum* lipids in various concentrations of FCS, 0 % CF leakage was observed. This may be evaluated as evidence that, unlike ester liposomes, ether liposomes have a resistance against high density lipoproteins in blood, plasma or serum because of their bilayer-spanning tetraether lipids (25). Concerning pulmonary delivery, this bilayer-spanning property of TEL also explains the resistance against Alveofact. Even though the stability decreases after 5 hours of incubation in Alveofact solution for all formulations in comparison to FCS, the % CF Leakage in Alveofact is similar to the leakage in FCS incubation. And still 10:0 TEL:Ph formulation shows the highest stability.

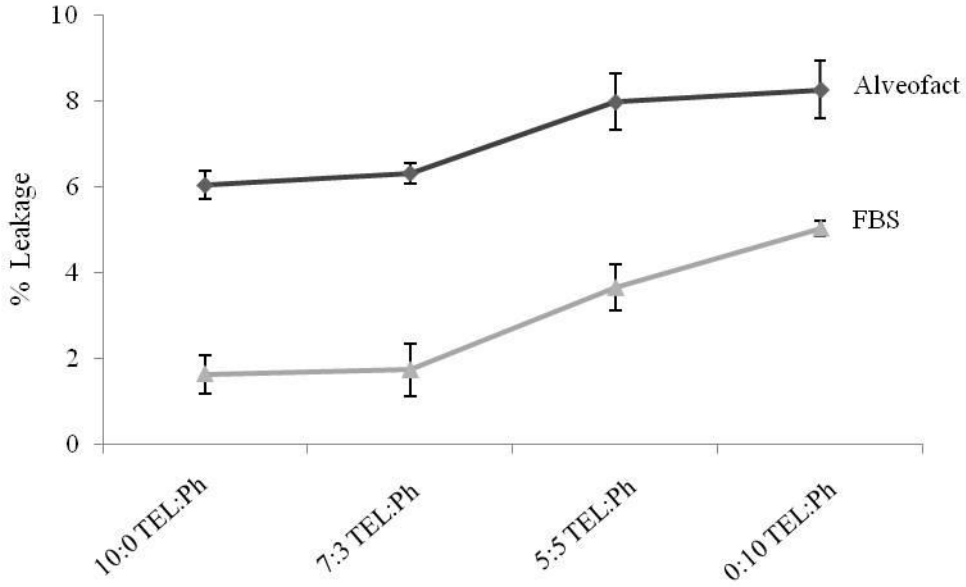

Figure 5. % CF leakage of 10:0, 7:3, 5:5, 0:10 TEL:Ph liposome formulations after 5 hours incubation in Alveofact and FCS.

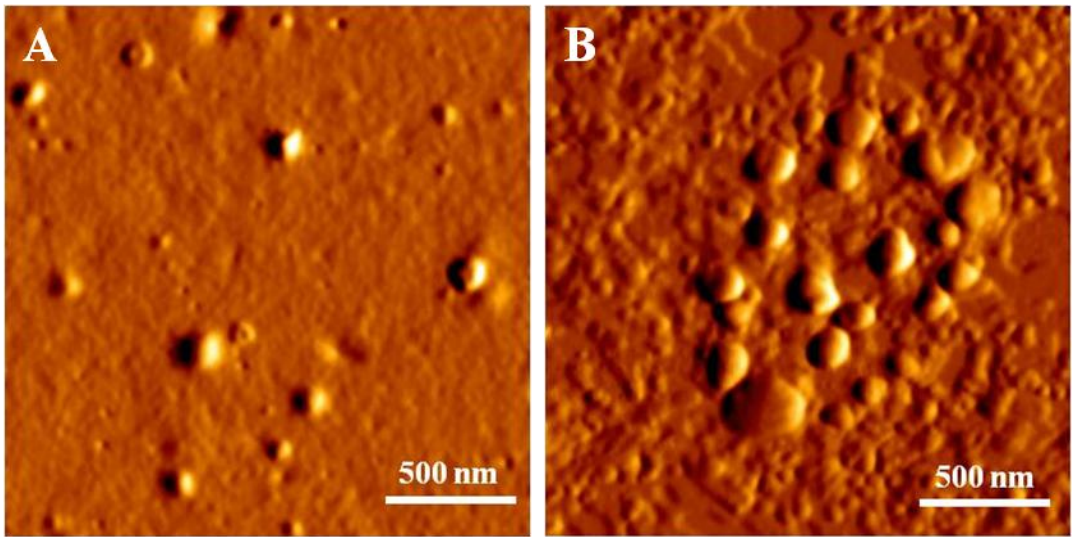

Figure 6. Figure A displays the AFM image of initial 7:3 TEL:Ph liposomes and Figure B shows the AFM image of 7:3 TEL:Ph liposomes after 4 hours of incubation.

3.5 Discussion

In this study the stability properties of liposomes according to potential applications in lung and gastrointestinal environment have been addressed. The liposomal formulations containing TEL could be prepared with well-defined sizes. It was considered that liposomes with more than 90 % of bipolar tetraetherlipids of total polar lipid extracted from *Thermoplasma acidophilum* are more stable than diester/diether lipid liposomes (4). This approach proves that the TEL molar ratio has a distinctive effect on stability against various pH and temperature conditions, biological environments (FCS and surfactant) and autoclavation.

It is reported that the permeability of tetraether lipid liposomes is less sensitive to temperature changes (26). In our study, mean diameters of all liposome formulations were measured and found to be below 0.2 µm and tetraether lipid fraction exhibits large negative zeta potential in agreement to Komatsu *et al.* (27)*;* as the temperature increases to 60^{o} C, the size of liposomes formed with pure Phospholipon 100H increases too. These results show that TEL liposomes are less temperature-sensitive than phospholipon containing liposomes, which was reported to be the result of membrane permeability and viscosity properties of the extracted membrane lipids (28). The PDI values for each composition under different temperatures indicate similar stability behaviour except for the liposomes consisting of pure Phospholipon.

Benvegnu *et al*. have also shown that the addition of synthetic TEL to conventional liposomes increases their stability (3). This study shows that the diameters of liposomes are highly stable at different pH values if sufficient amount of TEL is added to the formulation. At very low pH (pH 2), liposome sizes only show minor fluctuations. On the other hand, Elferink *et al.*

reported that liposomes prepared from tetraether lipid mixtures offer much lower proton permeability (19). This unique property is an adaptation of the archaea cell membrane to extreme environmental conditions, in order to maintain the intracellular pH of the cell. The results shown in Figure 4 can be explained with the liposome membrane integrity at low pH, provided by the lipid backbone, orientation of tetraether lipids and also by bi-polar head groups in their structures. Although *Thermoplasma acidophilum* grows optimally at pH 2, it has an internal pH of 6.9 (29, 30). To cope with this huge pH difference, *Thermoplasma acidophilum* has developed cytoplasmic membrane lipids which consist of asymmetrical, negatively-charged phosphate headgroups (31, 32). Therefore, with increasing TEL component of the liposome formulation, proton permeability decreases resulting in increased pH stability.

It is indicated that that TEL enables liposomes to be sterilized via autoclavation. Especially the pure TEL formulation showed no significant change after autoclavation in regard to size and PDI. As the Phospholipon concentration exceeds 50 %, stability starts to decrease gradually with an increasing PDI value. Stamm *et al*. have shown the potential of sterilization by filtration of liposomes through 0.2 µm filters and in this study we have presented a more reliable sterilization method (33).

The TEL proportion seemed to have a certain stabilising effect under serum and lung surfactant incubation. Patel *et al.* pointed out that low % leakage of CF occurred in TEL liposomes during the incubation in fetal calf serum albumin because of vesicle disruption rather than increasing permeability. (34). In contrast, the AFM image of liposomes after 5 hours of FCS incubation (Figure 6B) shows well-shaped particles; however, low % CF leakage indicates a low vesicle disruption rate, which makes it difficult to interpret the results.

The % CF leakage results presented in Figure 5 are in good agreement with Choquet *et al*. (Tetraether lipid liposomes from *Thermoplasma acidophilum* showed 0 % CF leakage in 20 %, 50 % and 100 % serum concentrations) (28).

The % leakage of CF in different compositions both in Alveofact and FCS indicates that TEL also has a positive impact on retention.

3.6 Conclusion

Our study demonstrates that TELs enhance the stability of liposomes, especially if they represent more than 50 % of the formulation. Since the TELs are adapted to very high temperatures, sterilization of liposomes by autoclavation is possible and provides considerable advantages for clinical applications. Significant stability with only slight variations in size, PDI and retention in serum and lung surfactant were observed. Thus, these liposomes offer attractive possibilities for treatment applications aiming at the pulmonary system and the gastrointestinal tract.

3.7 Acknowledgements

This project was supported by Deutscher Akademischer Austausch Dienst DAAD (A.O), the Deutsche Forschungs-Geminschaft DFG Forschergruppe 627 “Nanohale” and Forschergruppe 495 “Biohybridverbindungen” (U.B.) and Surface and interface Technologies GmbH (Germany). The authors thank Christian Hobler for his help with fluorescence studies.

3.8 References

1. Bangham, A. D., Standish, M. M., and Watkins, J. C. (1965) Diffusion of univalent ions across lamellae of swollen phospholipids. Vol. 13 pp. 238-252, J Mol Biol
2. Wang, G., Wang, I. E., Siahaan, T. J. E., and Soltero, R. E. (2005) Liposomes as drug delivery vehicles. pp. 411-434, Drug Delivery: Principles and Applications, John Wiley&Sons
3. Benvegnu, T., Rethore, G., Brard, M., Richter, W., and Plusquellec, D. (2005) Archaesomes based on novel synthetic tetraether-type lipids for the development of oral delivery systems. pp. 5536-5538, Chem Commun
4. Chong, P. L. (2010) Archaebacterial bipolar tetraether lipids: Physico-chemical and membrane properties. Vol. 163 pp. 253-265, Chem Phys Lip
5. Ozcetin, A., Mutlu, S., and Bakowsky, U. (2010) Archaebacterial Tetraetherlipid Liposomes. Vol. 605 pp. 87-96, Met Mol Biol
6. Darland, G., Brock, T. D., Samsonoff, W., and Conti, S. F. (1970) A thermophilic, acidophilic mycoplasm isolated from a coal refuse pile. Vol. 170 pp. 1416-1418, Science
7. Langworthy, T. A., Wolfe, C. R., and (Ed), Woese, R. S. (Ed) (1985) The bacteria, a treatise on structure and function. Vol. 8 pp. 459-496, Academic Press, New York
8. Kimura, T., and Gregoriadis, G. E. (1988) Transmucosal passage to liposomal drugs. pp. 635-647, Liposomes as Drug Carriers, Wiley Chichester
9. Gilligan, C. A., and Li Wan po, A. (1991) Oral vaccines: Design and delivery. Vol. 75 pp. 1-24, Int J Pharma

10. Richards, M. H., and Gardner, C. R. (1978) Effects of bile salts on the structural integrity of liposomes. Vol. 543 pp. 508-522, Biochim Biophys Acta

11. Freisleben, H. J., Zwicker, K., Jezek, P., John, G., Bettin-Bogutzki, A., Ring, K., and Nawroth, T. (1995) Reconstitution of bacteriorhodopsin and ATP synthase from Micrococcus luteus into liposomes of the purified main tetraether lipid from Thermoplasma acidophilum: proton conductance and light-driven ATP synthesis. Vol. 78(2) pp. 137-147, Chem Phys Lip

12. Niven, R. W. (1995) Delivery of biotherapeutics by inhalation aerosol. Vol. 12 pp. 151-231, Crit Rev Ther Drug Carrier Syst

13. Anabousi, S., Kleemann, E., Bakowsky, U., Kissel, T., Schmehl, T., Gessler, T., Seeger, W., Lehr, C. M., and Ehrhardt, C. (2006) Effect of PEGylation on the Stability of Liposomes During Nebulisation and in Lung Surfactant. Vol. 6 pp. 3010-3016, J Nanosci Nanotechnol

14. Bode, M. L., Buddoo, S. R., Minnaar, S. H., and du Plessis, C. A. (2008) Extraction, isolation and NMR data of the tetraether lipid calditoglycerocaldarchaeol (GDNT) from Sulfolobus metallicus harvested from a bioleaching reactor. Vol. 154(2) pp. 94-104, EPUB Chem Phys Lipids

15. Ishii, F., and Y., Nii. (2001) Simple and convenient method for estimation marker entrapped in liposomes. Vol. 22 pp. 97–101, J Dispersion Sci Technol

16. Abu-Dahab, R., Schäfer, U. F., and Lehr, C. M. (2001) Lectin-functionalized liposomes for pulmonary drug delivery: effect of nebulisation on stability and bioadhesion. Vol. 14 pp. 37-46, Eur J Pharm Sci

17. Kronberg, B., Dahlman, A., Carlfors, J., and Karlsson, J. (1990) Preparation and Evaluation of Sterically Stabilized Liposomes: Colloidal Stability, Serum Stability, Macrophage Uptake and Toxicity. Vol. 79(8) pp. 667-671, J Pharm Sci

18. Rufini, S., Cesaroni, P., Desideri, A., Farias, R., Gubensek, F., Gutierrez, J. M., Luly, P., Massoud, R., Morero, R., and Pederson, J. Z. (1992) Calcium ion independent membrane leakage induced by phospholipase-like myotoxins. Vol. 31 pp. 12424-12430, Biochem

19. Elferink, M. G. L., de Wit, J. G., Driessen, A. J. M., and Konings, W. N. (1994) Stability and proton-permeability of liposomes composed of archaeal tetraether lipids. Vol. 1193 pp. 247-254, Biochimica et Biophysica Acta

20. Kikuchi, H., Carlsson, A., Yachi, K., and Hirota, S. (1991) Possibility of heat sterilization of liposomes. Vol. 39 pp. 1018-1022, Chem Pharm Bull

21. Konings, A. W. T., and Gregoradis, G. E. (1984) Lipid peroxidation in liposomes. Vol. I pp. 139-163, Liposome Technology CRC Press, Boca Raton, FL

22. Goldbach, P., Brochart, H., Wehrle, P., and Stamm, A. (1995) Sterile filtration of liposomes: retention of encapsulated carboxyfluorescein. Vol. 117 pp. 225-230, Int J Pharm

23. Ertel, A., Marangoni, A. G., Marsh, J., Hallett, F. R., and Wood, J. M. (1993) Mechanical properties of vesicles. I. Coordinated analysis of osmotic swelling and lysis. Vol. 64 pp. 426-434, Biophys J

24. Hallett, F. R., Marsh, J., Nickel, B. G., and Wood, J. M. (1993) Mechanical properties of vesicles. II. A model for osmotic swelling and lysis. Vol. 64 pp. 435-442, Biophys J

25. Choquet, C. G., Patel, G. B., Beveridge, T. J., and Sprott, G. D. (1994) Stability of pressure-extruded liposomes made from arhaeobacterial ether lipids. Vol. 42 pp. 375-384, Appl Microbiol Biotechnol

26. Jarrell, H. C., Zukotynski, K. A., and Sprott, G. D. (1998) Lateral diffusion of the total polar lipids from Thermoplasma acidophilum in multilamellar liposomes. Vol. 1369 pp. 259-266, Biochim Biophys Acta

27. Komatsu, H., and Chong, P.L.-G. (1998) Low Permeability of Liposomal Membranes Composed of Bipolar Tetraether Lipids from Thermoacidophilic Archaebacterium Sulfolobus acidocaldarius. Vol. 37 (1) pp. 107–115, Biochem

28. Choquet, C. G., Patel, G. B., Beveridge, T. J., and Sprott, G. D. (1994) Stability of pressure-extruded liposomes made from archaeobacterial ether lipids. Vol. 42 pp. 375-384, Appl Microbiol Biotechnol

29. Cobley, J. G., and Cox, J. C. (1983) Energy Conservation in Acidophilic Bacteria. Vol. 47(4) pp. 579–595, Microbiol Rev

30. Krulwich, T. A., and Guffanti, A. A. (1983) Physiology of Acidophilic and Alkalophilic Bacteria. Vol. 24 pp. 173–214, Adv Microb Physiol

31. De Rosa, M., Gambacorta, A., and Nicolaus, B. (1983) A new type of cell membrane in thermophilic archaebacteria, based on bipolar ether lipids. Vol. 16 pp. 287-294, J Membr Sci

32. Morii, H., and Koga, Y. (1994) Asymmetrical topology of diether- and tetraether-type polar lipids in membranes of Methanobacterium thermoautotrophicum cells. Vol. 269 pp. 10492–10497, J Biol Chem

33. Stamm, A., Goldbach, P., Brochart, H., and Wehrle, P. (1995) Sterile filtration of liposome: retention of encapsulated carboxyfluorescein. Vol. 117 pp. 225-230, Int J Pharm

34. Patel, B. G., Agnew, B. J., Deschatelets, L., Fleming, L. P., and Sprott, G. D. (2000) In vitro assessment of archaeosome stability for developing oral delivery systems. Vol. 194 pp. 39-49, Int J Pharm

4 Selective Interactions of Concanavalin A-modified Tetraether Lipid Liposomes

Paper accepted in Pysica Status Solidi

DOI: 10.1002/pssc.201001175 (2011)

4.1 Abstract

For the development of site specific liposomes, high stability and long circulation properties are very promising for the improvement of drug targeting and drug delivery system as well as improvement of bioavailability of efficient bioactive drugs. Tetraether lipids (TELs) are very stabile lipids, extracted from *Thermoplasma acidophilum.* Because of its high chemical stability and its biocompatibility, Tetraether lipid liposomes prepared with TELs are excellent candidates for liposomal drug delivery. In this study a model protein, Concanavalin A (ConA) was chosen for a simulation of a specific adsorbtion onto mannan surface. Concanavalin A (ConA) is a lectin, extracted from *Canavalia ensiformis*, which interacts with sugar domains localized on inflammatory active tissues or tumors. In this study, stable TEL liposomes were prepared and characterized. Furthermore to develop side specific liposomes, tetraether lipids were activated and, ConA was covalently bond onto the surface of the prepared liposomes. Interaction of ConA conjugated liposomes with mannan-modified surfaces was investigated by Biomolecular Interaction Analysis (BIA) via Reflectometric Interference Spectroscopy (RIfS). This provides real time observation of interactions between carbohydrate structure and TEL liposomes. Specific interaction was also visualised by AFM imaging subsequent to the RIfS measurements. According to the results, with ConA conjugated liposomes, high specific adsorption efficiency was observed. Consequently, this specific adsorption assay between ConA and mannan surface can be considered as a model for the further studies utilized with specific biomarkers for a selective active agent transfer to tumors and inflammatory active tissues.

4.2 Introduction

In the past several decades, the progress in the field of liposomal technology has shown promising results with respect to minimization of side effects of pharmaceuticals due to longer circulation of liposomal formulations and tumor specific targeting. However, stability of liposome is of great concern. In contrast to many other conventional liposomes, Tetraether lipid (TEL) liposomes prepared with highly stable TEL possess extended circulation properties. TELs can be isolated from thermoacidophilic archaeon *Thermoplasma acidophilum* (1). *Thermoplasma acidophilum* is able to survive in extreme external condition of pH 2 and at temperatures up to 59° C because of very stable chemical structure of their membrane lipids. Unlike most bacterial membrane lipids, Archeal membrane lipids include pentacycles in hydrocarbon chains and ether bonds instead of esters. TEL does not have any double bonds in its chemical structure which causes a superior stability to TEL liposomes under harsh conditions (2). Because of these properties, they are rather promising for therapeutical applications.

In a model investigation, interactions between lectin and carbohydrates present on inflamed tissue were intensively investigated (3). The lectin-carbohydrate interaction mediated leukocyte rolling throughout the vascular surface to provide inflammation-response inspired leukocyte targeting. This interaction was also utilized in site-specific drug delivery in cancer therapy to reduce side effects of the drugs (4). Effective targeting of a drug carrier towards tumor tissue provides efficient therapy with low amounts of drug and low side effects (see Figure 1).

Hence as a model marker, the first commercially available lectin, Concanavalin A (ConA) was selected as a ligand for this study. ConA is a plant lectin extracted from *Canavalia*

ensiformis. It contains two metal binding sites, which bind to sugar domains localized on inflammatory active tissues or tumors (5-7). This model receptor was covalently bound to outer surface of bilayer membrane of liposomes. This interaction provides aspects for further studies with the use of specific biomarkers.

In this study specific interaction of ConA modified liposomes with mannan surface were investigated by Biomolecular Interaction Analysis (BIA) via Reflectometric Interference Spectroscopy (RIfS) and Atomic Force Microscopy (AFM). RIfS was previously described by Proll *et al.* (8,9) and provides a direct optical detection of the chemically designed surface.

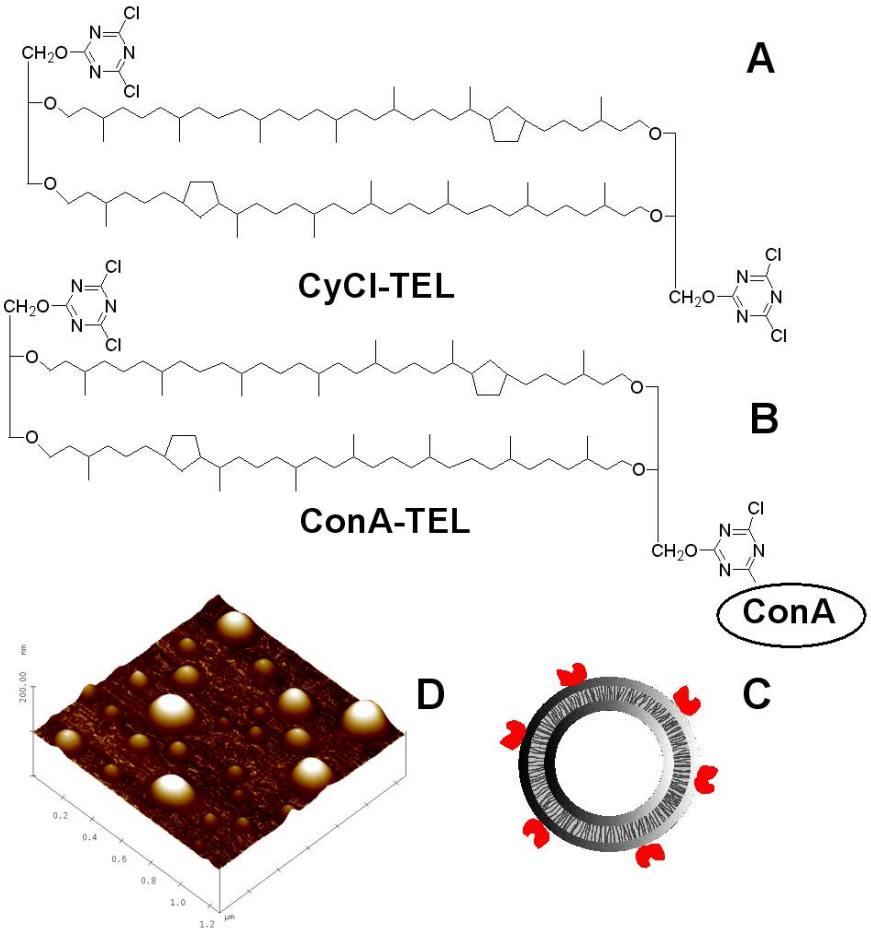

Figure 1. Molecular structure of the tetraether lipid A.) cyanuric chloride activated TEL and B.) activated TEL conjugated with ConA, C.) AFM image (height) of the TEL:DPPC:ConA-TEL (65:30:5) liposomes, D.) schematic illustration of ConA conjugation onto the liposome surface.

4.3 Experimental

4.3.1 Chemicals

Tetraether lipids were a kind gift of SIT GmbH and Interfeace Technologies (Rosenhof/Heiligen Stadt, Germany). L-Alpha-dipalmitoyl phosphatidylcholine (DPPC) was obtained from Acros Organics (USA). ConA was obtained from Vector Laboratories (USA). Chloroform and methanol were both HPLC grade and purchased from Fischer Scientific (UK). Cyanuric chloride, sodium hydroxide, sulphuric acid, hydrogen peroxide, sodium-tetraborate decahydrate, 1.4 butanediol diglycidyl ether and mannan were purchased from Sigma Aldrich (USA). Sodium borohydride obtained from Fluka (Germany) and 3-aminopropyl-triethoxysilane was purchased from Sigma Aldrich (China). All chemicals were of analytical grade.

4.3.2 Instruments

Reflectometric Interference Spectroscopic (RIfS) measurements were performed with a BIAffinity device from Analytik Jena AG (Jena, Germany). The bio-chips necessary for BIA measurements were a kind gift of Analytik Jena AG (Jena, Germany). AFM imaging was performed with a JPK NanoWizard™ (sensor measurements JPK Instruments, Berlin, Germany) equipped with silicon cantilevers NSC 16 AlBS, Micromasch (Estonia) and a Bioscope Nanoscope IV (liposome visualisation, Veeco Instruments, Mannheim Germany). The measurements were performed as described previously (10, 11).

4.3.3 Preparation of non-activated tetraether lipid liposomes

TEL was extracted from biomass of *Thermoplasma acidophilum* in the presence of chloroform:methanol (2:1 v/v) (12-14). TEL was mixed with DPPC in the concentration of 1 mg/ml (70:30 molar ratio) and dried under vacuum at 50° C in round bottomed flask in order to obtain a thin lipid film. The film was hydrated with PBS buffer pH 7.4 containing 0.1 M NaCl. To achieve a clear dispersion, the sample was exposed to ultrasound treatment with a tip-type sonicator for 8 min. (30 sec sonication followed by 30 sec rest). After sonication, the sample was filtered and extruded through a 0.1 µm polycarbonate membrane. Before BIA analysis, the sample was diluted with PBS buffer in 1/30 ratio.

Table 1: Size and zeta potential were measured by PCS (Photon Correlation Spectroscopy), AFM, and zeta potential. TEL:DPPC:CyCl-TEL are the activated TEL liposomes and TEL:DPPC:ConA-TEL are the same liposomal formulation but after ConA conjugation.

liposome	zeta potential [mV]	size d [nm]		size range
		PCS ± SD (PDI)	AFM ± SD	
DPPC	-17.5 ± 3.24	122.7 ± 9.8 (0.17)	132.4 ± 17.1	110 nm - 150 nm
TEL	-15.3 ± 0.82	137.5 ± 4.8 (0.15)	149.4 ± 14.6	90 nm - 170 nm
TEL:DPPC (70:30)	-14.7 ± 0.61	163.4 ± 18.2 (0.17)	176.7 ± 15.6	90 nm - 220 nm
TEL:DPPC:CyCl-TEL (65:30:5)	-12.7± 2.14	165.8 ± 15.7 (0.23)	169.4 ± 25.1	90 nm - 250 nm
TEL:DPPC:ConA-TEL (65:30:5)	-11.1± 1.03	185.8 ± 25.7 (0.21)	199.6 ± 22.4	90 nm - 250 nm

4.3.4 Preparation of Concanavalin A-modified TEL liposomes

Tetraether lipids from biomass of *Thermoplasma acidophilum* were extracted in the presence of chloroform:methanol (2:1 v/v) as described above (12). After extraction, organic solution was removed by drying of the sample under vacuum at 50°C to prevent the oxidative effect of methanol on activated TEL (CyCl-TEL). For preparation of TEL:DPPC:CyCl-TEL (65:30:5 molar ratio), initially activated TEL (CyCl-TEL) was prepared, by mixing of TEL with cyanuric chloride (2:1 molar ratio) in the presence of chloroform according to the method previously reported. (6). The mixture was stirred at Room Temperature (RT) overnight to provide the one side activated TEL. CyCl-TEL was mixed with TEL and DPPC in the molar ratio of 70:30 and in the concentration of 1 mg/ml, and dried under vacuum at 50° C in a round bottomed flask to obtain a thin lipid film. The final preparation process was continued similarly to the non-activated TEL:DPPC liposomes. The film was hydrated with PBS buffer pH 7.4 containing 0.1 M NaCl. A clear dispersion was obtained by ultrasound treatment as described above. After sonication, the sample was filtered and extruded through a 0.1 µm polycarbonate membrane. As the non-activated liposomes, the obtained liposomes had a diameter between 100-200 nm with a polydispersity index (PDI) of 0.1-0.2 and zeta potential between – 11 and –18 mV (see Table 1). 100 µl aliquot of the prepared sample was added to 2.9 ml borate buffer pH 8.8 containing 0.1 mM $MnCl_2$ and $CaCl_2$ (15). For lectin ConA was added (1:1000 protein:lipid ratio) into this mixture and stirred at RT overnight (16). Samples were stored at +4° C until the application of RIfS measurements.

4.3.5 Bio-chip design

Mannan coated bio-chips were prepared by covalent binding of mannan molecules according to a modified method previously reported by Hartmann *et al.* (17). A glass chip (1.3x1.3 cm, 100 µm thickness) was activated by incubation of 2 min with 6 M sodium hydroxide solution, and activated with piranha solution (H_2SO_4 96 % H_2O_2 30 % (v/v) 60:40) for 30 min. Amino-functionalization was done with 3-aminopropyl-triethoxysilane (APTS). Chips were incubated in 1 % (v/v) APTS in toluene for an hour and then washed with toluene to remove the loosely physisorbed APTS. Then, the chips were incubated at 105° C for an hour. Afterwards, bio-chips were immersed into 0.2 M sodium-tetraborate decahydrate buffer (pH 10.0) containing 1.4 butanediol diglycidyl ether (3 ml/10 ml buffer) and sodium borohydride (6 mg/ml buffer) for 12 h. Finally, 5 mg/ml mannan was dissolved in this buffer and glass chips were immersed and incubated in this solution for 24 h at RT. Before RIfS measurements, bio-chips were rinsed with Millipore® water and dried.

4.3.6 RIfS measurements

Interactions between the prepared chip and ConA were performed in accordance to Hartmann *et al.* and by Nikitin *et al.* (17,18). The real time interaction was observed by the BIAffinity device. Interactions of ConA modified liposomes and non-modified (plain) liposomes with the mannan coated chip were investigated. BIA was performed at RT within PBS buffer solution pH 7.4 including a washing step of about 2,100 sec for ConA conjugated liposomes and of about 1,700 sec for non activated liposomes over an interaction time of 3,050 sec. For analysis of obtained sensograms, BIAffinity-software (BIAM) was applied. As a result of this

analysis, it was possible to observe a clear differentiation of ConA modified liposomes and non-activated liposomes interactions onto sugar coated surface. Related results were discussed in section 3.1.

4.3.7 AFM measurements

The activation of liposomes with ConA was also confirmed by AFM. After RIfS measurements of specific interaction between both ConA modified liposomes and unmodified liposomes and the mannan coated bio-chips, the coverage of bio-chip surfaces with the liposomes was investigated by imaging the surface with AFM. For this purpose, the chips were removed from the RIfS device and then washed with Millipore® water and dried in air flow. AFM imaging was performed on a JPK NanoWizard™ and a Bioscope Nanoscope IV. Silicon cantilevers with ultra sharp tips (radius of the tip curvature <10 nm), resonance frequency ~170 kHz and a nominal force constant of ~40 N/m were used. To avoid damaging of the surfaces, intermittent contact (air) mode and Tapping mode™ were chosen. The scan speeds were proportional to the scan sizes. ImageJ software was used to calculate surface coverage with ConA modified and unmodified liposomes from 10 x 10 µm AFM images. Surface coverage was calculated as percentage of surface covered with liposomes divided by the whole surface.

4.4 Results and Discussions

4.4.1 RIfS analysis of ConA interactions

The interaction between the TEL:DPPC liposomes, which were functionalized with the lectin ConA, were investigated by Reflectometric Interference Spectroscopic (RIfS) measurements. The interactions between liposomes and mannan surface are illustrated in Figure 3D). Mannan coated chips were used to screen the difference in the attachments of unmodified TEL:DPPC liposomes in comparison with TEL:DPPC liposomes surface modified with ConA. After injection of unmodified liposomes into RIfS device (control measurement), a negligible number of liposomes was able to adhere to the mannan surface due to the unspecific interaction (Figure 2). In conrast; adhesion was relatively high for ConA conjugated liposomes. After equilibrium in order to designate the specific specific adsorption of liposomes onto mannan surface, a standard buffer washing application was administered. As easily visible, bounded liposomes could be nearly completely removed indicating that these liposomes were bound to the surface in an unspecific manner. It was observed that the signal of unmodified TEL:DPPC liposomes decreased up to 44 %, however for modified liposomes this value was only 14 % After the washing step, a nearly constant signal followed. Representative sensograms are shown in Figure 2. Association and dissociation phases are clearly visible for loaded and unloaded liposomes. The adsorption behaviour of TEL liposomes was characterized by calculation of dissociation rate constant (*KD*). *KD =kdiss/kass*. *Kass* is association rate constant and *kdiss* is dissociation rate constant. The *KD* value was calculated according to Edwards *et al.* and Proll *et al.* (19,20). *Kdiss* found to be 3.70×10^{-3} s^{-1}. *Kass* was 1.37×10^{5} $s^{-1}M^{-1}$ and the *KD* value was 2.70×10^{-8} M. The *KD* value

was in a good agreement with the *KD* value calculated by Smith *et al.* which was 2.00×10^{-8} (21).

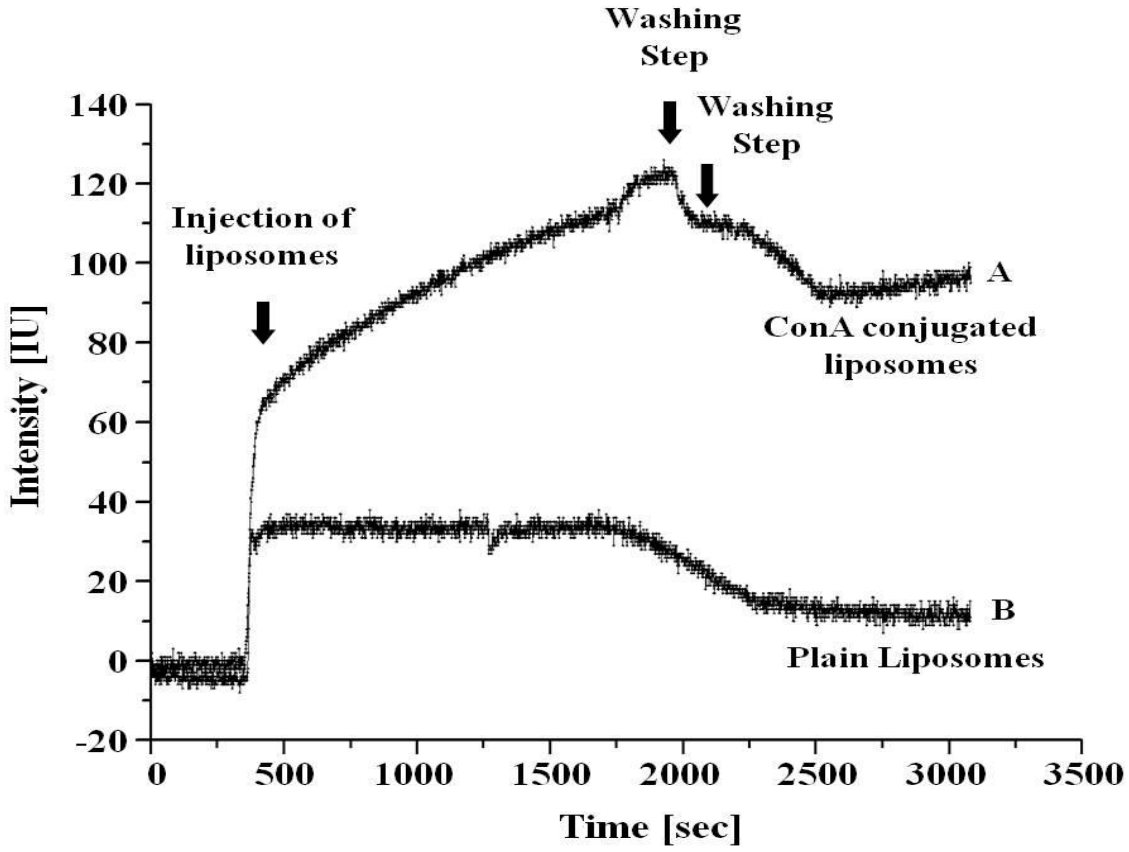

Figure 2. Reflectometric Interference Spectroscopic (RIfS) measurements: A.) liposomes conjugated with ConA, which were added to a mannan-coated surface. B.) control channel with plain liposomes. After 400 sec, liposomes were added (association). After 1,700 sec, dissociation was started.

4.4.2 Investigation of ConA interactions with AFM

Additionally to RIfS investigations, interaction of ConA conjugated TEL was also investigated by means of AFM. After each measurement of adsorption with BIA, bio-chips were removed and rinsed with Millipore® water and investigated by AFM by using tapping mode. Figure 3 a,b,c indicate the difference between non-activated and without ConA conjugated TEL and ConA conjugated TEL (ConA-TEL). TEL:DPPC liposomes were attached onto the surface of a mannan coated bio-chip, when liposomes were conjugated with ConA. In contrast, non-activated TEL liposomes were attached only in small amount onto mannan surface in an unspecific manner. Figure 3A illustrates the mannan coated surface. Specific interactions between modified liposomes are illustrated in Figure 3C. Figure 3B shows the control experiment with unmodified liposomes. These results clearly show that the mannan surface only shows little unspecific interactions. The AFM images were evaluated via the software ImageJ in order to compare the relative surface coverage properties. The result showed that ConA conjugated liposomes provided 5.68 ± 0.02 % surface coverage on the other hand this value was only 0.57 ± 0.07 % for unmodified liposomes. Remarkable similarity with RIfS measurements ensured the specific adsorption of ConA modified TEL:DPPC liposomes onto the mannan surface.

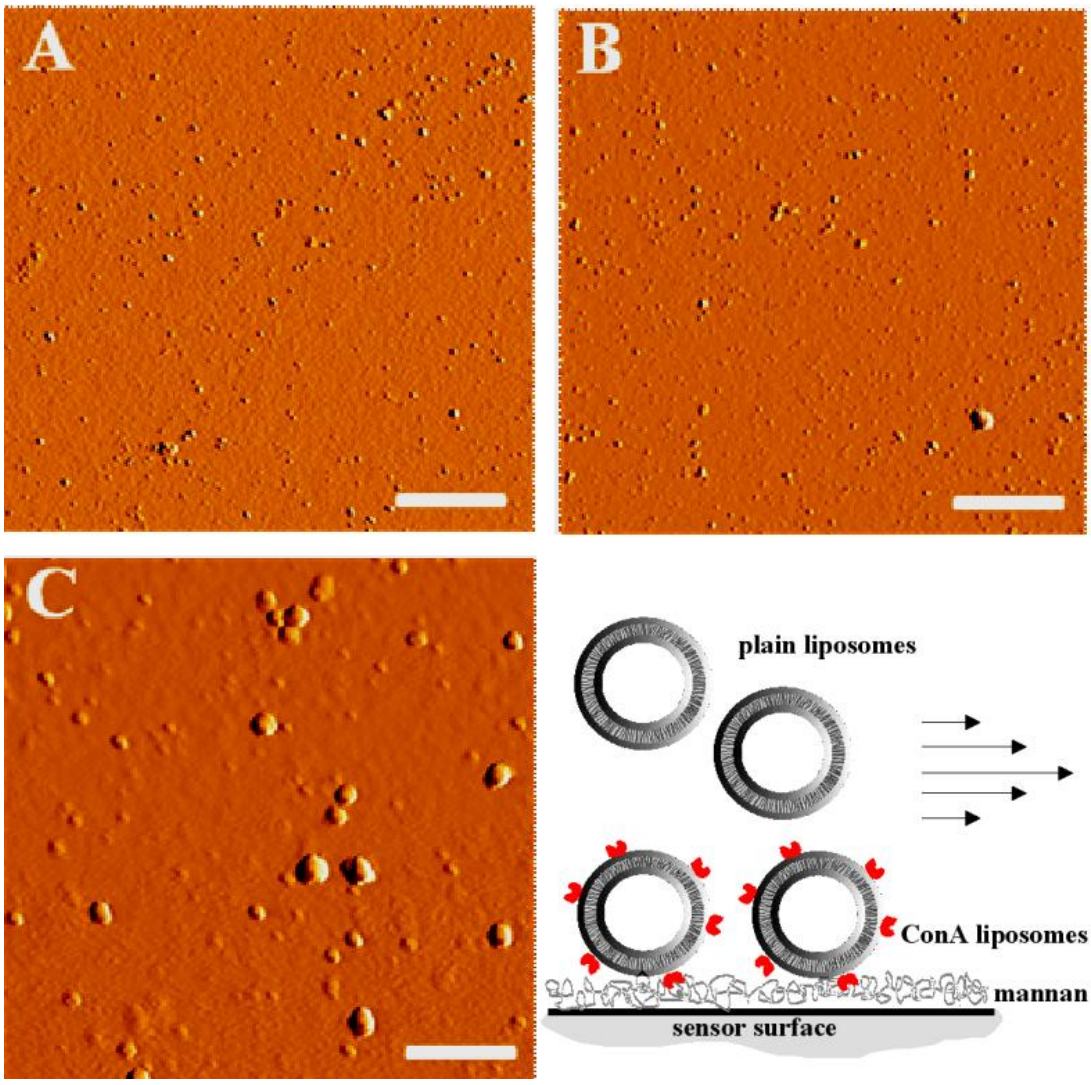

Figure 3. Schematic of the mannan modified sensor surface and the attachement of ConA conjugated liposomes. AFM images of A.) mannan coated glass chip, B.) attachment of TEL:DPPC (70:30 molar ratio) liposomes onto mannan coated glass chip C.) attachment of ConA-modified liposomes (TEL:DPPC:ConA-TEL), 65:30:5 molar ratio) onto mannan coated glass chip. Each bar represents 1µm. D.) The sketch shows the adhesion of ConA conjugated liposomes onto the mannan surface.

4.5 Conclusion

Tetraether lipids have unique stability properties because of their chemical structures. Unlike conventional lipids, they are attached to glycerol backbone via ether bonds. Tetraether lipids have saturated carbon bonds which provide high oxidation resistance (22). Due to these chemical properties high stability under extreme conditions such as low pH values (23) or high temperatures (24) can be acheived. Because of enhanced structural stability and eligibility of various protein modifications tetraether lipids are atractive as side-specific targeting agents in many biotechnological applications.

Until now various phospholipid ConA interactions were studied (25). In this study particularly TEL liposomes were used to prepare specific liposomes in order to specifically target tumors or inflammatory active tissues. These site specific liposomes minimize the side effects of the therapeutic drugs. Therefore, in this study TEL liposomes with highly stabile lipids were prepared and characterized. The ConA conjugations of TEL liposomes serve as a drug targeting model for the future studies. This adsorption model based on mannan coated chips was established in order to provide screening of modified and unmodified TEL liposomes according to their adsorption properties. RIfS measurements in combination with AFM measurements provide information about the interactions characteristics of liposomes in a wide range. ConA shows high affinity to the mannan and this adsorption behaviour was already discussed by Goldstein *et al*. (26).

The present study might provide an important aspect to determine interactions of other lectins. Lectin conjugated TEL liposomes are promising for drug targeting systems to be used as specific therapy with low amount of drug and low side effects with regard to drug targeting of tumor cells, lectins are an alternative to antibodies, antibody fragments and aptamers.

4.6 Acknowledgements

Deutscher Akademischer Austausch Dienst (DAAD) is gratefully acknowledged for promotion grant for A.O and also authors kindly thank to Forschergruppe 495 “Biohybridverbindungen” for financial support and Nico Harbach, Elvira Belz, Christoph Hemetsberger, Christian Seiler for their technical support. We thank Analytik Jena AG (Jena, Germany) and SIT Heiligenstadt GmbH (Germany) for their technical support (BIAffinity device).

4.7 References

1. Darland, G. Brock, T. D. Samsonoff, W., and Conti, S. F. (1970) Specific interactions of Concanavalin A with glycolipid monolayers. Vol. 170 pp. 1416-1418, Science
2. Langworthy, T. A. Woese, C. R., (Ed) and Wolfe R. S. (Ed) (1985) The Bacteria, A Treatise on structure and function Vol. 8 pp. 459-496 Academic. Press, New York,
3. Lasky, L. A. (1995) Selectins-carbohydrate interactions and the initiation of the inflammatory response. Vol. 64 pp.113-39, Annu Rev Biochem
4. Bakowsky, H. Richter, T. Kneuer, C. Hoekstra, D. Rothe, U. Bendas, G. Ehrhardt, C., and Bakowsky, U. (2008) Adhesion characteristics and stability assessment of lectin-modifies liposomes for site-specific drug delivery Vol. 1778 pp. 242-249, Biochim Biophys Acta
5. Read, B. D., Demel, R. A., Wiegandt, H., and Deenen, L. L. M. (1977) Specific interactions of Concanavalin A with glycolipid monolayers. Vol. 470 pp. 325-330, Biochim Biophys Acta
6. Kneuer, C., Ehrhardt C., Radomski, M. W., and Bakowsky U. (2006) Selectins-potential pharmacological targets? Vol. 21-22 pp. 1034-1040, Drug Dis Today
7. Ehrhardt, C. Kneuer, C., and Bakowsky, U. (2004) Selectins- an emerging target for drug delivery Vol. 56 pp. 527-549, Adv Drug Del Rev
8. Vornholdt, W. Hartmann, M., and Keusgen, M. (2007) Adhesion characteristics and stability assessment of lectin-modified liposomes for site-specific drug delivery Vol. 22 pp. 2983-8 Biosens Bioelectron,
9. Proll, G. Markovic, G. Steinle, L., and Gauglitz, G. (2009) Reflectometric Interference Spectroscopy Vol. 503 pp.167-178, Biosens Biodetect

10. Nguyen, J. Reul, R. Betz, T. Dayyoub, E. Schmehl, T. Gessler, T. Bakowsky, U. Seeger, W., and Kissel, T. (2009) J nanocomposited of lung surfactant and biodegradable cationic nanoparticles improve transfection efficiency to lung cells. Vol. 140(1) pp. 47-54, J Cont Rel

11. Schäfer, J. Höbel, S. Bakowsky, U., and Aigner, (2010) A. Liposome-polyethylenimine complexes for enhanced DNA and siRNA delivery, Vol. 31(26) pp. 6892-900, Biomater

12. Bode, M. L, Buddoo, S. R. Minnaar, S. H. and du Plessis, C. A., (2008) Extraction, isolation and NMR data of the tetraether lipid calditoglycerocaldarchaeol (GDNT) from *Sulfolobus metallicus* harvested from a bioleaching reactor . Vol. 154 pp. 94-104 Chem Phy Lipids

13. Vidawati, S. Sitterberg, J. Bakowsky, U., and Rothe, U. (2010) AFM and ellipsometric studies on LB films of natural asymmetric and symmetric bollamphiphilic archaebacterial tetraether lipids on silicon wafers. Vol. 78 (2) pp. 303-9, Coll Sur B Biointer

14. Ozcetin, A. Mutlu S., and Bakowsky, U. (2010) Archaebacterial Tetraetherlipid Liposomes. Vol. 605 pp. 87-96, Met Mol Biol

15. Copland, M. J. Baird, M. A. Rades, T. McKenzie, J. L. Becker, B. Reck, F. Tyler, P. C., and Davies, N. M. (2003) Liposomal delivery of antigen to human dendritic cells Vol. 21 pp. 883-890, Vaccine

16. Gosk, S. Moos, T. Gottstein, C., and Bendas, G. (2008) VCAM-1 directed immunoliposomes selectively target tumor vasculature in vivo. Vol. 1778 pp. 854-863, Biochim Biophys Acta

17. Hartmann, M. Nikitin, P., and Keusgen, M. (2006) Innovative analytic system for screening of lectins. Vol. 22(1) pp. 28-34, Biosens Bioelectron

18. Nikitin, P. I. Gorshkov, B. G. Valeiko, M. V., and Rogov, S. I. (2000) Spectral-phase interference method for detecting biochemical reactions on a surface. Vol. 30 pp. 1099-1104, Quant Electron

19. Edwards, P. R., and Leatherbarrow, R. J., (1997) Determination of association rate constants by an optical biosensor. Vol. 246 pp. 1–6, Anal Biochem

20. Proll, G. Kumpf, M. Mehlmann, M. Tschmelak, J. Griffith, H. Abuknesha, R., and Gauglitz G. (2004) Monitoring an antibody affinity chromatography with a label-free optical biosensor technique. Vol. 292 pp.35– 42, J Immunol Met

21. Smith, E. A. Thomas, W. D. Kiessling, L .L., and Corn, R. R. (2003) Surface Plasmon Resonance Imaging Studies of Protein-Carbonhydrate Interactions. Vol. 125(20) pp. 6140–6148, J Amer Chem Soc

22. Sprott, G. D. (1992) Structures of Archaeobacterial membrane lipids. Vol. 24 pp. 555-566, J Bioenerget Biomembr

23. Freisleben, H. J. Henkel, L. Gutermann, R. Rudolph, P. John, G. Sternberg, B. Winter, S., and Ring, K. (1994) Fermentor cultivation of *Thermoplasma acidophilum* for the production of cell mass and of the main phospholipid fraction. Vol. 40 pp.745-752, Appl Microbiol Biotechnol

24. Choquet, C. G. Patel, G. B. Beveridge, T. J., and Sprott, G. D. (1994) Stability of pressure-extruded liposomes made from archaeobacterial ether lipids. Vol. 42(2-3) pp. 375-384, Appl Microbiol Biotechnol

25. Bakowsky, U. Rettig, W. Bendas, G. Vogel, J. Bakowsky, H. Harnagea, C., and Rothe, U. (2000) Characterization of the interactions between various hexadecylmannoside-phospholipid model membranes with the lectin Concanavalin A. Vol.2 pp. 4609-4614, Phys Chem Chem Phys

26. Goldstein, I. J. Hollerman, C. E., and Smith, E. E. (1965) Protein-carbohydrate interaction. II. Inhibition studies on the interaction of Concanavalin A with polysaccharides. Vol. 4(5) pp. 876–883, Biochem

5 Imatinib Encapsulated Tetreaether Lipid Liposomes as Novel Cancer Therapeutics

5.1 Abstract

Extremely stable tetraether lipids isolated from *Thermoplasma acidophilum* were used for encapsulation of tyrosine kinase inhibitor Imatinib (Glivec®- STI 571). Imatinib inhibits the BCR-ABL, KIT, and platelet-derived growth factor receptor (PDGFR) tyrosine kinases. Imatinib containing TEL liposomes were examined for their anti-angiogenesis effect in a CAM assay. The Chorioallantoic Membrane (CAM) assay is very appropriate for both angiogenesis and anti-angiogenesis studies because of a very dense capillary network, low cost and eligibility of continuous microscopic visualization and screening of the implants and tissue reactions. The gelatine sponges were absorbed with MB49 (the mouse urothelial carcinoma) cell suspension. These sponges were placed onto the CAM and treated with imatinib containing TEL:DPPC liposomes, whereafter gradual deformation in vascularisation on CAM was clearly detectible. Moreover, it was shown that upon encapsulation in liposomes a lower concentration of imatinib was needed to suppress the enhanced phosphorilation of Extracellular-signal Regulated Kinase 1/2 (p-ERK 1/2) and to cause sustained decrease of its activity.

5.2 Introduction

Since 1970 liposomes have become very attractive as pharmaceutical carriers of great potential. Liposomes are already being used as industrial products for clinical applications because of many attractive biological properties such as biocompatibility, both hydrophilic and hydrophobic pharmaceutical incorporation capability, as well as efficient delivery into cells and even into individual cellular compartments (1). Doxil® Liposomal doxorubicin was the first liposomal chemotherapy product to be approved in US (2). Since then the application of liposomal drug delivery systems has achieved considerable success for the treatment of solid tumors in patients, and is promising for further investigations (3). However, liposomal drug carriers prepared from conventional phospholipids exhibit several drawbacks, especially considering stability (4).

To overcome these stability drawbacks, very stable lipids from *Thermoplasma acidophilum* were used for the preparation of liposomes in this study. The thermoacidophilic archaeon *Thermoplasma acidophilum* was isolated and described by Darland *et al*. (5). The suitable living conditions of this archaeon are around pH 2 and 56° C. Resistance against these extreme environmental conditions is gained through unique chemical and physical properties of core membrane lipids of archaeal bilayer membranes. Bipolar tetraether lipids consist of saturated chains with methyl branches attached to the ether bonds instead of ester bonds. These properties are also discussed in depth by Jacquement *et. al.,* Freisleben *et al.,* Bakowsky *et al.,* Hanford *et al.* (6-9). The chemical and physical properties of tetraether lipids provide improved stability to the liposomes allowing a larger spectrum of application (10). In this article we have addressed the encapsulation of a water soluble protein-tyrosine kinase inhibitor „Imatinib" (Glivec®- STI 571). According to the *in vitro*, *in vivo* and cellular

evaluations, Imatinib (Glivec®) inhibits the BCR-ABL, c-KIT and platelet-derived growth factor receptor (PDGFR) tyrosine kinases (11-13). In cancer and benign proliferative disorders, protein-tyrosine kinases play a fundamental role in signal transduction. Foreign substances like imatinib can affect the tyrosine kinase signal cascade (14). After Phase III trials, Imatinib was approved for first-line treatment of chronic myeloid leukemia and malignant gastrointestinal stromal tumors (GIST) (15, 16). It has been stated that the use of Imatinib could also induce antiangiogenic and/or antivascular effects in GIST (17). This antiangiogenic effect is mediated by the platelet-derived growth factor receptor (PDGFR) (18). Prevention of angiogenesis is anticipated to suppress tumor progression. In our study we have addressed stable liposomal nano-particles which encapsulated Imatinib (STI 571) for the approach of anti-angiogenesis as a novel anti-cancer strategy (19-21).

To provide a different perspective on investigation of anti-angiogenesis effect of Imatinib with and without liposomal encapsulation, a chorioallantoic membrane (CAM) assay was performed. Until the development of the CAM assay, several other angiogenesis assays were performed, among them rabbit ear chamber, rodent eye cornea, hamster check pouch and cornea, rodent dorsal skin and air sac. In practice these assays appeared to be complicated to apply, unsuitable for high quantity of test compounds, expensive and in most cases required specific surgical skills (22, 23). CAM is an extraembryonic membrane of a developing chick embryo; it is very attractive for angiogenesis and anti-angiogenesis studies because of its very dense capillary network, easy and rapid methodology, low cost and no sterility requirement. Also the immune system of the chick is not fully developed during the embryo stage, meaning the rejection system is not yet exerted. Besides these advantages, the CAM assay is preferential for angiogenesis and anti-angiogenesis studies because of its suitability for testing high quantities of various compounds (23-25). Furthermore, the CAM assay allows continuous rapid microscopic visualization and screening of the implants and tissue reactions

(26). During the CAM assay, the chick embryo may be removed from the egg shell (*ex ovo*) to provide large screening techniques. Because of several limitations such as low embryo survival rate, difficult methodology and no possibility to properly reflect the physiological conditions, we performed the traditional shell model (*in ovo*) as described by Knighton *et. al.* (27). Drug administration onto the tumor implants on the CAM was performed with the use of topical, intraperitoneal and intravenous delivery methods. Unlike topical, the other methods can result in lower survival rate, as well as lowering of the actual concentration of the drug during blood circulation (28). Topical administration of liposomes on CAM has been investigated elsewhere for efficiency of drugs and liposomal encapsulated drugs (29-31).

In this study we have not only investigated the anti-angiogenic effect of the topical application of a tyrosine kinase inhibitor but also the anti-angiogenic effect of a tyrosine kinase inhibitor encapsulated in very stable liposomes. These liposomes were tailored with tetraether lipids besides conventional lipid fractions. Furthermore, we implanted MB49 (the mouse urothelial carcinoma) as a model cell line onto the CAM and we investigated the activity of topical application of liposomal formulations *in ovo*.

5.3 Materials and Methods

5.3.1 Extraction of Tetraether lipids

Tetraether lipids (TEL) were extracted from freeze-dried *Thermaplasma acidophilum* according to modified method Bode *et al.* (31). *Thermaplasma acidophilum* biomass was a kind gift from SIT GmbH and Interference Technologies (Rosenhof/Heiligenstadt, Germany). 10 g biomass was refluxed at 60° C for 12 hours in presence of 500 ml $CHCl_3$:MeOH (2:1, v/v) (Fischer Scientific, Loughborough, UK; Carl Roth, Karlsruhe, Germany (both HPLC Grade). After cooling down, the mixture was filtered through 300 g 0.02-0.045 mm silica 60 gel (Merck, Darmstadt, Germany). The collected brown lipid solvent was adjusted to 10 mg/ml concentration in $CHCl_3$: MeOH (2:1 v/v) and this stock solution was kept at -20° C until the preparation of liposomes.

5.3.2 Preparation of tyrosine kinase inhibitor encapsulated TEL liposome formulations

For the preparation of blank liposomes, 2 ml aliquots of extracted TEL and DPPC mixtures in a molar ratio of 7:3 with the concentration of 1 mg/ml were transferred into a round bottom flask and evaporated at 45° C and 300 mbar with rotation (Heidolph, Laborota 400, Schwabach, Germany) to obtain a TEL:DPPC lipid film, according to the method we have reported previously (10). This molar ratio was chosen to provide sufficient stability to the liposomes in the circulation but not to prevent the cellular lysosome (10) The lipid film was hydrated with 2 ml PBS containing 0.5 M NaCl and for homogenization, the solution was sonicated by probe type sonication for 8 minutes at a level of 6 from 10 of intensity (30 sec sonication followed by 30 sec rest) (G. Heinemann Ultraschall und Labortechnik

Schwöbosch, Germany). Afterwards filtration through 0.45 µm filter and 21 times of extrusion through 0.2 µm polycarbonate membrane filters (Avanti, Otto Nordwald GmbH, Hamburg, Germany) followed subsequently. During the preparation of imatinib encapsulated liposomes, another 2 ml aliquot was prepared as described above and the lipid film was hydrated with imatinib solution in a 2:1 Lipid:Drug molar ratio prepared in PBS containing 0.5 M NaCl (32). The same procedure for the preparation of imatinib encapsulated liposomes was repeated as explained above for blank liposomes. The formulations are listed in Table 1 and Table 2.

Table 1. Imatinib encapsulated TEL:DPPC liposome formulations.

Abbreviation	Liposome Formulation	Imatinib Concentration (μM)
TA	7:3 TEL:DPPC liposomal formulation	3.43
TB		1.14
TC		$3.43x10^{-1}$
TD		$1.14x10^{-1}$
TE		$3.43x10^{-2}$
TO	(Blank Liposomes)	0
TP	Without liposomal Formulation	PBS

Table 2. Free imatinib Solutions for topical applications

Abbreviation	Liposome Formulation	Imatinib Concentration (mM)
A	Free imatinib imatinib without liposomal formulation	1.00
B		$3.30x10^{-1}$
C		$1.00x10^{-1}$
D		$3.30x10^{-2}$
E		$1.00x10^{-2}$
P	Without liposomal Formulation	PBS

5.3.3 Size and PDI Determination of Liposomes

The mean diameter and the polydispersity index (PDI) of the vesicles were determined by photon correlation spectroscopy (PCS) (Malvern instruments GmbH, Germany) with a scattering angle 90° C at 25° C temperature. During the size measurements a 10 μl liposome suspension diluted with distilled water in a ratio of 1:6 (v:v).

5.3.4 Determination of encapsulation efficiency

According to the modified procedures of Papahadjopoulos and Fishman *et al.*, after preparation of imatinib encapsulated TEL:DPPC liposomes, the 0.5 ml aliquots of the vesicle suspension were transferred into small dialysis bags with MWCO 14000 (Carl Roth GmbH, Karlsruhe, Germany) which were pre-EDTA-washed according to the manufacturer instructions (33, 34). After 4 h dialysis of free imatinib in 500 ml buffer containing 0.5 M NaCl at RT, the aliquots were transferred into individual Eppendorf tubes. Total amount of the entrapped Imatinib was calculated after terminal lysis of the liposomes with Tween 20 (1.0 vol % final concentration) (35). To minimize the absorption of the detergent, for the absorbance measurements of drug content, Tween 20 was chosen. 1.0 vol % final concentration of Tween 20 was mixed with the vesicle suspensions and stirred in order to release the encapsulated drug to the solvent. Encapsulation efficiency was calculated according to Ishii *et al*. (36).

$$\text{Encapsulation efficiency (\%)} = \frac{C_{total} - C_{out}}{C_{total}} \times 100$$

Concentrations of the drug C_{out} and C_{total} were quantitatively analyzed by spectrophotometer (UV Mini 1240, Shimadzu, Suzhou instruments Manufacturing Co. Ltd. Suzhou Jiangsu, China) at a wavelength of 256 nm.

5.3.5 AFM Measurements

Topographic investigations of imatinib encapsulated liposomes were done with Atomic Force Microscopy. Blank and imatinib encapsulated liposomes were separately dropped onto a sample carrier glass and dried in air flow and AFM imaging was performed afterwards. The imagining was carried out with JPK NanoWizard^{TM} (JPK Instruments, Berlin, Germany) equipped with silicon cantilevers NSC 16 AIBS, (Mikromasch, Estonia) with intermittent contact (air) mode. During the imaging, silicon cantilevers with ultra sharp tips were used (radius of the tip curvature <10 nm, resonance frequency ~170 kHz and nominal force constant of ~40 N/m). The scan speeds were proportional to the scan size, and the collected images were 5 x 5 µm.

5.3.6 Cell Lines

Murine Urothelial Carcinoma cell line MB49 (kind gift from Dr. Ulrich Rothe) cultured in Iscove's Modified Dulbecco's Media (IMDM) medium (PAA, Coelbe, Germany) containing 10 % fetal calf serum (FCS) (PAA, Coelbe, Germany) and 1:100 (v/v) Penicillin, Streptomycin mixture. Until implantation, cells were incubated at 37° C with 5 % CO_2.

5.3.7 WST-1 Viability Assay

WST-1 Assay was performed on imatinib and imatinib encapsulated TEL liposomes according to Mueller *et al.* (37). 5000 MB49 cells/well (Murine Urothelial Carcinoma cell line) was incubated for 24 h at 36.5° C and 5 % CO_2 in the growth medium. On the following

day, the medium was changed to IMDM + 0.5 % FCS and incubation continued for 2-4 h at 36.5° C and 5 % CO_2 before treatment. The cells were incubated with various imatinib concentrations of free imatinib solution and imatinib encapsulated TEL solution. The imatinib concentrations of imatinib solutions were: 1.00, $3.30x10^{-1}$, $1.00x10^{-1}$, $3.30x10^{-2}$, $1.00x10^{-2}$, $3.30x10^{-3}$, $1.00x10^{-3}$ mM and the imatinib concentrations in TEL:DPPC liposomes were: 3.43, 1.14, $3.34x10^{-1}$, $1.14x10^{-1}$, $3.43x10^{-2}$, $1.14x10^{-2}$, $3.43x10^{-3}$ µM. To determinate cell viabilities after 24 hours, the cells were incubated in WST-1 reagent (2-(4-iodophenyl)-3-(4-nitrophenyl)-5-(2,4-disulfophenyl)^2 [H] tetrazolium monosodium salt) (Roche, Mannheim Germany), and after 30 minutes the cell viability was assessed according to the manufacturers recommendations and detected by an ELISA micro plate reader at 450 nm, with a 75 W Tungsten halogen lamp light source (Dynatech Laboratories inc. MRX Chantilly, VA, USA). To determine the cell viability after 48 hours, incubation in WST-1 reagent and cell viability detection by the ELISA reader were repeated as explained above. All formulations used for this assay were tested in triplicates and average values were plotted against applied concentrations and presented as sigmoidal curves with OriginPro 8.0 SRO (OriginLab Corporation, USA). The 50 % growth-inhibitory concentration IC_{50} was calculated from interpolations of the graphical data (Mean ± S.E.M).

5.3.8 CAM Assay

Fertilized VALO-SPF eggs were obtained from Lohmann Tierzucht GmbH (Cuxhaven, Germany) and incubated at 37.5° C und with 60 % relative humidity. On the 5th day of incubation approximately 6-7 ml albumin was removed from the fertilized egg to detach the shell from the CAM, as the first described traditional shell model by Knighton *et al*. (27). Subsequently from the upper part of the egg, a window was opened which was approximately

2.5 cm in diameter. To prevent dehydration, the opened shell was sealed with Parafilm® and incubated in under the conditions mentioned above until implantation. On the 10th day sterile gelatin sponges, Gelfoam (Pfizer, Pharmacia & Upjohn Company Kalamazoo, USA) were cut in pieces of approximately 2 mm^3 size and absorbed with 10 µl of cell suspension (approximately 30 000 cell per sponge) of MB49 cell line. Also as negative control group, 2 mm^3 sterile sponges were absorbed with 10 µl of PBS. The sponges were planted gently onto the CAM, to a region where the vessel density was high (38). The egg was sealed again with parafilm and incubated until the 18th day at standard conditions as mentioned above. Daily observations were carried out with a Stereomicroscope (Olympus SZX12, Japan) connected to a Moticam 2000 digital camera (Motic China Group, China). Each image was captured using the software of Motic Images Plus 2.0 ML (China). On the 18th day, tumor samples were cut from CAM, transferred into individual Eppendorf tubes, quickly immersed into liquid nitrogen and stored at -80° C until investigation with Western Blot Analysis.

5.3.9 Western Blot

The tumors cut out from CAM were collected in RIPA lysis buffer (50 mM Tris–HCl, 1 % Nonidet P-40, 150 mM NaCl, 1 mM EDTA,) with 1:20 (v/v) protease (Roche, Mannheim, Germany) and 1:100 (v/v) phosphatase inhibitors (Sigma, Missouri, USA) and homogenised and centrifuged at 2500 rpm for 10 min. at 4° C subsequently. Protein concentration of the supernatant was determined by Bradford protein assay (39, 40). After denaturation at 95° C the proteins for Extracellular signal-regulated kinases 1/2 (ERK 1/2) (20 µg/lane) and for p-ERK (30 µg/lane) into separate gels were loaded into each lane of a 10 lane gel and were size fractionated by 10 % SDS–polyacrylamide gel electrophoresis (Invitrogen, Paisley, UK) and transferred to a nitrocellulose membrane (Whatman, Dassel, Germany). Expression of

proteins was detected by using rabbit primary antibodies, p42/44 MAPK (ERK) and phospho-p24/44 MAPK (p-ERK) (Cell Signalling, Danvers, USA) and an anti-rabbit secondary antibody HRP (GE Healthcare Buckinghamshire, UK) at a dilution of 1:1000 for ERK 1/2 and 1:500 for p-ERK 1/2. Visualization of antibody binding was done by enhanced chemoluminescence (Thermo Scientific, Rockford, USA). To determine the suppression of the protein from the implant samples on the photographic film, the imageJ program (National Institutes of Health, USA) was used.

5.3.10 Statistics

All values are expressed as mean ± standard error of mean (S.E.M). The results of CAM model assays were analyzed by Student's T-Test to determine significant differences in multiple comparisons using SigmaPlot 12.0 (Systat Software, USA). All experiments were carried out in triplicates.

5.4 Results

5.4.1 Mean sizes and polydispersity index of tyrosine kinase inhibitor encapsulated TEL liposome formulations

Unilammelar TEL:DPPC liposomes were generated by pressure extrusion through 0.1 µm polycarbonate membrane filters. The mean diameter for blank TEL:DPPC liposomes were determined as 235.30±2.63 nm with a PDI value of 0.241±0.005. On the other hand the mean diameter of imatinib encapsulated TEL:DPPC liposomes were shifted to 248.83±5.78 nm and PDI to 0.290±0.010.

5.4.2 Encapsulation efficiency

Percent encapsulation efficiency (EE %) was determined as a ratio of imatinib portion remaining inside of the TEL:DPPC liposomes to the amount of total imatinib after filtration and before dialysis, because loss of liposomes was observed during the filtration. To avoid errors, only the lipid amount which contributed to encapsulation was taken into account for the efficiency calculation which was carried on as it was described in the material and methods section. At pH 7.4 EE % of TEL:DPPC liposomes were 86,36 ± 0.88 %. Initial imatinib used for encapsulation was $2.88x10^{-1}$ mM. After filtration and liposome formation, the total encapsulated imatinib amount inside the liposomes was 3.43±0.14 µM. Encapsulation efficiency was calculated according to Nii *et la.* (41).

5.4.3 Morphology

AFM images of TEL:DPPC liposomes with and without entrapped imatinib are shown in Figure 1A and 1B. Both of the formulations showed homogenous and well-defined contours surfaces. Incorporation of imatinib into liposomes resulted in larger vesicles size (Figure 1B). The diameter of these vesicles was between 250-300 nm. This indicated that the interaction between the drug and liposomes involved the size increase in which more liposomes tend to associate. This property of imatinib with DPPC lipids interactions was reported by Beni *et al.* (32).

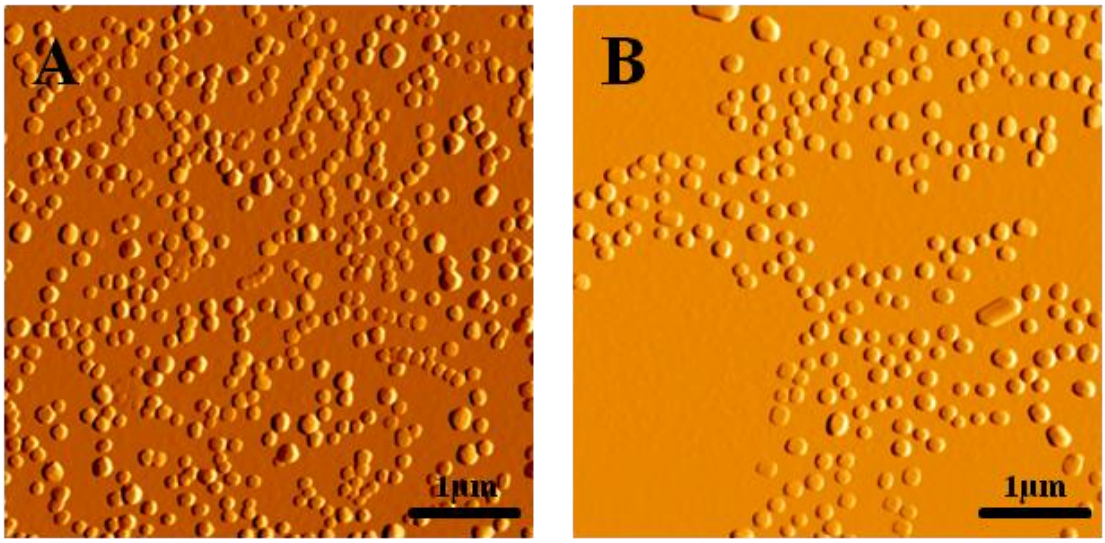

Figure 1. (A) blank TEL:DPPC; (B) imatinib encapsulated TEL:DPPC.

5.4.4 WST-1 Viability Assay

We investigated the viability of blank TEL:DPPC liposomes, imatinib encapsulated TEL:DPPC liposomes and also free imatinib by utilizing a cell proliferation kit containing WST-1. Figure 2A and 2B demonstrate the cell viability after 24 hours incubation (36° C 5 % CO_2). At A_{450} plateaus were determined for blank TEL, imatinib encapsulated TEL and non-encapsulated TEL. With the % cell viabilities, the IC_{50} values for imatinib at 24 hr and 48 hr were calculated. IC_{50} imatinib after 24 hr: $9.68x10^{-2}$ mM; IC_{50} of imatinib after 48 hr: $3.12x10^{-2}$ mM; and IC_{50} of TEL: DPPC liposome after 24 hr: $3.67x10^{-1}$ µM, IC_{50} of TEL: DPPC liposome after 48 hr: $3.14x10^{-1}$ µM. To define the effect of TEL: DPPC (7:3) blank liposome, WST-1 assay was repeated for this formulation as well. The blank liposomes were prepared in concentrations of $6.25x10^{-1}$, $2.08x10^{-1}$, $6.25x10^{-2}$, $2.08x10^{-2}$, $6.25x10^{-3}$, $2.08x10^{-3}$ mM. The IC_{50} of blank TEL: DPPC liposome after 24 hr: 0.066 mM, after 48 hr: 0.085 mM.

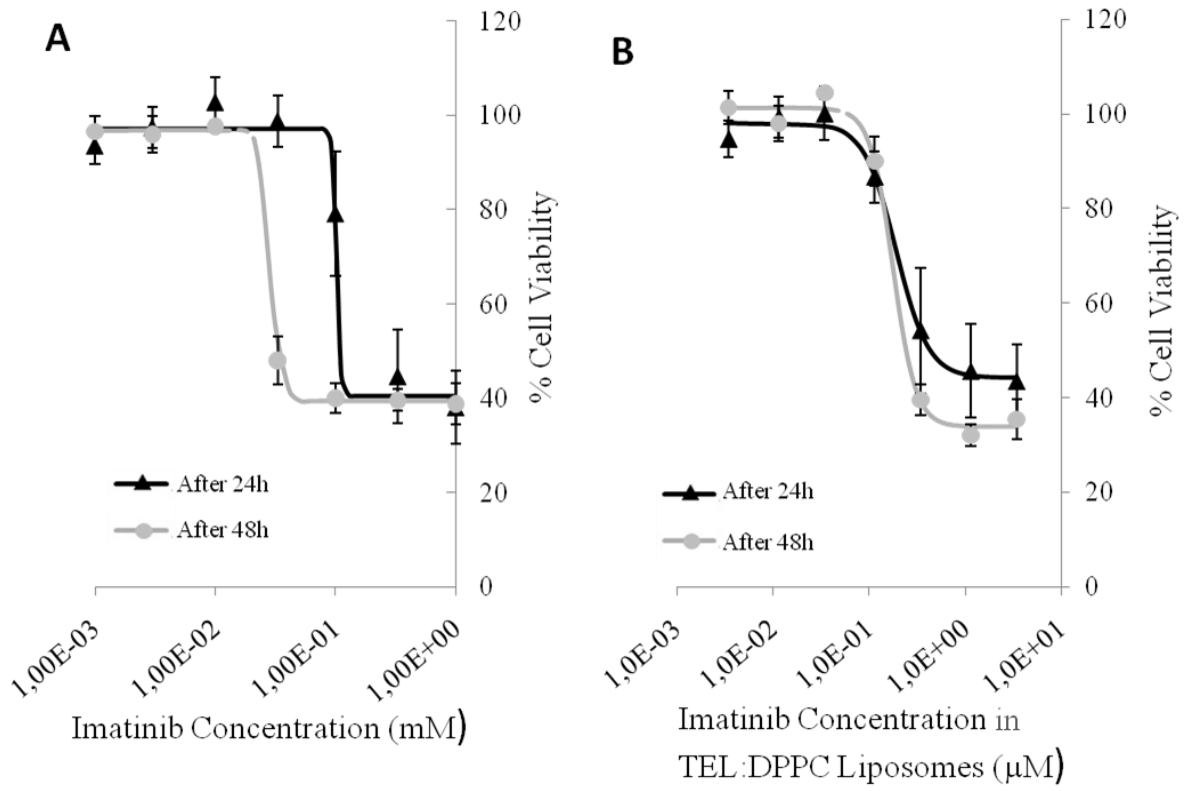

Figure 2. A WST-1 assay was used to quantify MB49 cell viability versus various concentrations of imatinib and imatinib concentrations in TEL:DPPC liposomes. (A) % Cell viability versus imatinib concentration (mM). The imatinib concentrations of imatinib solutions were: 1.00, $3.30x10^{-1}$, $1.00x10^{-1}$, $3.30x10^{-2}$, $1.00x10^{-2}$, $3.30x10^{-3}$, $1.0x10^{-3}$ mM. (B) % cell viability versus the imatinib concentration in TEL:DPPC liposomes, which were: 3.43, 1.14, $3.43x10^{-1}$, $1.14x10^{-1}$, $3.43x10^{-2}$, $1.14x10^{-2}$, $3.43x10^{-3}$ μM. The IC_{50} values were determined as: IC_{50} imatinib after 24 hr: $9.68x10^{-2}$ mM; IC_{50} of imatinib after 48hr: $3.12x10^{-2}$ mM; and IC_{50} of TEL: DPPC liposome after 24 hr: $3.67x10^{-1}$ μM, IC_{50} of TEL: DPPC liposome after 48 hr: $3.14x10^{-1}$ μM.

5.4.5 CAM Assay

Daily microscopic measurements of parallel series of experiments from day 10 to day 18 were undertaken on MB49 cell implants onto CAM, in a total of 39 eggs. From day 13 to the last day of treatment (day 18), imatinib solution (with the concentrations of A:1.0, B:$3.30x10^{-1}$, C:$1.00x10^{-1}$, D:$3.3x10^{-2}$, E:$1.00x10^{-2}$ mM, P: PBS Solution as a negative control) as well as suspensions of imatinib encapsulated TEL:DPPC liposomes (with the imatinib concentrations of TA:3.43, TB:1.14, TC:$3.43x10^{-1}$, TD:$1.14x10^{-1}$, TE:$3.34x10^{-2}$ μM, TO: Blank TEL:DPPC liposomes without imatinib content, TP:PBS Solution as a negative control) with the volume of 10 μl were topically applied to the implants.

The anti-angiogenic responses to free imatinib and imatinib encapsulated TEL:DPPC liposomes in the time-course were monitored from day 13 until day 18.

The implants were treated with various imatinib concentrations of the imatinib encapsulated liposome and free imatinib solution as well as blank liposomes and PBS. Both free imatinib and imatinib encapsulated liposomal treatments resulted in significant responses to the anti-angiogenic agent, with the decrease of the number of allantoic vessels proportionally to the concentration of the agent (Figure 4, 5, 6 and 7). The anti-angiogenic responses were illustrated with “vessel total diameter/ tumor circumference” and “vessel total diameter/vessel amount” versus treatment day, to provide a distinctive aspect to the anti-angiogenic effect on vessel deformation independently from the implant size. The illustration of the data in the form of “vessel total diameter/tumor circumference” serves this cause. Also the “vessel total diameter/vessel amount” versus treatment day provides a perspective on the anti-angiogenic effect on the blood vessels. On the 5^{th} day of treatment the highest concentration of the imatinib (A) or encapsulated imatinib liposome (TA), a few blood vessels could still be

recognized. Indeed, with PBS topical application on to the implant on CAM (Figure 3), no anti-angiogenic effect was exerted. Beside implant surface area numerous allantoic vessels developed in a spoked-wheel pattern towards the implant. Supplementary Table 1 and 2 provide the quantification of the anti-angiogenic response performed from day 13 to day 18 with standard error of the mean of all triplicates. The results shown in Figure 4, 5, 6 and 7 confirmed the morphological observations. When highest concentration of imatinib solution (A) was applied topically on the implant, vessel total diameter/tumor circumference ratio and vessel total diameter/vessel amount ratio were significantly decreased in comparison to the control implants. It was shown that the anti-angiogenic effect was strictly dependent on the concentration of the imatinib solution. On the other hand, during the liposomal treatment this concentration difference showed no significant effect. Also we observed a relatively late anti-angiogenesis response to the liposomal treatment compared to free imatinib solution. Moreover blank liposomes applied to the implants indicated no significant difference in comparison to control group.

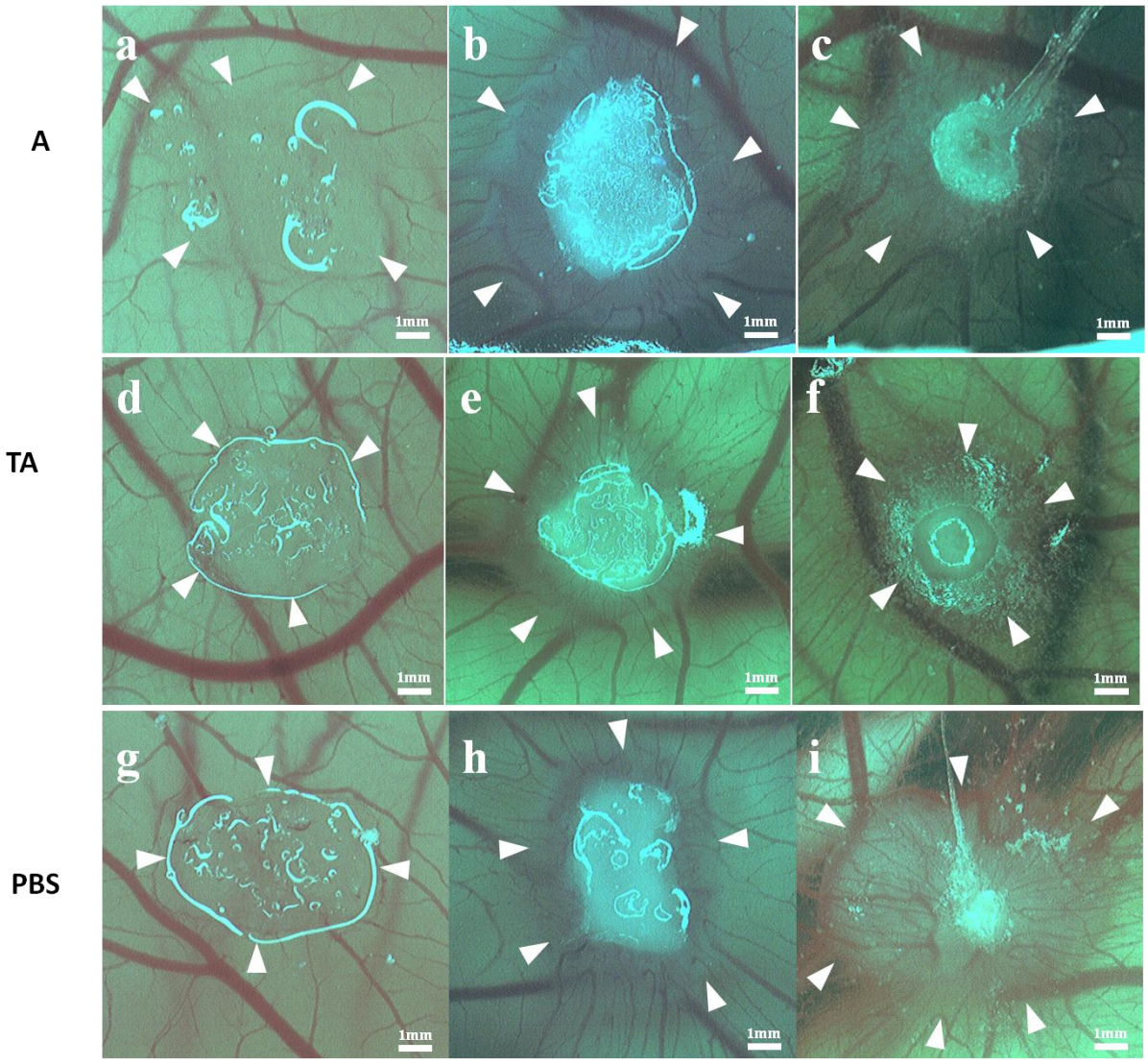

Figure 3. Time-course of the macroscopic appereance of a CAM implant. The sponges absorbed with 30.000 MB49 cells were implanted on day 10 (a, d, g). On day 13 before first topical treatments, vascular reaction was detected (b, e, h). On day 18 before the removal of implants the tumor and vessel morphology were investigated (c, f, i). On all images, numerous allantoic vessel were oriented towards the implant in a spoked-wheel pattern. In group A, the implants were treated with imatinib solution (1.0 mM) (b, c). Group TA was treated with imatinib encapsulated in TEL:DPPC liposomes (3.43 µM) (e, f). PBS: negative control group (h, i). Arrowheads indicate tumor outline.

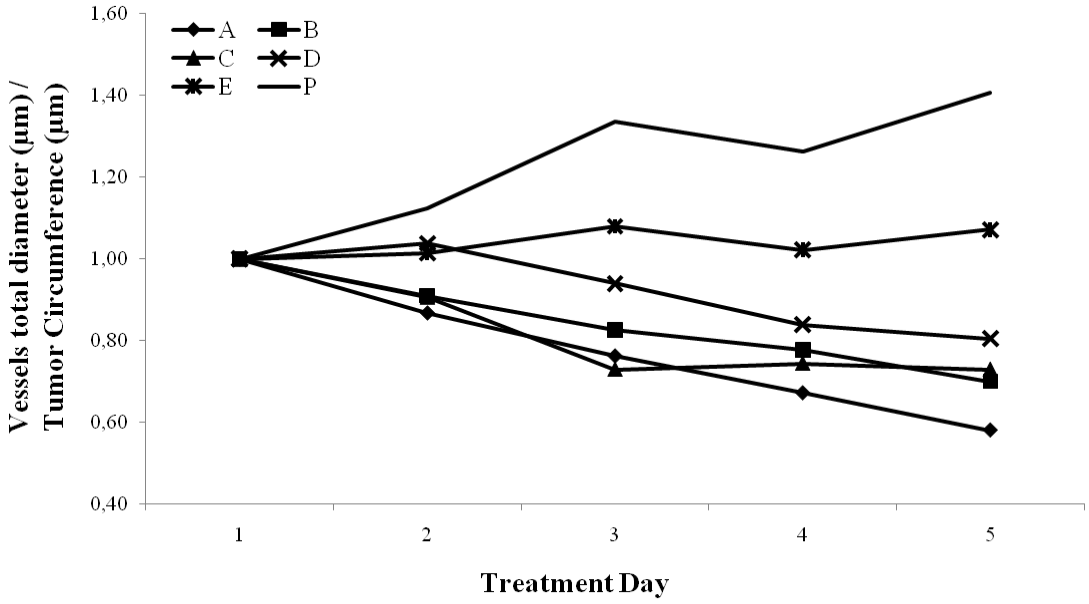

Figure 4. Vessel total diameter (µm) /Tumor circumference (µm), after the treatment with imatinib solution with various concentrations of imatinib (A:1.0, B:$3.30x10^{-1}$, C:$1.00x10^{-1}$, D:$3.30x10^{-2}$, E:$1.0x10^{-2}$ mM, P: PBS solution as negative control). $P < 0.05$ for A, B, C, D versus PBS treatment, $P< 0.1$ for E versus PBS treatment.

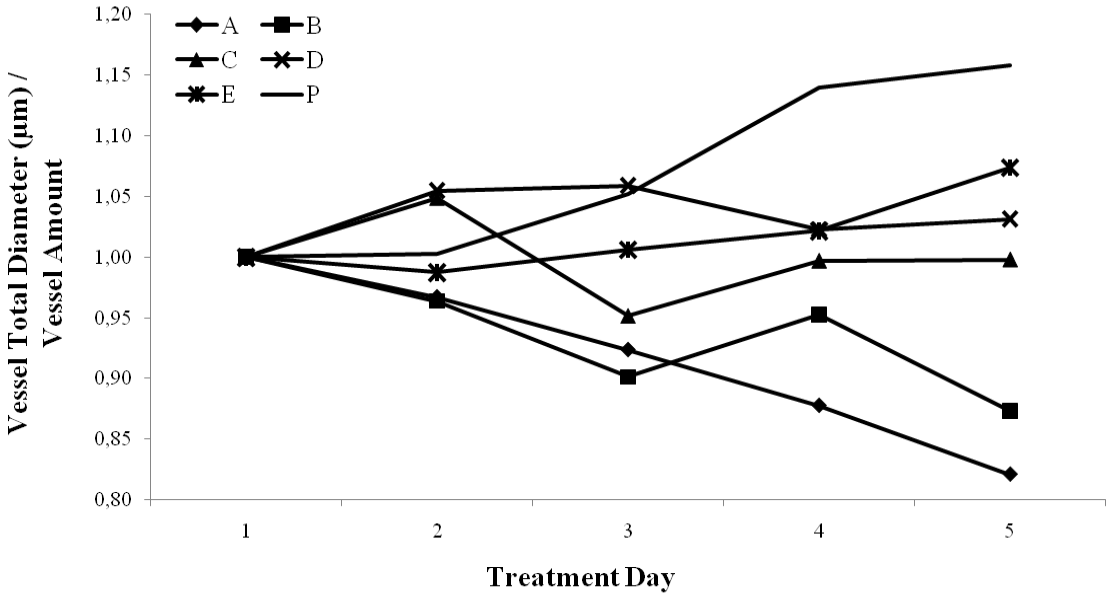

Figure 5. Vessel total diameter (µm) /Vessel amount, after the treatment with imatinib solution with various concentration of imatinib (A:1.0, B:$3.30x10^{-1}$, C:$1.00x10^{-1}$, D:$3.30x10^{-2}$, E:$1.00x10^{-2}$ mM, P: PBS solution as negative control). $P < 0.05$ for A, B, C, D versus PBS treatment, $P < 0.1$ for E versus PBS treatment.

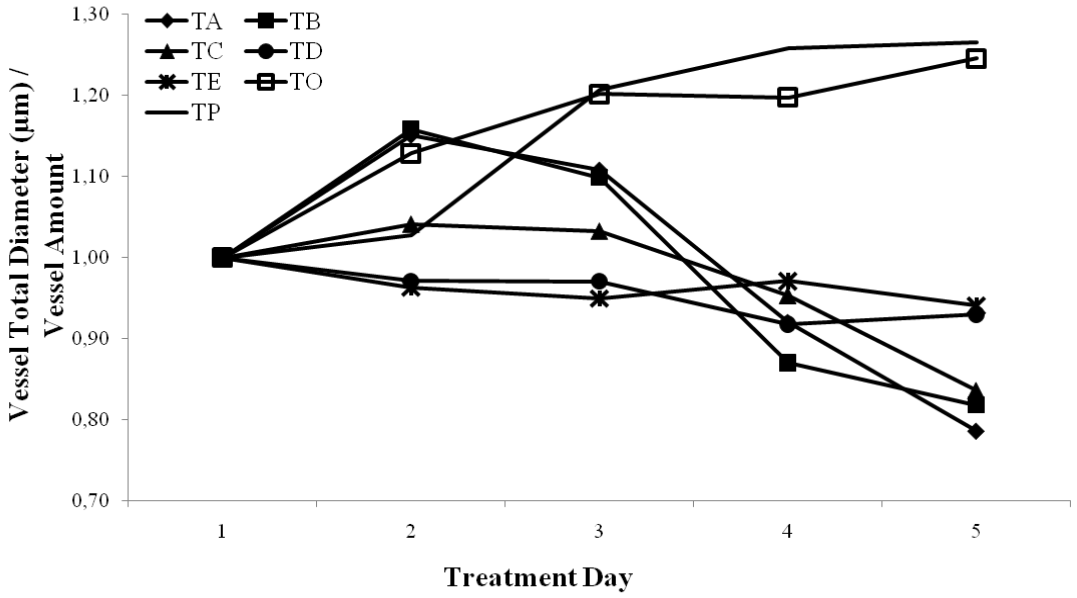

Figure 6. Vessel total diameter (µm) /Vessel amount, after the treatment with imatinib encapsulated TEL:DPPC liposomes with various concentrations of imatinib (TA:3.43, TB:1.14, TC:$3.43x10^{-1}$, TD:$1.14x10^{-1}$, TE:$3.43x10^{-2}$ µM TO: TO: Blank TEL:DPPC liposomes without imatinib content, TP:PBS solution as negative control). $P < 0.001$ for TA, TB, TC, TD versus PBS treatment, $P < 0.05$ for TE versus PBS treatment, $P < 0.7$ for TO versus PBS treatment.

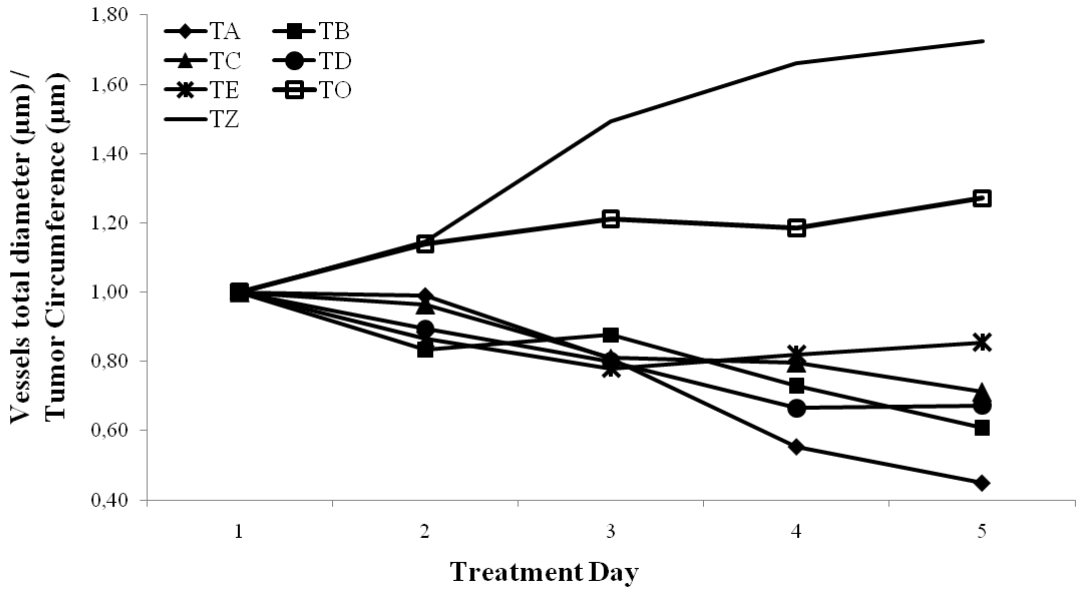

Figure 7. Vessel total diameter (µm) /Vessel amount, after the treatment with imatinib encapsulated TEL:DPPC liposomes with various concentration of imatinib (TA:3.43, TB:1.14, TC:$3.43x10^{-1}$, TD:$1.14x10^{-1}$, TE:$3.43x10^{-2}$ µM, TO: Blank TEL:DPPC liposomes without imatinib content, TP:PBS solution as a negative control). $P < 0.001$ for TA, TB, TC, TD versus PBS treatment, $P < 0.05$ for TA, TB, TC, TD versus PBS treatment, $P < 0.6$ for TE versus PBS treatment, $P < 0.8$ for TO versus PBS treatment.

5.4.6 Western Blot

The analysis of the anti-angiogenesis effect of imatinib encapsulated in TEL:DPPC liposomes on the implants on CAM was also carried out via Western Blot. In Western Blot measurements, proteins were prepared from the CAM implants and loaded onto the gel (20 µg for total ERK 1/2 and 30 µg for p-ERK 1/2). We took MB49 cell lysate and PBS treated implants from the CAM as negative controls. Western Blot results using both ERK 1/2 and p-ERK 1/2 antibodies indicate that there were differences of expression between PBS treated

and other treated implant samples removed from the CAM. Our results suggest that the highest inhibition was achieved with the treatment of TA group (Figure 8 and 9). Although the imatinib concentration applied to TA group was much lower than imatinib solution applied to (A) group. The TEL:DPPC blank liposome (TO) showed no significant difference to the control group. From the samples we have tested, only TA showed a significant difference to the control group.

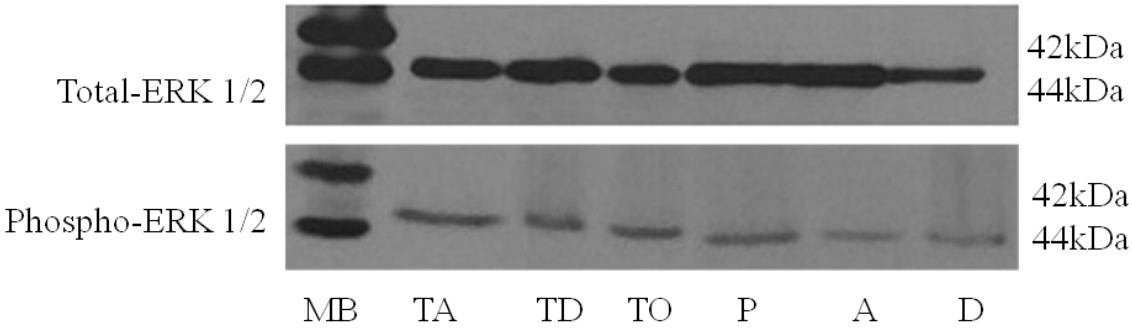

Figure 8. The total ERK 1/2 and phosphorilation of ERK 1/2 were determined by Western Blot analysis. For total ERK 1/2, 20 µg protein/lane, for phosphorilation ERK 1/2, 30 µg protein/lane were used. MB: MB49 cell lysate. TA, TD: implant groups removed from the CAM, treated with TEL:DPPC liposomes, entrapped imatinib concentrations: TA:3.43, TD:1.14×10^{-1} µM. A, D: implant groups removed from the CAM, treated with free imatinib solutions, concentrations A:1.0, D:3.30×10^{-2} mM. P: implant group, treated with PBS, negative control.

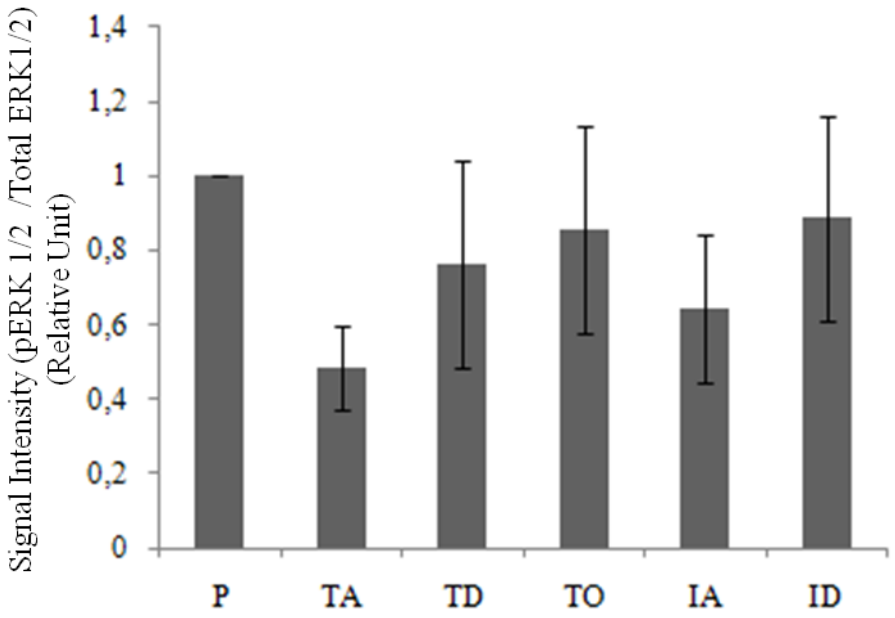

Figure 9. Signal Intensity of pERK 1/2 Total ERK 1/2. P values were calculated versus P (with PBS treatment) TA: $p < 0.01$, TD: $p < 0.5$, TO: $p < 0.7$, IA: $p < 0.2$, ID: $p < 0.7$. Mean ± S.E.M.

5.5 Discussion and Conclusion

In cancer therapy the use of chemotherapeutics is limited due to common damaging side effects. Hence, drug delivery systems have gained importance for lowering the daily doses and preventing side effects. However, there are several drawbacks that restrain the use of conventional liposomal carriers (42). Thus we employed TEL liposomes incorporated with a tyrosine kinase inhibitor. TEL liposomes were characterized by mean diameter, PDI and morphology. The mean size diameters of the liposomes were limited by extrusion through polycarbonate membrane filters; nevertheless, it was observed that imatinib encapsulated liposomes yielded larger than blank liposomes. Beni *et al.* has reported aggregation between DPPC liposomes due to molecular interaction of imatinib a DPPC liposomes (32). Although we have tailored the liposomes with 7:3 molar ratio of TEL:DPPC lipids, we observed smoothly shaped particles with a low ratio of aggregation in AFM images. This might be caused by a relatively high proportion of stable TELs in the liposome formulation. The TELs that we have employed in this study were extracted from biomass. As they were not purified, all cell components dissolved in $CHCl_3$:MeOH (2:1, v/v) were present during the liposome preparations. During the experiment, we have filtered liposome suspensions through 0.45 mm filters. It was assumed that imatinib encapsulated liposomes may have grown larger and remained on the filter and could not flow through. This could provide an explanation to the decrease of the final concentration of imatinib encapsulated within TEL liposomes. Despite the relatively low final imatinib concentration, we observed effective anti-angiogenesis and anti-tumor effects during WST-1 and CAM assays.

We monitored the anti-angiogenic effect of imatinib and imatinib encapsulated within TEL:DPPC liposomes in a CAM assay during chick embryo development. The CAM assay is

a well-defined assay to provide a large perspective on blood vessels through angiogenic and anti-angiogenic responses. In this study it was demonstrated that MB49 cells induced vasoproliferation on CAM until treatment. After the first day of topical application of imatinib solution and imatinib encapsulated TEL:DPPC liposomes on the implants, this vasoproliferative effect showed significant decrease in comparison to the control treatment (PBS). Imatinib is a protein tyrosine kinase inhibitor, which has been defined to have a suppressive effect on Bcr-Abl, c-kit and platelet-derived growth factor receptor (PDGFR) (43). PDGFR is also known to be over-expressed during several vasculoproliferative diseases (44). Kim *et al.* reported that imatinib has an anti-angiogenesis effect due to targeting PDGF/PDGFR-signalling pathway beside in addition to an anti-tumor effect (45). A few years ago also anti-angiogenic effects of imatinib were reported by Kim *et al.* and Kvasnicka *et al.* (20, 45). Therefore in the current study we focused on imatinib mediated angiogenic suppression. It was reported that imatinib reduces the Bcr-Abl mediated secretion on VEGF (46). In the literature there is a lack of data concerning the anti-angiogenesis effect of imatinib encapsulated TEL. Hence, we have examined free imatinib and imatinib encapsulated liposomes to provide a clear perspective of their effects on CAM micro-vessels. However, it was relatively difficult to distinguish the total anti-angiogenesis effect of free imatinib and encapsulated imatinib on the CAM assay. Highest concentration of imatinib (A) has a similar effect on anti-angiogenesis as the imatinib encapsulated liposomes (TA). On the other hand, lower concentration of encapsulated imatinib in TEL:DPPC liposomes (TE) exhibits no significant difference to higher concentration of liposomal encapsulated imatinib (TA). This indicates that with the encapsulated drug, a much lower concentration is sufficient to provide a similar anti-angiogenic effect.

Before *in ovo* applications, we determined the effect of free imatinib and imatinib encapsulated liposomes on cell viability via WST-1 assay. After incubation with various

imatinib concentration of for free imatinib and liposomes, after 24 hours and 48 hours, a significant change was observed in comparison to control group on MB49 cells. It was also determined that the imatinib encapsulated liposomes -although having much lower concentration of imatinib- provided a similar effect on cell viability as the free imatinib itself. The maximum effect of free imatinib on the WST-1 assay was reached after 48 hours (Figure 2A). In contrast, imatinib encapsulated liposomes already reached maximum efficiency after 24 hours (Figure 2B). The blank TEL:DPPC liposomes might have caused an impact on cell viability as well. It was found that after 24 hours the IC_{50} of blank TEL:DPPC liposomes was $6.6x10^{-2}$ mM; this value was almost stable after 48 hours: 0.085 mM (data not shown). This characteristic could support imatinib function and therefore be a reason for better inhibition despite much lower imatinib concentration encapsulated in liposomes. These results were also supported by Western blot analysis (Figure 9).

The cell proliferation on the CAM occurred diversely because of different circumstances during the cell growth process on the CAM due to the vascularisation and the distance to the vascular dense regions. Due to the nature of the procedure, during the removal of the implant from the CAM, connected egg tissue, such as membrane, blood vessels, blood, chorioallantoic fluid were removed together with the implant and involved in the Western Blot assay. Hence the assay always included some variable amount of quantified kinase from untreated tissue, resulting in a larger error value. Nevertheless, the Western blot results support the findings from the CAM assay. It is known that the ERK 1/2 pathway leads to the expression of VEGF; it is activated by multiple extracellular stimuli, including growth factors and it is a downstream target of Bcr-Abl (47). The treatment with imatinib encapsulated TEL:DPPC liposomes at the highest concentration of imatinib (TA) was found to result in a lowered concentration of pERK 1/2 (Figure 9) and therefore might have a significant effect on inhibition of VEGF expression.

Our results show that the imatinib encapsulated TEL:DPPC liposomes, despite much lower imatinib content than used with free imatinib, elicited an anti-angiogenic response which was correlated to the inhibition of the tyrosine kinase signal transduction cascade.

In conclusion, during the first five days after free imatinib treatment and imatinib encapsulated liposome treatment, a significant anti-angiogenesis response was detected. The suppression efficiency was concentration dependant.

Considering applications in cancer therapy, very stable TEL liposomes with appropriate release properties may play an important role in minimizing side effects of potentially harmful pharmaceuticals by reducing the amount of applied drug.

Supplementary Table 1. The Normalized Values of Vessels total diameter (μm)/Tumor Circumference (μm) and Normalized Values of Vessel Total Diameter (μm) /Vessel Amount with the treatment of various concentrations of free imatinib data were presented in the presence of mean ± S.E.M

Formulation	Treatment Day	Normalized Values of Vessels total diameter (μm) /Tumor Circumference (μm) ± S.EM.	Normalized Values of Vessel Total Diameter (μm) /Vessel Amount ± S.E.M
A	**1**	1.00 ± 0.00	1.00 ± 0.00
	2	0.87 ± 0.05	0.97 ± 0.06
	3	0.76 ± 0.08	0.92 ± 0.07
	4	0.67 ± 0.09	0.88 ± 0.09
	5	0.58 ± 0.08	0.82 ± 0.07
B	**1**	1.00 ± 0.00	1.00 ± 0.00
	2	0.91 ± 0.06	0.96 ± 0.05
	3	0.83 ± 0.09	0.90 ± 0.01
	4	0.78 ± 0.15	0.95 ± 0.04
	5	0.70 ± 0.13	0.87 ± 0.02
C	**1**	1.00 ± 0.00	1.00 ± 0.00
	2	0.91 ± 0.16	1.05 ± 0.20
	3	0.73 ± 0.12	0.95 ± 0.15
	4	0.74 ± 0.17	0.99 ± 0.14
	5	0.73 ± 0.16	0.99 ± 0.14
D	**1**	1.00 ± 0.00	1.00 ± 0.00
	2	1.04 ± 0.03	1.05 ± 0.08
	3	0.94 ± 0.05	1.06 ± 0.09
	4	0.84 ± 0.07	1.02 ± 0.07
	5	0.80 ± 0.08	1.03 ± 0.09
E	**1**	1.00 ± 0.00	1.00 ± 0.00
	2	1.01 ± 0.09	0.99 ± 0.06
	3	1.08 ± 0.12	1.01 ± 0.07
	4	1.02 ± 0.18	1.02 ± 0.05
	5	1.07 ± 0.14	1.07 ± 0.06
P	**1**	1.00 ± 0.00	1.00 ± 0.00
	2	1.12 ± 0.09	1.00 ± 0.01
	3	1.33 ± 0.13	1.05 ± 0.01
	4	1.26 ± 0.17	1.14 ± 0.09
	5	1.41 ± 0.29	1.16 ± 0.10

Supplementary Table 2. The Normalized Values of Vessels total diameter (µm)/Tumor Circumference (µm) and Normalized Values of Vessel Total Diameter (µm) /Vessel Amount with the treatment of various concentrations of imatinib encapsulated TEL:DPPC liposomes data were presented in the presence of mean ± S.E.M

Formulation	Treatment Day	Normalized Values of Vessels total diameter (µm) /Tumor Circumference (µm) ± S.EM.	Normalized Values of Vessel Total Diameter (µm) /Vessel Amount ± S.E.M
TA	**1**	1.00 ± 0.00	1.00 ± 0.00
	2	0.99 ± 0.14	1.15 ± 0.11
	3	0.80 ± 0.06	1.10 ± 0.06
	4	0.55 ± 0.01	0.92 ± 0.04
	5	0.44 ± 0.08	0.79 ± 0.07
TB	**1**	1.00 ± 0.00	1.00 ± 0.00
	2	0.83 ± 0.03	1.16 ± 0.03
	3	0.87 ± 0.05	1.10 ± 0.13
	4	0.72 ± 0.09	0.87 ± 0.12
	5	0.60 ± 0.05	0.82 ± 0.10
TC	**1**	1.00 ± 0.00	1.00 ± 0.00
	2	0.96 ± 0.05	1.04 ± 0.06
	3	0.81 ± 0.08	1.03 ± 0.14
	4	0.80 ± 0.07	0.95 ± 0.07
	5	0.71 ± 0.06	0.84 ± 0.10
TD	**1**	1.00 ± 0.00	1.00 ± 0.00
	2	0.89 ± 0.07	0.97 ± 0.03
	3	0.80 ± 0.05	0.97 ± 0.07
	4	0.67 ± 0.08	0.92 ± 0.07
	5	0.67 ± 0.13	0.93 ± 0.08
TE	**1**	1.00 ± 0.00	1.00 ± 0.00
	2	0.86 ± 0.12	0.96 ± 0.09
	3	0.78 ± 0.07	0.95 ± 0.08
	4	0.82 ± 0.15	0.97 ± 0.13
	5	0.86 ± 0.16	0.94 ± 0.11
TO	**1**	1.00 ± 0.00	1.00 ± 0.00

	2	1.14 ± 0.12	1.13 ± 0.08
	3	1.22 ± 0.21	1.20 ± 0.10
	4	1.18 ± 0.20	1.20 ± 0.05
	5	1.27 ± 0.22	1.25 ± 0.11
TP	**1**	1.00 ± 0.00	1.00 ± 0.00
	2	1.15 ± 0.02	1.03 ± 0.08
	3	1.49 ± 0.13	1.21 ± 0.15
	4	1.66 ± 0.20	1.26 ± 0.18
	5	1.72 ± 0.20	1.27 ± 0.16

5.6 References

1. Gregoriadis, G. (1991) Overview of Liposomes. Vol. 28 B pp. 39-48, J Antimicrob Chemother
2. James, J. S. (1995) DOXIL approved for KS. Vol. 236:6, AIDS Treat News
3. Torcilin, V. P. (2005) Recent advances with liposomes as pharmaceutical carriers. Vol. 4 pp. 145-160, Nat Rev Drug Dis
4. Storm, G., and Crommelin, D. J. A. (1998) Liposomes: quo vadis? Vol. 1 pp. 19-31, PSTT
5. Darland, G., Brock, T. D., Samsonoff, W., and Conti, S. F. (1970) A thermophilic, acidophilic mycoplasm isolated from a coal refuse pile. Vol. 170 pp. 1416-1418, Science
6. Jacquemet, A., Barbeau, J., Lemiégre, L., and Benvegnu, T. (2009) Archaeal tetraether bipolar lipids: Structures, functions and applications. Vol. 91(6) pp. 711-717, Biochimie
7. Freisleben, H. J., Henkel, L., Gutermann, R., Rudoph, P., John, G., Sternberg, B., Winter, S., and Ring, K. (1994) Fermentor cultivation of *Thermoplasma acidophilum* for the production of cell mass and of the main phospholipid fraction. Vol. 40 pp. 745-752, Appl Microbiol Biotechnol
8. Bakowsky, U., Rothe, U., Antonopoulos, E., Martini, T., Henkel, L., and Freisleben, H. K. (2000) Monomolecular organization of the main tetraether lipid from Thermoplasma acidophilum at the water-air interface. Vol. 105 pp. 31-42, Chem Phys Lip

9. Hanford, M. J., and Peeples, T. L. (2002) Archaeal Tetraether Lipids Unique Structures and Applications. Vol. 97(1) pp. 45-62, Appl Biochem Biotechnol

10. Ozcetin, A., Mutlu, S., and Bakowsky, U.. (2010) Archaebacterial Tetraetherlipid Liposomes. Vol. 605 pp. 87-96, Met Mol Biol

11. Buchdunger, E., Cioffi, C. L., Law, N., Stover, D., Ohno-Jones, S., Druker, B. J., and Lydon, N. B. (2000) Abl protein-tyrosine kinase inhibitor STI571 inhibits in vitro signal transduction mediated by c-Kit and platelet-derived growth factor receptors. Vol. 295 pp. 139-145, J Pharmacol Exper Ther

12. Joensuu, H., Roberts, P. J., Sarlomo-Rikala, M., Andersson, L. C., Tervahartiala, P., Tuveson, D., *et al.* (2001) Effect of the tyrosine kinase inhibitor STI571 in a patient with a metastatic gastrointestinal stromal tumor. Vol. 344 pp. 1052-1056, N Engl J Med

13. Sjöblom, T., Shimizu, A., O'Brien, K. P., Pietras, K., Dal Cin, P., Buchdunger, E., Dumanski, J. P., Ostman, A., and Heldin, C. H. (2001) Growth inhibition of dermatofibrosarcoma protuberans tumors by the platelet-derived growth factor receptor antagonist STI571 through induction of apoptosis. Vol. 61 pp. 5778-5783, Cancer Res

14. Lugo, T. G., Pendergast, A. M., Muller, A. J., and Witte, O. N. (1990) Tyrosine kinase activity and transformation potency of bcr-abl oncogene products. Vol. 247 pp. 1079-1082, Science

15. Peggs, K., and Mackinnon, S. (2003) Imatinib mesylate—the new gold standard for treatment of chronic myeloid leukemia. Vol. 348 pp. 1048-1050, N Engl J Med

16. Peng, B., Hayes, M., Druker, B., Talpaz, M., Sawyers, C., Resta, D., *et al.* (2000) Clinical pharmacokinetics and pharmacodynamics of STI571 in a Phase I trial in

chronic myelogenous leukemia (CML) patients. Vol. 41 pp. 544, Proc Am Assoc Cancer

17. De Giorgi, U., Aliberti, C., Benea, G., Conti, M., and Marangolo, M. (2005) Effect of Angiosonography to Monitor Response During Imatinib Treatment in Patients with Metastatic Gastrointestinal Stromal Tumors. Vol. 6171 pp. 158-162, Clin Cancer Res
18. Prabhash, K., Sastry, P. S. R. K., Biswas, G., Bakshi, A., Prasad, N., Menon, H., and Parikh, P. M. (2005) Pregnancy outcome of two patients treated with imatinib. Vol. 12 pp. 1983-1984, Ann Oncol
19. Rocha, A., Azevedo, I., and Soares, R. (2007) Anti-angiogenic effects of imatinib target smooth muscle cells but not endothelial cells. Vol. 10 pp. 279-286, Angiogenesis
20. Kvasnicka, H. M., Thiele, J., Staib, P., Schmitt-Graeff, A., Griesshammer, M., Klose, J., Engels, K., and Kriener, S. (2004) Riversal of bone marrow angiogenesis in chronic myeloid leukemia following imatinib meslate (STI571) therapy. Vol. 103(9) pp. 3549-3552, Blood
21. Folkman, J. (1971) Tumor angiogenesis: therapeutic implications. Vol. 285 pp. 1182–1186, N Engl J Med
22. Schaeffer, H. E., and Krohn, D. (1982) Liposomes in topical drug delivery. Vol. 22(2) pp. 220-227, Invest Ophthalmol Vis Sci
23. Ribatti, D. (2008) Chick Embryo Chorioallantoic membrane as a useful tool to study angiogenesis. Vol. 270 pp. 181-224, Int Rev Cel Mol Biol
24. Ribatti, D., and Vacca, A. (1999) Models for studying angiogenesis in vivo. Vol. 14 pp. 207-213, Int. J. Biol Markers

25. Leene, W., Duyzings, M. J. M., and Von Steeg, C. (1973) Lymphoid stem cell identification in the developing thymus and bursa of Fabricius of the chick. Vol. 136 pp. 521–533, Z Zellforsch

26. Zwadlo-Klarwasser, G., Gorlitz, K., Hafemann, B., Klee, D., and Klosterhalfen, B. (2001) The chorioallantoic membrane of the chick embryo as a simple model for the study of the angiogenic and inflammatory response to biomaterials. Vol. 12 pp. 195–199, J Mater Sci, Mater Med

27. Knighton, D., Ausprunk, D., Tapper, D., and Folkman, J. (1977) Avascular and vascular phases of tumor growth in the chick embryo. Vol. 35 pp. 347–356, Br J Cancer

28. De Magalhaes, N., Liaw, L.-H. L., and Berns, M. (2010) An Instruction on the In Vivo Shell-Less Chorioallantoic Membrane 3-Dimensional Tumor Spheroid Model. Vol. 62 pp. 279–283, Cytotechnol

29. Hammer-Wilson, M. J., Cao, D., Kimel, S., and Berns, M. W. (2002) Photodynamic parameters in the chick chorioallantoic membrane (CAM) bioassay for photosensitizers administered intraperitoneally (IP) into the chick embryo. Vol. 1 pp. 721–728, Photochem Photobiol Sci

30. Hornung, R., Hammer-Wilson, M. J., Kimel, S., Liaw, L. H., Tadir, Y., and Berns, M. W. (1999) Systemic application of photosensitizers in the chick chorioallantoic membrane (CAM) model: photodynamic response of CAM vessels and 5-aminolevulinic acid uptake kinetics by transplantable tumors. Vol. 49 pp. 41–49, J Photochem Photobiol, B Biol

31. Pastorino, F., Brignole, C., Di Paolo, D., Nico, B., Pezzolo, A., Marimpietri, D., Pagnan, G., Piccardi, F., Cilli, M., Longhi, R., Ribatti, D., Corti, A., Allen, T. M., and Ponzoni, M. (2006) Targeting liposomal chemotherapy via both tumor cell-specific

and tumor vasculature-specific ligands potentiates therapeutic efficacy. Vol. 66 pp. 10073–10082, Cancer Res

32. Béni, S., Budai, M., Noszal, B., and Grof, P. (2006) Molecular interactions in imatinib–DPPC liposomes. Vol. 27 pp. 205–211, Eur J Pharma Sci

33. Papahadjopoulos, D. (1970) III. Antagonistic Effets of Ca^{2+} and local anesthetics the permeability of phosphatidylserine Vesicles. Vol. 211 pp. 467-477, Biochim Biophys Acta

34. Fishman, P. H., Peymon, G. A., and Lesar, T. (1986) Intravitreal Liposome-Encapsulated Genfamicin in a Rabbit Model. Vol. 27 pp. 1103-1106, Invest Ophthalmol Vis Sci

35. Lelkes, P. I., and Tandeter, H. B. (1982) Studies on the methodology of the carboxyfluorescein assay and on the mechanism of liposome stabilization by red blood cells in vitro. Vol. 716 pp. 410-419, Biochim Biophysica Acta

36. Ishii, F., and Nii, Y. (2001) Simple and convenient method for estimation marker entrapped in liposomes. Vol. 22 pp. 97–101, J Dispersion Sci Technol

37. Mueller, L., Goumas, F. A., Himpel, S., Brilloff, S., Rogiers, X., and Broering, D. C. (2007) Imatinib mesylate inhibits proliferation and modulates cytokine expression of human cancer-associated stromal fibroblast from colorectal metastases. Vol. 250 pp. 329-338, Cancer Lett

38. Ribatti, D., Gualandris, A., Bastaki, M., Vacca, A., Iuraro, M., Roncali, L., and M., P. (1997) New model for the study of angiogenesis antiangiogenesis in the chick embryo chorioallantoic membrane: the gelatine sponge/chorioallantoic membrane assay. Vol. 34 pp. 455-463, J Vasc Res

39. Bradford, M. M. (1976) A rapid and sensitive method for the quantitation of microgram quantities of protein utilizing the principle of protein-dye binding. Vol. 72 pp. 248-254, Anal Biochem

40. Kruger, N. J., and Walker J. M. (Ed) (1996) The Protein Protocols Handbook. DOI:1007/978-1-60327-257-9_4 pp. 15-20, Humana Press Inc., Totowa, NJ

41. Nii, T., and Ishii, F. (2005) Encapsulation efficiency of water-soluble and insoluble drugs in liposomes prepared by the microencapsulation vesicle method. Vol. 298 pp. 198-205, Int J Pharma

42. Andresen, T. L., Jensen, S. S., and Jørgense, K. (2005) Advanced strategies in liposomal cancer therapy: Problems and prospects of active and tumor specific drug release. Vol. 44(1) pp. 68-97, Prog Lipid Res

43. Meco, D., Riccardi, A., Servidei, T., Brueggen, J., Gessi, M., Riccardi, R., and Dominaci, C. (2005) Antitumor activity of imatinib mesylate in neuroblastoma xenografs. Vol. 228 pp. 211-219, Cancer Lett

44. Ostman, A. (2004) PDGF receptors-mediators of autocrine tumor growth and regulators of tumor vasculature and stroma. Vol. 15 pp. 275–286, Cytokine Growth Factor Rev

45. Kim, R., Emi, M., Arihiro, K., Tanabe, K., Uchida, Y., and Toge, T. (2005) Chemosensitization by STI571 targeting the platelet-derived growth factor/Platelet-derived growth factor receptor-signaling pathway in the tumor progression and angiogenesis of gastric carcinoma. Vol. 103(9) pp. 1800–1809, Cancer

46. Ebos, J. M., Tran, J., Master, Z., Dumont, D., Melo, J. V., Buchdunger, E., and Kerbel, R. S. (2002) Imatinib mesylate (STI571) reduces Bcr-Abl-mediated vascular endothelial growth factor secretion in chronic myelogenous leukemia. Vol. 1 pp. 89-95, Mol Cancer Res

47. Legros, L., Bourcier, C., Jacquel, A., Mahon, X.-F., Cassuto, J.-P., Auberger, P., and Pagés, G. (2004) Imatinib mesylate (STI571) decreases the vascular endothelial growth factor plasma concentration in patients with chronic myeloid leukemia. Vol. 104(2) pp. 495-501, Blood

6 Summary and Perspectives

6.1 Summary

Liposomes currently have a broad spectrum of medical applications, especially in diagnostics and therapy. Stability of the liposomal drug carriers is one of the most important limitations, which concerns fast elimination of vesicles in the human body. Therefore in this thesis, very stable tetraether lipid liposomes were prepared and characterized. The study consists of the investigation of stability properties of tetraether lipid liposomes, the lectin conjugation onto the liposomal membrane, tyrosine kinase inhibitor encapsulation and characterization of these liposomes. These investigations were structured in five chapters:

Chapter 1 introduced the tetraether lipid liposomes, their extraction and preparation methods, stability properties and pharmaceutical applications. In this context, modification and application of the tetraether lipid liposomes as drug delivery systems were also discussed. This chapter focused on the application of liposomes in the field of cancer therapy as anti-angiogenic drug carriers.

Chapter 2 describes the tetraether lipid liposomes which were tailored with an archaeal lipid, Glycerol Dialkyl Nonitol Tetraether (GDNT), isolated from the thermoacidophilic archaeon *Sulfolobus acidocaldarius.* Investigations of thermal stability, stability during autoclavation and pH stability were carried out. Furthermore, morphological images were presented. In this chapter a special lipid was isolated and purified for the preparation of liposomal vesicles. Liposomes tailored with GDNT showed high stability in various pH and temperature conditions. The results showed that the GDNT liposomes are even stable after autoclavation. The second chapter was presented in the form of a protocol.

Chapter 3 describes stability properties of tetraether lipid liposomes under conditions simulating the pulmonary system and gastrointestinal tract. The tetraether lipids were isolated from the thermoacidophilic archaeon *Thermoplasma acidophilum.* In contrast to the liposome formulations presented in Chapter 2, these liposomes were prepared with total tetraether lipids instead of a specific type of tetraether lipid. In addition to studies of pH stress and stability during autoclavation, the stability properties of these liposomes were investigated in fetal calf serum and lung surfactant conditions. The TEL content of the liposomes provides extreme stability to the liposomes which is very promising for drug delivery and targeting systems. The results of this work are considered as a preliminary study to elucidate the optimal ratio of tetraether lipid and conventional lipid for the following studies.

Chapter 4 deals with lectin-carbohydrate interactions. The model lectin Concanavalin A (ConA) extracted from the Jack-bean *Canavalia ensiformis* was used to modify tetraether lipid liposomes. ConA binds to sugar domains localized on inflamed tissues or tumors. The ConA modified TEL liposomes provide an effective targeting mechanism to the inflamed area or tumors. The polymeric form of the sugar mannose, "mannan", was used for the surface modification of a bio-chip. This bio-chip simulated the carbohydrate residues on the cell surface. The binding properties of ConA- modified liposomes onto the mannan coated chip surface were investigated with Reflectometric Interference Spectroscopic (RIfS) measurements which were performed with a BIAffinity device and subsequently with Atomic Force Microscopy (AFM). These measurements provide full information about the binding characteristics of ConA onto the mannan surface. In this regard, ConA can be considered as a useful model for the investigation of specific biomarkers. In the future, ligand conjugated TEL liposomes may serve as efficient carriers for specific drug targeting.

Chapter 5 presents an anti-angiogenic effect of a tyrosine kinase inhibitor entrapped in tetraether lipid liposomes to protect the drug and to decrease the adverse effects on the organism. The anti-angiogenic effect was determined by investigation of blood vessels on a chorioallantoic membrane (CAM) model, especially because of its dense capillary network and eligibility of continuous screening of the implant. Besides *in ovo* investigations, anti-angiogenic effects of the tyrosine kinase inhibitor "imatinib" entrapped tetraether liposomes were elucidated with cell viability and Western blot assays. According to the comparative results of application between imatinib solution and imatinib encapsulated tetraether lipid liposomes, tetraether lipid liposomes were considered to be promising carriers for tyrosine kinase inhibitors due to the high anti-angiogenesis efficiency with much lower drug concentration. This approach yields to decrease the undesirable side effects of the drug and reduces the amount of drug necessary for an efficient therapy.

6.2 Perspectives

Within the scope of this thesis, investigations of tetraether lipid (TEL) liposomes were performed in two sections, which were namely liposomal targeting and liposomal drug delivery. Since both aspects were examined separately, an essential future perspective of this study is the investigation of a combined application of those two systems to finally provide a tetraether lipid liposomal drug carrier with a targeting mechanism.

To achieve an effective drug delivery and targeting model, the stability of ligand conjugated liposomes and tyrosine kinase inhibitor entrapped TEL liposomes obviously needs to be explored under different thermal, pH, fetal calf serum, lung surfactant and other conditions concerning the application region.

In ***Chapter 4***, a ligand modification of tetraether lipid liposomes was tailored with a model ligand Concanavalin A, to investigate lectin-carbohydrate interactions of the tetraether lipid liposomes to the carbohydrate surface. This interaction is an unspecific interaction. For an effective targeting model, more specific ligands need to be investigated with Reflectometric Interference Spectroscopy.

In ***Chapter 5,*** the CAM model, which is known as an *in ovo* method, was investigated. A posterior step to the *in ovo* experiments is the *in vivo* study of ligand conjugated TEL liposomes with an encapsulated drug in order to evaluate the systemic effect of a tyrosine kinase inhibitor entrapped in ligand conjugated /nonconjugated tetraether lipid liposomes to a living organism.

6.3 Zusammenfassung

Liposomen bieten ein breites Spektrum an medizinischen Anwendungsmöglichkeiten, besonders in der Diagnostik und der Therapie. Die Stabilität der Liposomen als Wirkstoffträger stellt dabei eine der größten Einschränkungen in der Anwendung dar, da die Gefahr eines schnellen Abbaus der Vesikel im menschlichen Körper besteht. Daher wurden im Rahmen dieser Arbeit hochstabile Tetraetherlipid-Liposomen (TEL-Liposomen) hergestellt und charakterisiert. Die vorliegende Arbeit umfasst die Untersuchung der Stabilität von Tetraetherlipid-Liposomen, die Lectinbindung dieser Liposomen und schließlich Liposomen als Träger eines Anti-Angiogenese-Wirkstoffes. Diese Untersuchungen sind in fünf Kapiteln strukturiert.

Kapitel 1 gibt eine Einführung in Tetraetherlipid-Liposomen, stellt Methoden zur Extraktion und Reinigung vor und beschreibt pharmazeutische Anwendungsmöglichkeiten. Darüber hinaus werden Modifikationen von TEL-Liposomen und deren Nutzung zum Wirkstofftransport diskutiert. Der Fokus dieses Kapitels liegt auf dem Einsatz von Liposomen als Antiangiogenese-Wirkstofftransporter in der Krebstherapie.

Kapitel 2 charakterisiert Tetraetherlipid-Liposomen, die aus einem Archea-Lipid, Glycerol-Dialkyl-Nonitol-Tetraether (GDNT), hergestellt wurden, das aus dem thermoacidophilen Archaeon *Sulfolobus acidocaldarius* isoliert wurde. Es wurden Untersuchungen zur Thermostabilität, Stabilität während des Autoklavierens und pH-Stabilität durchgeführt. Weiterhin wurde eine morphologische Charakterisierung vorgenommen. In diesem Kapitel

wurde ein spezifisches Lipid isoliert und gereinigt, um Liposomen herzustellen. Liposomen aus GDNT weisen eine hohe Stabilität in unterschiedlichen pH- und Temperaturbedingungen auf. Es konnte gezeigt werden, dass GDNT-Liposomen sogar nach dem Autoklavieren stabil bleiben. Kapitel 2 liegt in Form eines Methodenprotokolls vor.

Kapitel 3 beschreibt die Stabilitätseigenschaften von Tetraetherlipid-Liposomen unter Bedingungen, die die physiologischen Gegebenheiten im Atmungssystem und Magen-Darm-Trakt simulieren. Hierzu wurden Tetraether-Lipide aus dem thermoacidophilen Archaeon *Thermoplasma acidophilum* isoliert. Im Gegensatz zu den in Kapitel 2 vorgestellten Liposomzusammensetzungen wurden hier Liposomen aus dem Gesamtumfang der isolierten Tetraether-Lipide anstatt aus einer bestimmten Fraktion hergestellt. Zusätzlich zu Untersuchungen der Stabilität unter pH-Stress und Autoklavierungs-Bedingungen wurden die Liposomen in fetalem Kälberserum und Lungen-Surfactant untersucht. Der TEL-Anteil in den Liposomen verhilft ihnen dabei zu hoher Stabilität. Dies ist vielversprechend für einen späteren Einsatz im zielgerichteten Wirkstofftransport. Diese Untersuchungen können als Vorversuche zur Ermittlung der optimalen Lipidzusammensetzung von Liposomen angesehen werden, die in den weiterführenden Studien genutzt werden sollen.

Kapitel 4 beschäftigt sich mit Lectin-Kohlenhydrat-Interaktionen. Das Lektin Concavalin A (ConA), gewonnen aus der Jackbohne *Canavalia ensiformis*, wurde hier zur Modifikation von Tetraetherlipid-Liposomen eingesetzt. ConA bindet an Zuckerdomänen, wie sie in entzündetem Gewebe oder Tumoren vorkommen. Die ConA – modifizierten TEL-Liposomen stellen somit eine effektive Methode zur gezielten Anwendung in solchen Geweben dar. Die

Polymerform des Zuckers Mannose, „Mannan“, wurde zur Beschichtung eines Bio-Chips genutzt, so dass Kohlenhydratreste auf einer Zelloberfläche simuliert werden konnten. Die Affinität der ConA – modifizierten Liposomen zum mannanbeschichteten Biochip wurde mittels Reflektrometrischer Interferenzspektroskopie untersucht, die mit einem BIAffinity-Gerät durchgeführt wurde, und weiterhin mittels Rasterkraftmikroskopie. Diese Messungen erlauben die vollständige Charakterisierung der Bindung von ConA an die Mannanoberfläche. In diesem Zusammenhang kann die ConA-Modifikation der TEL-Liposomen als Modellversuch für die Untersuchung spezifischer Biomarker betrachtet werden. Künftig könnten TEL-Liposomen als wirksame zielgerichtete Wirkstoffträger zum Einsatz kommen.

Kapitel 5 schildert den Antiangiogenese-Effekt des Tyrosinkinaseinhibitos „imatinib“, der in TEL-Liposomen eingschlossen wurde, um den Wirkstoff zu schützen und Nebenwirkungen auf den Organismus zu minimieren. Der Antiangiogenese-Effekt wurde an Blutgefäßen in einem CAM-Modell (Chorioallantoische Membran im Hühnerei) untersucht, insbesondere aufgrund des dichten Kapillarnetzwerks und der Eignung für kontinuierliche Beobachtung des Implantats. Neben den *in-ovo*-Untersuchungen wurde der Antiangiogenese-Effekt der imatinib-beladenen TEL-Liposomen mittels Zellviabilität- und Western-Blot-Analysen charakterisiert. Aufgrund der gewonnen Erkenntnisse im direkten Vergleich von imatinib-geladenen TEL-Liposomen mit imatinib-Lösung konnten die TEL-Liposomen als vielversprechende Vektoren für Tyrosinkinaseinhibitoren dargestellt werden, da sie eine hohe Antiangiogeneseeffizienz mit einer niedrigeren Wirkstoffkonzentration erreichen. Dieser Ansatz soll helfen, unerwünsche Nebeneffekte des verwendeten Wirkstoffes zu minimieren und reduziert die für eine Therapie notwendige Wirkstoffmenge auf ein Mindestmaß.

6.4 Ausblick

Im Rahmen dieser Arbeit wurden Tetraetherlipid-Liposomen unter zwei verschiedenen Aspekten untersucht: Liposomen-Targeting und Wirkstofftransport durch Liposomen. Da bisher beide Aspekte getrennt untersucht wurden, ist ein wichtiger nächster Schritt die Kombination beider Systeme, um schließlich ein Wirkstofftransportsytem mit Targetingfunktion auf der Basis von Tetraetherlipid-Liposomen etablieren zu können.

Bisher wurde die Stabilität von unmodifizierten TEL-Liposomen ohne Beladung untersucht – um ein erfolgreiches Wirkstofftransportsystem zu etablieren, müssen im weiteren Verlauf die ligandgebundenen Liposomen sowie Tyrosinkinaseinhibitor-beladene Liposomen unter Stressbedingungen wie hohe Temperaturen, verschiedene pH-Werte, Inkubation in fetalem Kälberserum und Lungen-Surfactant sowie anderer Bedingungen, die am gewünschten Einsatzort vorherrschen, untersucht werden.

In Kapitel 4 wurden mit dem Liganden Concavalin A gebundene TEL-Liposomen hergestellt, um Lectin-Kohlenhydrat-Interaktionen der modifizieren TEL-Liposomen mit einer kohlenhydratbeschichteten Oberfläche zu Untersuchen. Bei dieser Art der Interaktion handelt es sich um eine unspezifische. Für ein effektives Targeting sollten nun mittels Reflektrometrischer Interferenzspektroskopie Liganden untersucht werden, die eine spezifischere Interaktion ermöglichen.

Kapitel 5 beschreibt das CAM-Modell als eine Methode des *in-ovo*-Screenings. Ein notwendiger Folgeschritt zu den *in-ovo*-Beobachtungen beinhaltet *in-vivo*-Experimente mit wirkstoffbeladenen und ligandgebundenen TEL-Liposomen, um eine fundierte Einschätzung

des systemischen Effekts des Einsatzes Tyrosinkinaseinhibitor-beladener ligandgebundener TEL-Liposomen auf den Organismus treffen zu können.

7 Apendices

7.1 Abbreviations

AFM	Atomic Force Microscopy
abl	Abelson murine leukemia gene
bcr	Breakpoint cluster region gene
bFGF	Basic Fibroblast Growth Factor
BIA	Biomolecular Interaction Analysis
BM	Bone Marrow
CAM	Chorioallantoic Membrane
CF	5(6)-Carboxyfluorescein
CML	Chronic Myeloid Leukemia
ConA	Concanavalin A
DLS	Dynamic Light Scattering
DPPC	L-Alpha-dipalmitoyl phosphatidylcholine
EDTA	Ethylenediaminetetraacetic acid
EE	Encapsulation Efficiency
ELISA	Enzyme-Linked Immunosorbent Assay
ERK	Extracellular-Signal-Regulated Kinase
FCS	Fetal Calf Serum
HEPES	2-[4-(2-Hydroxyethyl)-1-piperazinyl]ethanesulfonic Acid
GDNT	Glycerol Dialkyl Nonitol Tetraether
GIST	Gastrointestinal Stromal Tumor
IC_{50}	Half-Inhibitory Concentration
IMDM	Iscove's Modified Dulbecco's Medium

LDA	Laser Doppler Anemometry
MAPK	Mitogen-Activated Protein Kinase
PBS	Phosphate Buffered Saline
PCS	Photon Correlation Spectroscopy
PDGF	Platelet-Derived Growth Factor
PDGFR	Platelet-Derived Growth Factor Receptor
PDI	Polydispersity Index
PECAM-1	Platelet Endothelial Cell Adhesion Molecule-1
PEG	Poly(ethylene Glycol)
Ph	Phospholipon 100H
RES	Reticulo-Endothelial System
RIfS	Reflectometric Interference Spectroscopy
RT	Room Temperature
SD	Standard Deviation of the Mean
SEM	Standard Error of the Mean
SPF	Specific Pathogen Free
TEL	Tetraether Lipid
TGF-β	Transforming Growth Factor Beta
VEGF	Vascular Endothelial Growth Factor
WST	Water Soluble Tetrazolium Salts

7.2 List of Publications

7.2.1 Articles

Aybike Ozcetin, Samet Mutlu, Udo Bakowsky (2009) "Archaebacterial Tetraetherlipid Liposomes" Vol. 605 pp. 87-96, Liposomes: Methods and Protocols, Volume 1: Pharmaceutical Nanocarriers Volkmar Weissig (Ed), Methods in Molecular Biology

Johannes Sitterberg, **Aybike Ozcetin**, Carsten Ehrhardt, Udo Bakowsky (2010) Utilising atomic force microscopy for the characterisation of nanoscale drug delivery systems, Review Article Vol. 74 (1), pp. 2-13, European Journal of Pharmaceutics and Biopharmaceutics

7.2.2 Poster Presentations

A. Özcetin, U. Bakowsky,

"The Application of Chorioallantoic Membrane Tumor Model for Potential Testing of Nanoscale Drug Delivery System",

Controlled Release Society German Chapter, 19.03.2009 Halle/Germany

A. Özcetin, S. Mutlu, N. Harbach, U. Bakowsky,

"New Highly stable Liposomal Formulations Based on Tetraetherlipids From the Archaeon Thermoplasma Acidophilum"

6th World Meeting of Pharmaceutics, Biopharmaceutics and Pharmaceutical Technology 07-10.04.2008 Barcelona/Spain

7.2.3 Oral Presentations

Aybike Özcetin "Tyrosine Kinase Inhibitor Encapsulated in Tetraetherlipid Liposome for Anti-angiogenic Applications"

20th Mountain/Sea Liposome Workshop, International Workshop 25.09.2009 Ameland/Holland

Aybike Özcetin XI. Summer Academy (DAAD and Studienstiftung des Deutschen Volkes), „Der extrakorporale frühe menschliche Embryo (efmE): „human being" („embryonaler Mensch") „human life" („potentiell zum Menschen Werdender") oder „special cell life" („humane Zellverbindung besonderer Art")?"

09.-22.08.2010, Rot an der Rot/Germany

Aybike Özcetin 19th Mountain/Sea Liposome Workshop, Oberjoch International Workshop "Tetraetherlipid-Liposomes: A New Class of Liposomal Drug Formations" 13th International Pharmaceutical Technology 10-14.03.2008, Oberjoch/Germany

7.2.4 Awards

DAAD Doctoral Studies Full Scholarship, September 2007-April 2011

7.3 Curriculum Vitae

Personalien:

Özcetin, Aybike

Geboren am 01.01.1981 **in** Izmit, Türkei

Staatsangehörigkeit: Türkisch

Ausbildung and Berufspraxis:

1996-1999	Atılım Gymnasium, Izmit, Türkei
2000-2005	Bachelours Chemie, Hacettepe Universitaet, Ankara, Türkei
Jan. - März 2001	Praktikum SakoSA industriell Garn und Reifen Cord GMBH, Izmit Türkei
Sep. - Okt.2003	Praktikum DupontSA Dupont Sabanci Polyester GMBH-Hamm, Uentrop Germany
2005-2007	Master Biochemie, Hacettepe Universitaet, Ankara, Türkei
April 2007-September 2007	Erasmus Prog., Institut für Physikalische Chemie, Kernchemie und Makromolekulare Chemie, Marburg, Philipps Universitaet, Marburg

Seit September 2007	Stipendiatin und Doktorandin im Institut für Pharmazeutische Technologie und Biopharmazie, Philipps-Universitaet Marburg

7.4 Danksagung

Abschliessend möchte ich allen danken, die durch ihre fachliche und persönliche Unterstützung zum Gelingen dieser Doktorarbeit beigetragen haben.

Mein besonderer Dank gilt Herrn Prof. Dr. Udo Bakowsky für die Vergabe und Betreuung meiner Doktorarbeit ebenso wie für die zahlreichen Ratschläge, hilfreichen Kommentare und seine freundschaftliche Wegbegleitung.

Weiterhin bedanke ich mich bei Herrn Prof. Dr. Achim Aigner, der mir stets Ansprechpartner für unser Kooperationsprojekt war und meine Arbeit durch seine Ideen, seine Anregungen und seine konstruktive Kritik bereicherte und darüber hinaus für die Erstellung des Zweitgutachtens.

Ich danke dem Deutschen Akademischen Austausch Dienst (DAAD), der mich während meiner gesamten Doktorarbeit finanziell unterstützt hat und ohne den ein erfolgreicher Abschluss nicht möglich gewesen wäre.

Für die Hilfe, Unterstützung und Freundschaft danke ich meinen Kollegen aus dem AK Bakowsky, besonders Johannes Sitterberg für die erfolgreiche Zusammenarbeit und Eyas Dayyoub für seine Bemühungen mit der Mikroskopie. Alle anderen, Bassam Al Meslmani, Leonie Baginski, Thomas Betz, Jana Brüssler, Nico Harbach, Elena Marxer, Jens Schäfer, Anett Sommerwerk, Maria Solovey, Boris Strehlow danke ich ebenfalls für gute Zusammenarbeit. Auch danke ich Herrn Prof. Thomas Kissel sowie seinen Mitarbeitern Moritz Beck-Broichsitter, Nadja Bege, Markus Benfer, Heiko Debus, Thomas Endres, Klaus Keim, Tobias Lebhardt, Sascha Maretschek, Olivia Merkel, Eva Mohr Frank Morell, Thomas

Renette, Regina Reul, Susanne Rösler, Olga Samsanova, Christoph Schweiger, Nina Seidel, Terry Steele, Nan Zhao für die nette Zeit im Institut und ihre Freundschaft.

Bei Christian Hobler und Elvira Betz vom Institut für Pharmazeutische Chemie möchte ich mich besonders für unsere nette Zusammenarbeit und für ihre technische Unterstützung während der Affinity-Messungen bedanken.

Für fachliche und technische Unterstützung danke ich allen Mitgleidern des AK Aigner die mir ein angenehmes und produktives Arbeiten erlaubt haben: Daniela Gutsch, Melanie Günther, Sabrina Höbel, Ahmed Ibrahim, Michael Rabe, Daniel Schulze, Ulrike Weirauch. Insbesondere möchte ich mich bei Andrea Wüstenhagen, Marga Losekam und Fatma Aktuna bedanken für die Zusammenarbeit bei den Messungen der Zellviabilität und beim Western Blot.

Bei Herrn Dr. Thomas Hofmann bedanke ich mich für seine wertvollen Ideen sowie sein großzügiges Angebot, sein Labor und seine Geräte zur allen Tages- und Nachtzeiten bzw. am Wochenende nutzen zu dürfen.

Ich möchte Herrn Dr. Ulrich Rothe und Christian Hübner vom Institut für Physiologische Chemie in Martin Luther Universitaet Halle-Wittenberg dafür danken, dass sie mir das CAM-Modell beigebracht haben so wie Nancy Funk für ihre nette Hilfe und ihre Freundschaft.

Ausserdem bedanke ich mich bei Frau Dr. Frauke Kepura und Tanja Pfeffer-Eckel ganz herzlich für ihre Freundschaft, ihre Unterstützung und angenehme Unterhaltungen.

Weiterhin bedanke ich mich bei Urs Lahrmann, Christian Seile und Robert Prinz für ihre technische Unterstützung und stundenlange nette Unterhaltungen.

Ich danke zudem Samet Mutlu vom Institut für Pharmakologie und Toxikologie des Biomedizinischen Zentrums der Universität Bonn ganz besonders für die nette Zusammenarbeit und seine wertvolle Freundschaft.

Auf privater Ebene danke ich meiner Familie für ihre Unterstützung und ihren Glauben an mich, die mir meine Doktorarbeit überhaupt erst ermöglicht haben.

Von tiefsten Herzen möchte ich meinem Freund Christoph Hemetsberger danken, der mich jederzeit seelisch und moralisch unterstützt, bestärkt, bei jedem Schritt des Schreibens geholfen und motiviert hat, mit besten wissenschaftlichen Gesprächen meine Perspektive erweitert hat und der mein Leben auf allen Ebenen viel schöner macht.

ERKLÄRUNG

Ich versichere, daß ich meine Dissertation

"Tetraether lipid Liposomes for the Preparation of Novel Liposomal Drug Carriers"

selbständig ohne unerlaubte Hilfe angefertigt und mich dabei keiner anderen als der von mir ausdrücklich bezeichneten Quellen bedient habe.

Die Dissertation wurde in der jetzigen oder einer ähnlichen Form noch bei keiner anderen Hochschule eingereicht und hat noch keinen sonstigen Prüfungszwecken gedient.

Marburg, den 14.03.2011

Aybike Özcetin